Technical Report Documentation Page

1. Report No.	2. Government Accession No.	3. Recipient's Catalog No.
Preliminary Review Copy		

4. Title and Subtitle	5. Report Date
DIAGNOSTIC LOAD TESTS OF A REINFORCED CONCRETE PAN-GIRDER BRIDGE	**June 2000**
	6. Performing Organization Code

7. Author(s)	8. Performing Organization Report No.
B. M. Velázquez, J. A. Yura, K. H. Frank, M. E. Kreger, and S. L. Wood	Research Report 7-2986-2

9. Performing Organization Name and Address	10. Work Unit No. (TRAIS)
Center for Transportation Research The University of Texas at Austin 3208 Red River, Suite 200 Austin, TX 78705-2650	11. Contract or Grant No. Research Study 7-2986

12. Sponsoring Agency Name and Address	13. Type of Report and Period Covered
Texas Department of Transportation Research and Technology Transfer Section, Construction Division P.O. Box 5080 Austin, TX 78763-5080	Research Report (9/95-8/99)
	14. Sponsoring Agency Code

15. Supplementary Notes

Project conducted in cooperation with the U.S. Department of Transportation

16. Abstract

This report presents the results from a diagnostic load test performed on a reinforced concrete pan-girder bridge located in Buda, Texas. A total of 45 strain gages and 5 displacement gages were attached to the bridge to measure the response. The results indicate the following: (a) the nonstructural curbs act integrally with the exterior girders and carry a large portion of the load, (b) the maximum positive moments in the bridge are similar to the maximum positive moments obtained from a line-girder analysis of a continuous beam, (c) the AASHTO load distribution factor is unconservative for girders with curbs and conservative for interior girders, and (d) rotational restraint was observed at both supports.

17. Key Words	18. Distribution Statement
	No restrictions. This document is available to the public through the National Technical Information Service, Springfield, Virginia 22161.

19. Security Classif. (of report)	20. Security Classif. (of this page)	21. No. of pages	22. Price
Unclassified	Unclassified	121	

Form DOT F 1700.7 (8-72) Reproduction of completed page authorized for FSEL Reports

Diagnostic Load Tests of a Reinforced Concrete Pan-Girder Bridge

by

B. M. Velázquez, J. A. Yura, M. E. Kreger, and S. L. Wood

Research Report 7-2986-2

Research Project 7-2986

BRIDGE LOAD TESTING PROGRAM

conducted for the

Texas Department of Transportation

in cooperation with the

U.S. Department of Transportation
Federal Highway Administration

by the

CENTER FOR TRANSPORTATION RESEARCH
BUREAU OF ENGINEERING RESEARCH
THE UNIVERSITY OF TEXAS AT AUSTIN

May 2000

Research performed in cooperation with the Texas Department of Transportation and the U.S. Department of Transportation, Federal Highway Administration.

ACKNOWLEDGEMENTS

We greatly appreciate the financial support from the Texas Department of Transportation that made this project possible. The support of the project director, Mike Lynch (BRG), and program coordinator, Ron Koester, is also very much appreciated. We thank Project Monitoring Committee members, .

DISCLAIMER

NOT INTENDED FOR CONSTRUCTION,
PERMIT, OR BIDDING PURPOSES

J. A. Yura, P.E., Texas #29859
M. E. Kreger, P.E. , Texas #65541
S. L. Wood, P.E., Texas #83804
Research Supervisors

TABLE OF CONTENTS

LIST OF FIGURES

LIST OF TABLES

SUMMARY

This report presents the results from a diagnostic load test performed on a reinforced concrete pan-girder bridge located in Buda, Texas. A total of 45 strain gages and 5 displacement gages were attached to the bridge to measure the response. The results indicate the following: (a) the nonstructural curbs act integrally with the exterior girders and carry a large portion of the load, (b) the maximum positive moments in the bridge are similar to the maximum positive moments obtained from a line-girder analysis of a continuous beam, (c) the AASHTO load distribution factor is unconservative for girders with curbs and conservative for interior girders, and (d) rotational restraint was observed at both supports.

CHAPTER 1: INTRODUCTION

Approximately 18,000 bridges in Texas do not meet the current design standards set by the American Association of State Highway and Transportation Officials (AASHTO). The Texas Department of Transportation (TxDOT) is concerned that these bridges lack the structural integrity to safely carry current and future traffic demands. As a result, TxDOT either posts or, more severely, closes the bridges in question. Posting a bridge is an attempt to limit the loads crossing the bridge. Posting of a bridge also requires regular costly inspections in order to determine the structural and physical condition. Furthermore, the posting of a bridge affects the trucking industry because direct routes may be eliminated.

The issue with posting or closing of bridges is that the procedure used does not represent the true strength of the bridge. This procedure known as load rating determines the live load-carrying capacity of an existing bridge [1]. Currently, load rating is derived from calculations based on simplified design procedures that do not consider the reserve strength of the bridge. Important decisions about posting and closing bridges are therefore based on this conservative load rating approach.

According to the AASHTO Manual for Condition Evaluation of Bridges (AASHTO Manual) [1], the load rating of a bridge should be evaluated at two levels: inventory and operating. The inventory rating level represents the live load that can safely use the bridge for an indefinite period of time. The operating rating level represents the maximum permissible live load to which the bridge may be subjected. An inventory load rating less than an HS20, the current design load, requires the bridge to be posted [1].

The main objectives of this research were to measure the response of a pan-girder bridge based on a diagnostic load test. Additionally, assessing the feasibility of performing such load test on this type of bridge was investigated. An important step was to develop a procedure to measure the response of a reinforced concrete pan-girder bridge and use the measured response to evaluate the bridge. Subsequent investigations will use the measured response to evaluate the reserve capacity of a pan-girder bridge.

This chapter presents a summary of nondestructive load testing procedures, previous research, the need for testing pan-girder bridges, and the objectives and scope of this research.

1.1 THE USE OF NONDESTRUCTIVE LOAD TESTING FOR LOAD RATING BRIDGES

Nondestructive load tests are performed on bridges to better assess their behavior and load-carrying capacity without destroying any of the structural elements. Steel bridges are among the most common types of bridges tested because they are easy to instrument, and the relationship between measured strain and stress is a constant material property. On the other hand, fewer reinforced concrete bridges have been tested because of varying material properties, undetermined extent of cracking, and difficulty instrumenting the bridge. Therefore, more load tests on reinforced concrete bridges must be conducted to determine better measuring techniques and to evaluate the significance of the measured data. Once these improved techniques become available, load tests may be conducted to assess the in situ strength of concrete bridges and to obtain a more accurate load rating. The two primary tests used for bridge evaluation and load rating are diagnostic and proof load testing.

1.1.1 Diagnostic Load Testing

Diagnostic load tests are conducted to determine the effects of a known load on various components of a bridge. During a diagnostic load test, the applied load is sufficiently large to model the physical behavior of the bridge without causing any distress to its components [2]. The disadvantage of diagnostic load tests is that the measured response must be extrapolated to find its load-carrying capacity. Because of restricted loading equipment and a lack of load testing results, this research project involved performing a diagnostic load test on a reinforced concrete pan-girder bridge.

1.1.2 Proof Load Testing

In a proof load test, loads are applied incrementally until early warning of possible distress or nonlinear behavior is observed. The advantage of proof load testing is that the measured response is near the actual capacity of the bridge, and extrapolation of results is unnecessary. The disadvantages of proof load tests are that special loading equipment is necessary to generate the incremental loading and the bridge is damaged during the test [2].

1.2 PREVIOUS TESTS OF PAN-GIRDER BRIDGES

A pan-girder bridge is constructed by using pan forms to create the slab and girder structural system. A typical pan-girder span is shown in Fig. 1.1 [3]. Pan-girder construction has many advantages such as (a) speed of construction, (b) light equipment and low labor requirements, (c) economy, and (d) ease of widening [4]. Because of these advantages, pan-girder bridges are very common throughout the United States.

Few field tests have been conducted on pan-girder bridges. One particular field test conducted by Armstrong, et al. (1969) provided important results describing the load distribution behavior of a pan-girder bridge located in Belton, Texas.

The field test was preceded by testing a 1/6-scale model of the pan-girder bridge in the laboratory. The model was developed to compare its measured response with the response obtained from the prototype. The loads placed on the model corresponded to service and ultimate levels. The actual bridge was tested using only service loads because the bridge was new. Therefore, the extent of cracking was more severe in the model than the prototype. The loading of the model with single and double truckloads produced similar strain results to those of the prototype bridge [3].

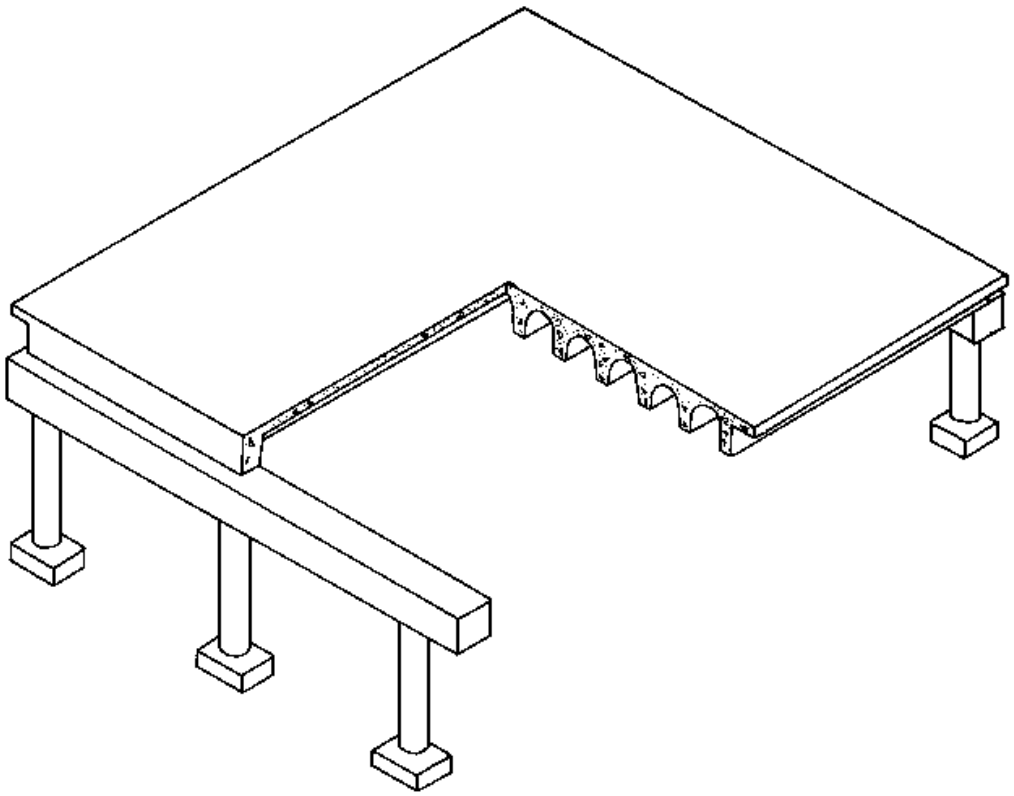

Figure 1.1 Typical Pan-Girder Span [3]

The objectives of the field test were twofold. One objective of the field test was to compare the prototype results with those from the model. A second objective was to investigate the feasibility of load distribution testing of a full-scale pan-girder bridge [4]. To achieve these objectives, strain gages were placed at various locations along the reinforcing bars, as shown in Fig. 1.2. Subsequently, trucks were positioned transversely across the bridge to obtain the strain distribution as a function of truck position.

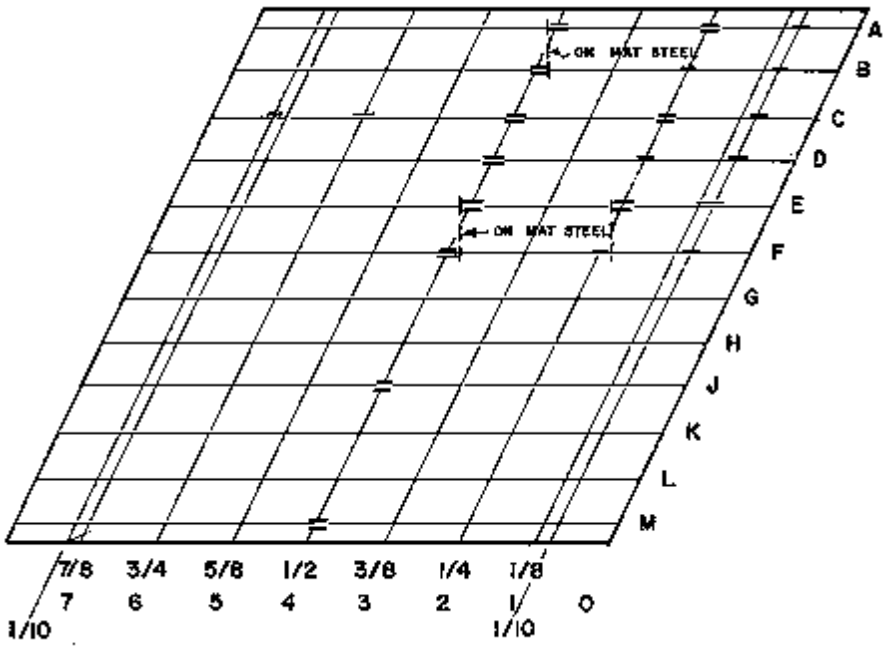

Figure 1.2 Strain Gage Layout for Bridge [4]

The strain results were used to obtain the AASHTO load distribution factor, K_A, for each load configuration used in the field test. The load distribution factor is calculated as follows:

$$K_A = \frac{S}{C} \tag{1.1}$$

where

K_A = AASHTO load distribution factor

S = average girder spacing in ft.

C = constant

The constant C is a function of the type of structural system and the number of traffic lanes. For the tested bridge, the constant used by the 1957 AASHO Specifications [9] was defined as 6.0 for one traffic lane. The constant changed to 6.5 for one traffic line in the 1965 AASHO Specifications [10]. The experimental strain data were used to obtain a constant representative of the load distribution among the girders. The equation for this constant based on the experimental strain data is as follows [5]:

$$C = \frac{S}{K_{GM}} * \frac{N_G}{N_W} \tag{1.2}$$

where

C = constant

S = average girder spacing in ft.

K_{GM} = ratio of longitudinal moment in a specific girder to the average longitudinal moment in all girders

N_G = number of longitudinal girders

N_W = number of equal wheel lines

From Eq. 1.2, the constant was calculated and compared with the constant determined by AASHTO. The results indicated that the AASHTO factor was overly conservative, and the percent difference between experimental and design load distribution factors depends on the loading of the bridge. For a single truck load, the AASHTO factor overestimated the moment in the individual beams between 10 to 100 percent. For two trucks, the AASHTO factor overestimated the moments between 2 to 80 percent.

In conclusion, the strains measured during a field test of a pan-girder bridge agreed with the strains measured in the laboratory tests. Also, the results indicated that the AASHTO load distribution factor was conservative for this type of bridge.

1.3 NEED FOR TESTING PAN-GIRDER BRIDGES

Pan-girder bridges are very common throughout Texas. Texas has approximately 4,000 pan-girder bridges of which sixty percent were designed with design loads less than the current standard [6]. These design loads were trucks weighing 10, 15, or 20 tons, commonly known as H10, H15, or H20 design vehicles, respectively. As mentioned, the current AASHTO design load is an HS20 design vehicle weighing 36 tons, and load rating is based on this HS20 design vehicle. Problems arise when many bridges do not meet the load rating standard.

TxDOT sponsored a project at The University of Texas at Austin which entails measuring the load response of four types of bridges: reinforced concrete slab on steel girders, reinforced concrete slab, prestressed concrete, and reinforced concrete pan-girder. These four types of bridges make up a majority of the bridges designed for less than HS20 design vehicles and thus are susceptible to posting or closing. Multiple load tests have been performed on all of these types of bridges.

1.3.1 Inventory of Current Pan-Girder Bridges in Texas

The following tables present an inventory of pan-girder bridges in Texas. These tables show design loads, skew angles, and span lengths of all pan-girder bridges in Texas. Table 1.1 shows the number of existing bridges that were designed for the given design vehicles. The skew angle and the span length of existing pan-girder bridges are desired because the measured response obtained from a load test could be a function of these parameters. Tables 1.2 and 1.3 show a range of skew angles, span lengths and their distribution.

Table 1.1 Summary of Design Loads for Pan-Girder Bridges [6]

Design Load	Number of Bridges
H10	7
H15	1033
HS15	6
H20	1241
HS20	1595
Other	24

Table 1.2 Distribution of Skew Angle of Pan-Girder Bridges [6]

Skew Angle, θ (°)	Number of Bridges
$\theta \leq 5$	3221
$5 < \theta \leq 10$	0
$10 < \theta \leq 20$	183
$20 < \theta \leq 30$	285
$\theta > 30$	218

Table 1.3 Distribution of Span Length of Pan-Girder Bridges [6]

Span Length, L (ft)	Number of Bridges
$L \leq 20$	1
$20 < L \leq 30$	1965
$30 < L \leq 40$	1585
$40 < L \leq 50$	325
$L > 50$	31

1.3.2 Reasons for Testing Pan-Girder Bridges

As shown in Table 1.1, a majority of the existing pan-girder bridges were designed for less than the 36 ton HS20 design vehicle. The bridges of primary concern are those whose inventory and operating rating levels are below an HS20 load rating. The legal vehicle load limit is 40 tons. These bridges must be checked to see if they can continue to carry the current legal loads, as well as carry increases in the legal load to accommodate heavier vehicles [7]. Therefore, a procedure must be developed to test pan-girder bridges and to assess any capacity not considered in the current load rating procedures [1].

1.4 OBJECTIVES AND SCOPE OF RESEARCH

The objectives of this thesis were to evaluate the measured response of a pan-girder bridge during a diagnostic load test. The following chapters discuss in detail the procedures taken to meet the stated objectives. Chapter 2 presents the structural characteristics of the bridge, a review of the original design procedure, and the results of a load rating based on the current AASHTO procedures [1]. Chapter 3 follows with a discussion of the instrumentation, setup, and procedures used for load testing the bridge.

The test results are presented in Chapter 4. Chapter 5 evaluates and discusses the measured response. Chapter 6 compares the load distribution results from the load test with those from a previous field test and those used by design specifications. Conclusions and recommendations for future testing are presented in Chapter 7.

CHAPTER 2: DESCRIPTION AND LOAD RATING OF BRIDGE

The pan-girder bridge selected for the diagnostic load test is located in Buda, Texas, approximately fifteen miles south of Austin, Texas. It was selected because of its good condition, ease of access, and its location near the research laboratory. The bridge consists of eleven 30 ft. spans, which are not skewed relative to the piers. The bridge serves as FM 967 over Onion Creek and has a traffic flow of approximately 3300 vehicles per day [6].

2.1 BRIDGE DESCRIPTION

The bridge was constructed of reinforced concrete, and its structural details are shown in Figure 2.1. The spans had a 3.5 in. slab on top of the girders. The nine longitudinal girders were spaced at three feet on center, and they served as the primary load-carrying elements. Within the slab, #5 reinforcing bars were placed in the transverse direction at a spacing of 10 ½ in. Three-inch diameter holes through the slab were located at the midpoint of each span, centered between the adjacent girders. The holes were cast during the construction process in order to provide access to the forms.

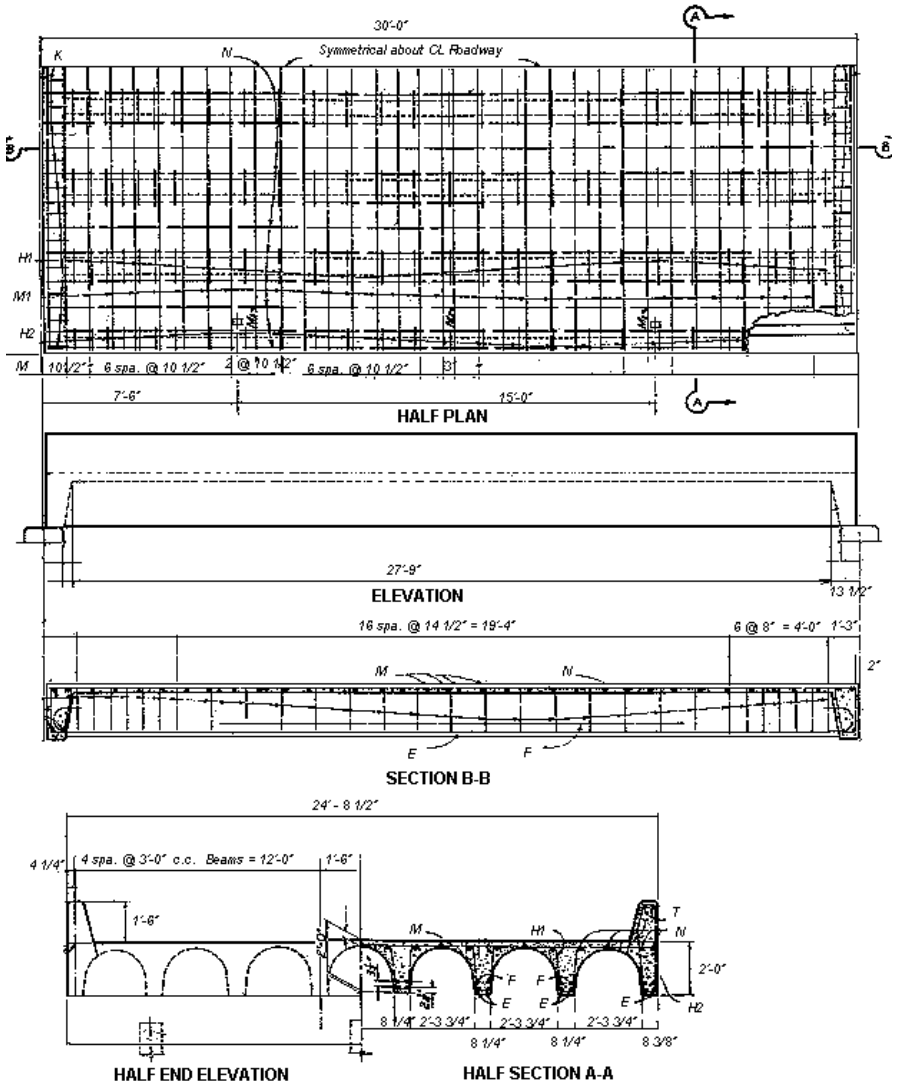

Figure 2.1 Structural Details of Pan-Girder Bridge in Buda, TX

The bridge cross section was composed of two typical cross sections. These are identified as the interior and exterior girder cross sections. The interior girder cross section is shown in Figure 2.2. The primary longitudinal reinforcing bars at the bottom of the girders are #7 and #11 bars. The longitudinal reinforcing bars located within the slab of this cross section were #4 bars. The exterior girder cross section is shown in Figure 2.3. The curb is assumed to act as a structural member in this investigation because the #3 stirrups tie the curb and the girder together. However, the bridge was designed assuming that the curbs were nonstructural.

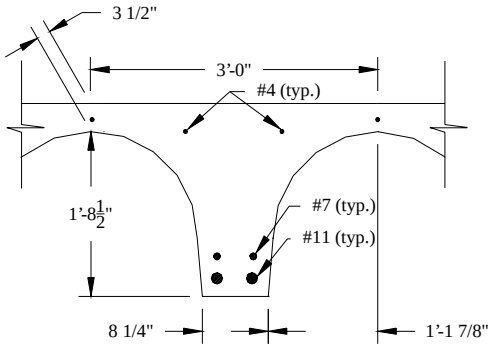

Figure 2.2 Interior Girder Cross Section

2.2 DESIGN PARAMETERS

The bridge was built in 1956. It was designed using working stress design procedures. The loads used for design were two H15 vehicles; each weighing 15 tons. Additionally, the 28-day concrete compressive strength used in the design calculations was 3000 psi, known as Class A concrete. The specified yield stress of the reinforcing bars was 40,000 ksi. The design calculations were based on each span behaving as a simply-supported beam.

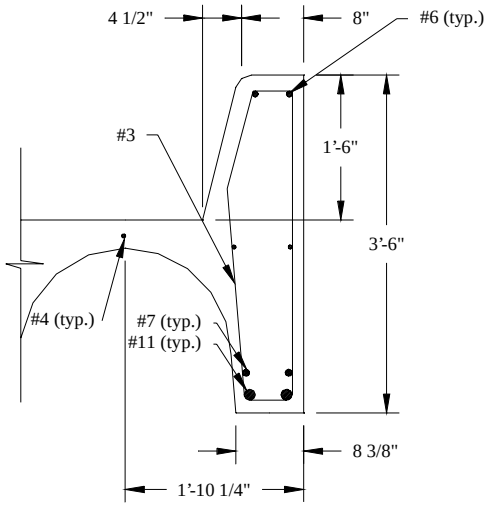

Figure 2.3 Exterior Girder Cross Section

2.3 BRIDGE LOAD RATING

This pan-girder bridge was last inspected in 1995, and its load rating was calculated using the material properties presented in Section 2.2. TxDOT calculated the inventory and operating load ratings for the bridge using the equations outlined in the AASHTO Manual, and both exceeded the AASHTO HS20 designation, as shown in Table 2.1. These results indicate the bridge can remain in service without being posted.

The AASHTO Manual incorporates the physical condition of the bridge into the load rating procedure. This load rating indicates that the physical condition of the bridge did not affect its load-carrying capacity. However, the physical condition of other bridges may decrease their load rating below the AASHTO HS20 standard. Therefore, an assessment of the physical condition is necessary as the first step in evaluating an existing bridge.

Table 2.1 Load Rating for Pan-Girder Bridge*

Inventory Rating	HS 22.8
Operating Rating	HS 24.7

* Calculated by TxDOT using specified material properties for design.

CHAPTER 3: INSTRUMENTATION SETUP AND LOAD TEST PROCEDURE

A pan-girder bridge located in Buda, Texas was tested. This bridge spans over Onion Creek and is a part of FM 967, which carries an average of 3300 vehicles daily [6]. Of the eleven spans crossing the creek, only four were accessible from below. Access was required for the research team to attach the strain and displacement gages. The second span from the west end was chosen for instrumentation because it was the easiest to access.

The instruments were located at midspan and one quarter of the span. Midspan was selected because the maximum strains and moments occur at this location in a simply-supported beam. Previous studies [7] indicated that appreciable end restraint can exist in reinforced concrete bridges that were designed as simply-supported spans. Additional instruments were located at the quarter-point in an attempt to quantify the amount of end restraint.

Pictures of the bridge, viewed from the side and below, are shown in Figures 3.1 and 3.2, respectively. Figure 3.2 shows a black stripe across midspan. This stripe is due to staining caused from run-off that travels through holes located at the top of each crown. As discussed in Chapter 2, the holes are from the pan forms used to cast the slab and the beams.

Figure 3.1 Instrumented Span Viewed from the South

Figure 3.2 Instrumented Span Viewed from Below

This chapter describes the physical condition of the bridge, the gages used to measure the response, the locations of the gages, the problems with instrumenting, and the load testing procedure, which includes the load vehicles and load paths used.

3.1 CONDITION ASSESSMENT OF BRIDGE

The pan-girder bridge on FM 967 was in good physical condition. No signs of corrosion, spalling, honeycombed concrete, or significant cracking of the girders were observed. There were some vertical cracks located at the midspan and quarter-span of all girders, as shown in Figure 3.3. The average crack width was 0.009 in. at midspan. Smaller hairline cracks, with crack widths less than 0.002 in., were observed approximately ten inches from the midpoint and the quarter-point of the girders. Longitudinal cracks were also observed in most crowns of the bridge. These cracks were continuous along the length of the span and located near the top of the crowns. The average width of the cracks was 0.008 in. Longitudinal cracks were not observed in the crowns adjacent to the curb however.

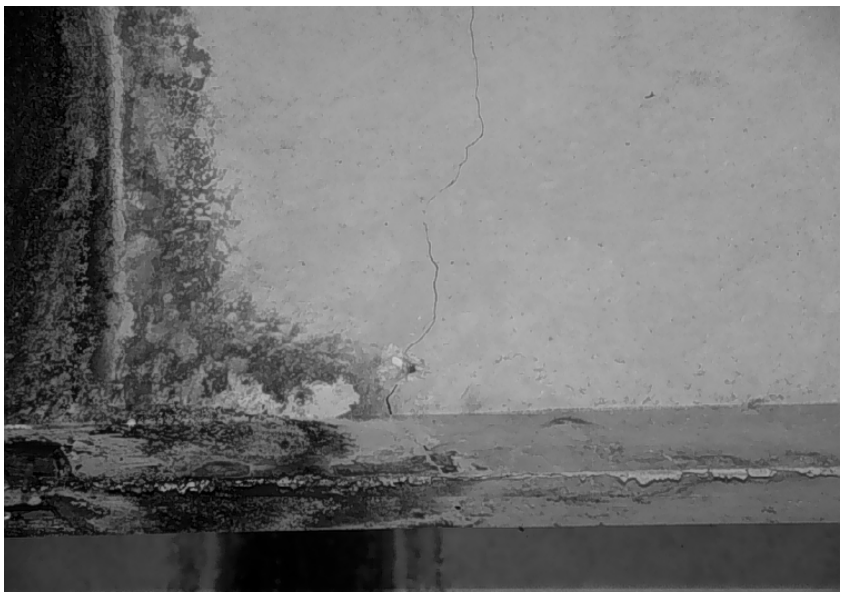

Figure 3.3 Vertical Crack in Girder

The in situ concrete compressive strength was determined using a Schmidt hammer. Measurements were taken at three locations: (1) the bottom of an interior girder, (2) the top of an interior crown, and (3) the top of the north curb. The surface of the concrete was prepared by grinding off approximately ¼ in. About 15 points, spaced between one and two inches apart were marked on the surfaces, but only ten readings are reported because the high and low points were eliminated, as specified in the instruction manual. Table 3.1 summarizes the results from the Schmidt hammer tests. The asterisk denotes that the rebound reading exceeded the maximum rebound value on the calibration chart. The mean compressive strength of all three locations was significantly greater than the 3000 psi compressive strength specified in design.

Table 3.1 Schmidt Hammer Results, psi

Location 1	Location 2	Location 3
6400	8700	10000*
6900	8400	10000*
6700	8400	10000
6400	8100	10000*
6400	7900	10000
6400	8100	9700
6900	7600	10000*
6900	8700	10000*
6400	8100	10000*
6700	7900	9700
Mean	8200	
Std. Dev.	1400	

3.2 INSTRUMENTATION AND DATA ACQUISITION SYSTEM

Strain gages and displacement transducers were attached to the bridge to monitor the service load response. Strains were measured on the surface of the concrete and on the surface of the reinforcing bars in microstrains, which were exposed for this test. The strain data were used to infer the moments carried by each of the girders and the degree of restraint at the ends of the span. Both the distribution of load among the girders and the end restraint were expected to differ from the assumptions made during design. The displacement transducers were used to measure vertical displacements at the midspan of the instrumented span. Therefore, instrumentation was selected in order to provide a detailed description of the actual bridge response.

A total of 45 strain gages and 5 displacement transducers were positioned on the bridge. Because each span of the bridge had been designed with simply-supported end conditions, the strains were expected to be the maximum at midspan. Therefore, as shown in Figure 3.4, the instruments were placed near midspan and at the east quarter-span. All of the instruments shown in Figure 3.5 were located four inches west of midspan to avoid the holes in the slab and the stirrups in the beams at midspan. A second line of instruments was located at the quarter-span (Figure 3.6) in an attempt to quantify the amount of rotational restraint at the ends of the span. The moments along the two lines of instrumentation can be calculated from the measured strains, and then the end moments can be calculated from statics. Figures 3.7 and 3.8 show the exact location of the concrete gages placed on the curbs and the reinforcing bars that were instrumented.

Twenty-five strain gages and five displacement transducers were located near midspan and twenty strain gages were located at the quarter-span. Figure 3.9 contains a photograph of both lines of instruments; midspan is denoted by the black stains on the surface of the concrete. The strain gages were divided into three groups based on the placement: (a) on the surface of the reinforcing bars, (b) on the surface of the concrete near the curbs, and (c) on the surface of the concrete on the crowns. Each of these groups is discussed in the following sections.

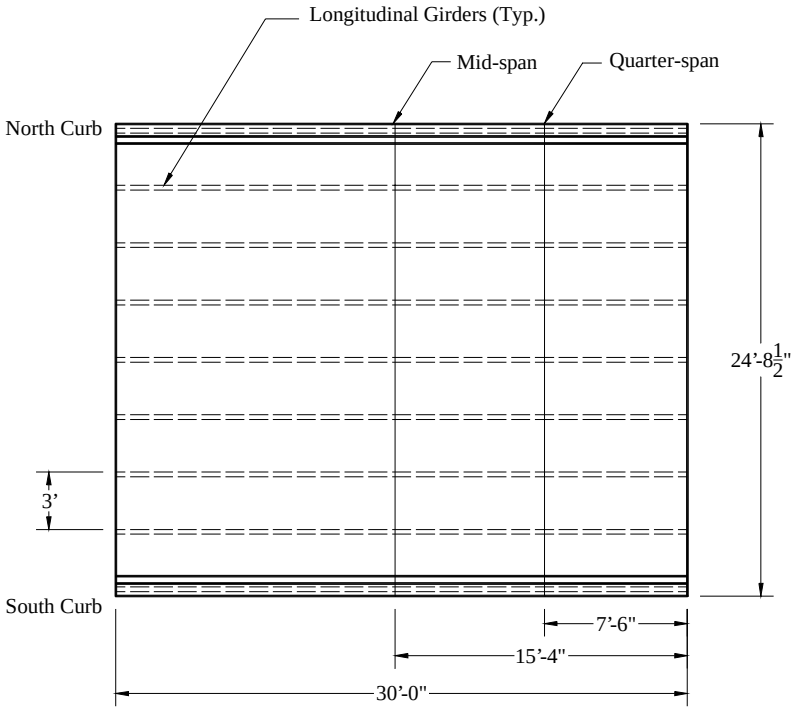

Figure 3.4 Plan View of Span Indicating Locations of Instruments

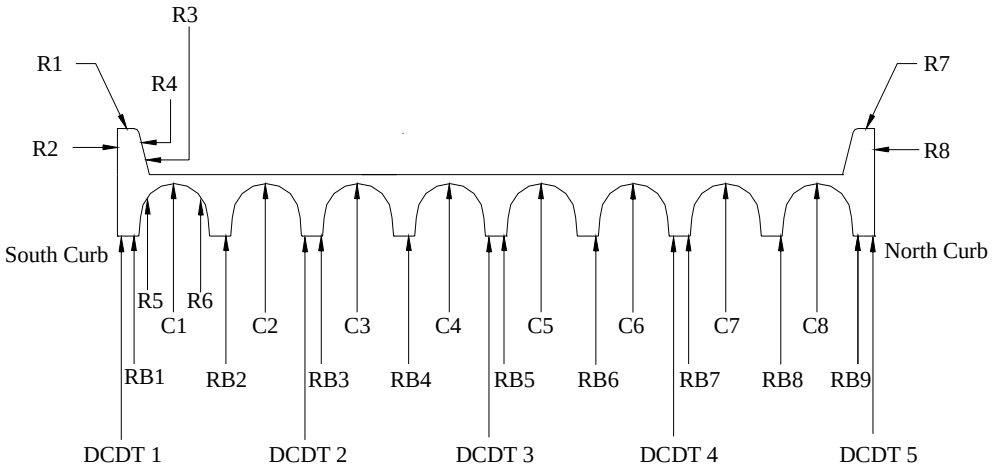

RB# - 6 mm foil strain gages attached to reinforcing bars
C# - 60 mm wire strain gages attached to the surface of the concrete in the crowns
R# - 60 mm wire strain gages attached to the surface of the concrete curbs
DCDT# - Displacement transducers attached to the bottom of the longitudinal girders

Figure 3.5 Location and Identification of Instruments at Midspan

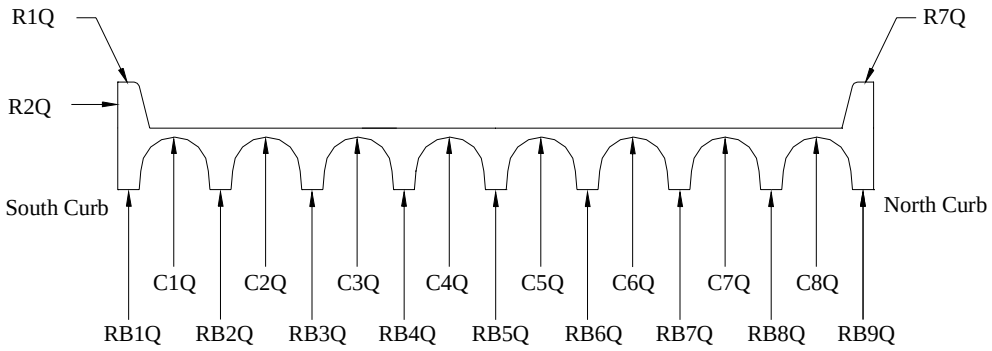

RB#Q - 6 mm foil strain gages attached to reinforcing bars
C#Q - 60 mm wire strain gages attached to the surface of the concrete in the crowns
R#Q - 60 mm wire strain gages attached to the surface of the concrete curbs

Figure 3.6 Location and Identification of Instruments at Quarter-span

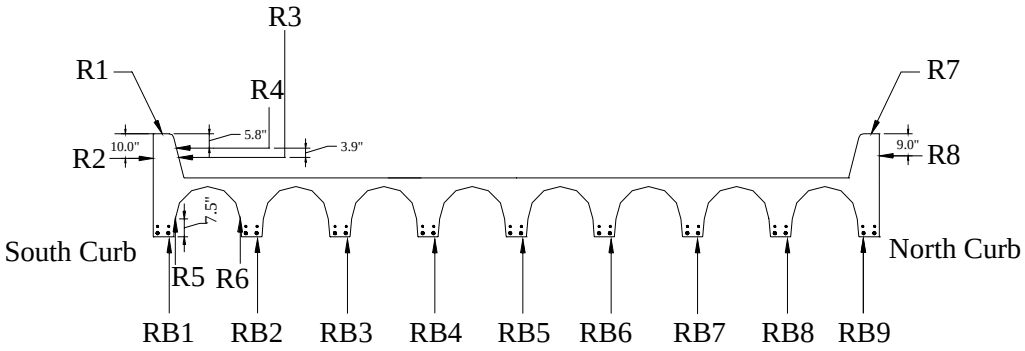

Figure 3.7 Exact Location of Curb Gages and Reinforcing Bar Gages at Midspan

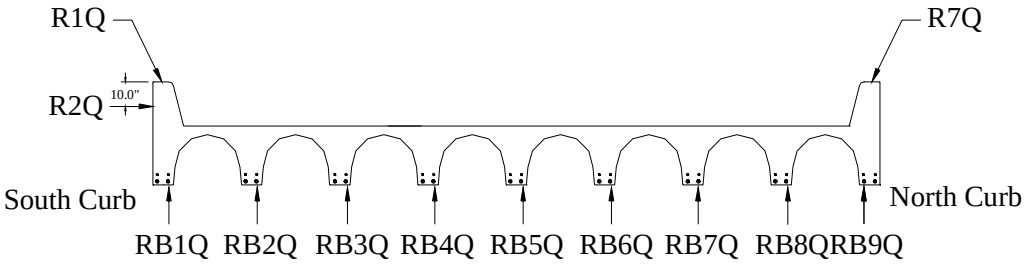

Figure 3.8 Exact Location of Curb Gages and Reinforcing Bar Gages at Quarter-Span

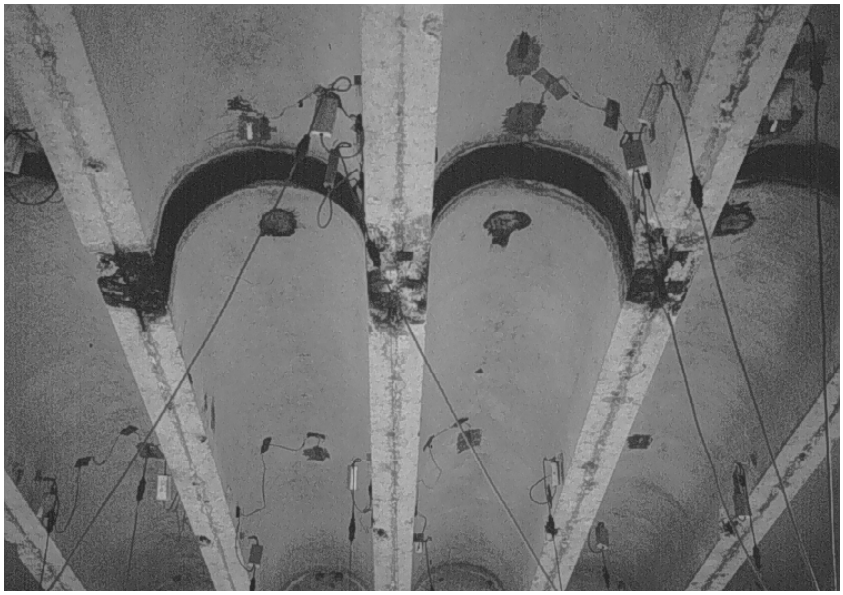

Figure 3.9 Instrumentation of Midspan and Quarter-Span

3.2.1 Strain Gages Attached to Surface of Reinforcing Bars

A total of nine, #11 reinforcing bars (one per girder), were instrumented with 6 mm foil strain gages, similar to the gage shown in Figure 3.10. As shown in Figures 3.5 and 3.6, the nine reinforcing bars were instrumented at the mid- and quarter-points accordingly.

In order to instrument each reinforcing bar, a volume of concrete approximately 4 x 6 x 2 in. was removed, as shown in Figure 3.11. The surface of the reinforcing bar was then ground until a flat surface was obtained. Next, the bar was cleaned with acetone to remove any dirt from the surface of the bar. The foil gage was then glued on the bar with a special adhesive. In order to weatherproof the foil gage, white acrylic and silicone rubber were placed on top of the gage.

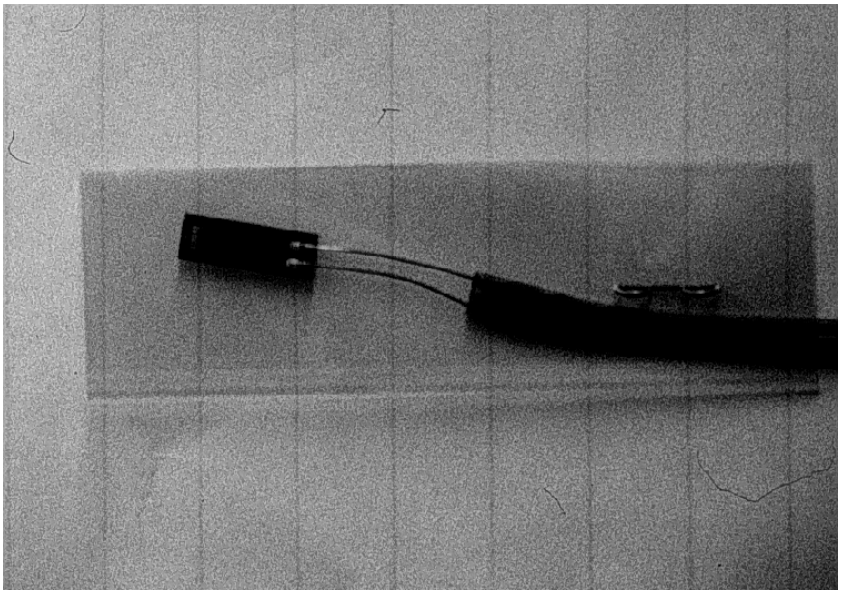

Figure 3.10 Foil Strain Gages for Reinforcement Bars

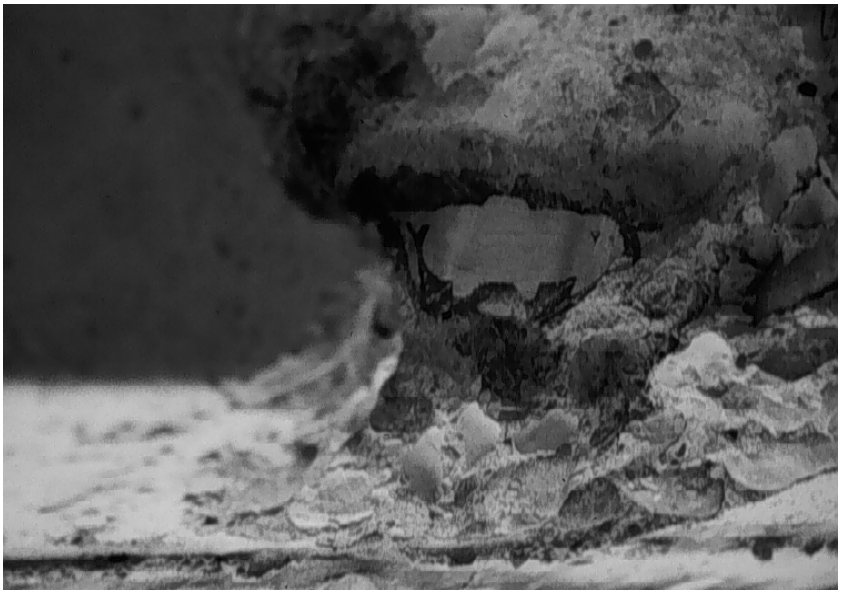

Figure 3.11 Exposed Reinforcing Bar at Midspan

3.2.2 Strain Gages Attached to Surface of Concrete

Twenty-seven 60 mm wire strain gages, similar to the one in Figure 3.12, were used to measure strain on the concrete surface. Like the strain gages attached to the reinforcing bars, these gages were placed at midspan and quarter-span. At each of these locations, wire strains gages were placed on the crowns and on the curb.

The surface of the concrete needed to be prepared before a wire strain gage was attached. Devcon 5-minute Epoxy was placed over the location where the gage was to be mounted. After the epoxy cured, it was sanded until a smooth surface was obtained. The purpose of the epoxy was to fill any voids located on the surface of the concrete so that the strain gage adhered to a continuous surface. The smoothed surface was then cleaned with water and dried. At this time, the strain gage was mounted with the same glue as used for mounting the reinforcing bar gages. The gages were weatherproofed with white acrylic and silicone rubber.

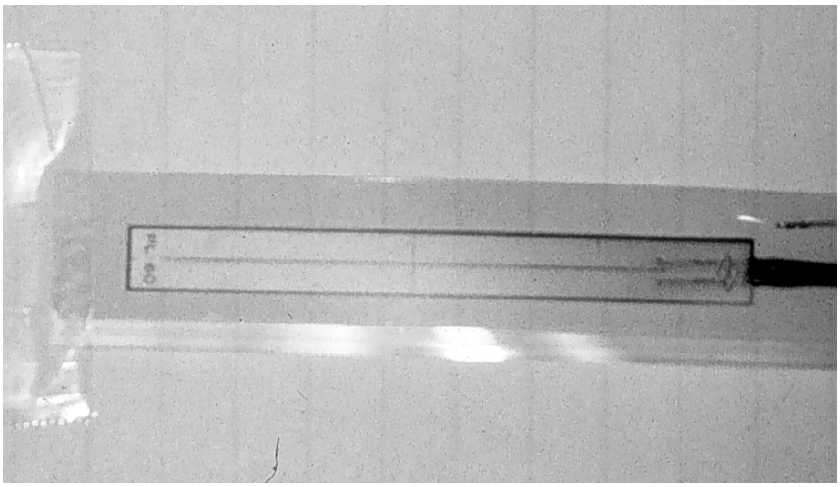

Figure 3.12 Wire Strain Gages for Concrete

3.2.2.1 Wire Strain Gages placed on the Curbs

Wire strain gages were placed on the curbs at midspan and the quarter-span. One gage was placed on the top surface of the curb at all four locations, as shown in Figures 3.5 and 3.6. A gage was also placed on the outside surface of the south curb at the mid- and quarter-spans and on the north curb at midspan. In addition, two gages were positioned on the inside surface of the south curb at midspan, and two gages were located beneath the slab between the south exterior and first interior girder at midspan. Information from these gages was used to determine the neutral axis depth in the exterior girders and to determine if the exterior girders were subjected to torsion, in addition to flexure.

3.2.2.2 Wire Strain Gages placed on the Crowns

In addition to placing wire strain gages on the curbs, gages were placed on each crown at midspan and quarter-span. These gages were placed immediately adjacent to the longitudinal cracks located at the top of the interior crowns.

3.2.3 Displacement Transducers

Direct Current Differential Transformers (DCDT) were used to monitor the vertical deflection response of the bridge. Five DCDTs were located at midspan (Figure 3.5). Figure 3.13 shows a DCDT during the test. The DCDT was clamped to a rod that was anchored in the ground. The core of the DCDT was attached to fishing wire, which was connected to the bottom of the girder. A weight was suspended from the bottom of the core in order to keep the fishing wire taut.

Figure 3.13 DCDT Mounted on Rod

3.2.4 Data Acquisition System

A Campbell Scientific CR9000 data acquisition system (Figure 3.14) was used to collect data during the test. This data acquisition system was configured so that 55 channels could be recorded simultaneously.

The system was designed such that five instruments were connected to a single junction box. Cables from eleven junction boxes attached directly to the CR9000. The advantage of the junction boxes was that they reduced the number of cables running from the individual instruments to the data acquisition system. Figure 3.15 shows two rows of cables suspended from the bottom of the bridge deck. The acquisition frequency for semistatic runs was 10 Hz, and for dynamic runs, the frequency was 100 Hz. The data acquisition system represents a significant improvement from the Campbell Scientific 21X Micrologger used in previous studies [7], which had a capacity of 8 channels.

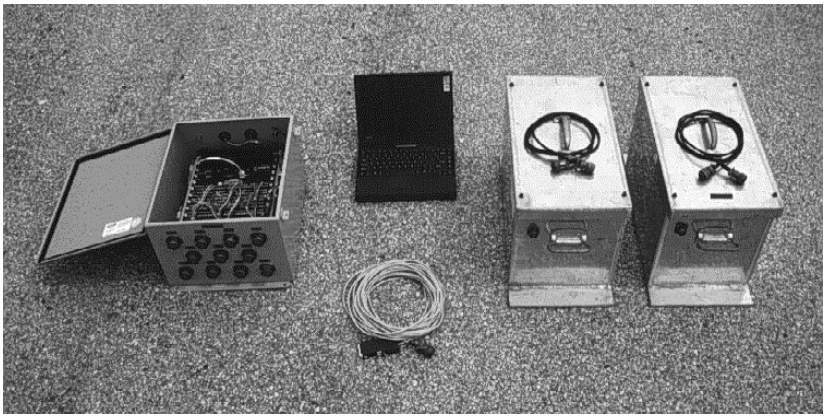

Figure 3.14 Campbell Scientific CR9000 Data Acquisition System

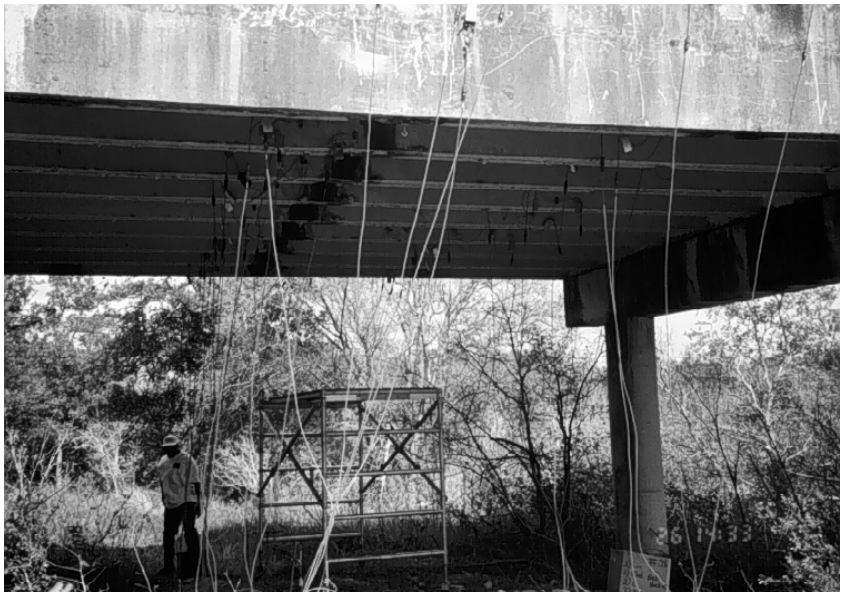

Figure 3.15 Cables Suspended from Bottom of Bridge

3.2.5 Problems with Installation of Instrumentation

Installation of the strain gages was time consuming. Five researchers installed the gages over a two-day period. Most of the gages were located on the bottom of the bridge, and the researchers used scaffolding for access. Removal of the concrete to expose the reinforcing bars was particularly laborious. Additional problems were encountered in instrumenting the crowns with wire strain gages. Placement of epoxy and sanding of the cured epoxy at the top of the crown were difficult due to the curvature of the crown and because curved tools were not available.

The flow of traffic made placing the strain gages on the top of the curb difficult and unsafe because the bridge did not have a shoulder and the bridge traffic was quite high. The researchers wore traffic vests to caution drivers to slow down.

3.3 LOAD TESTS

This section summarizes the load test and describes the loading vehicles. The test was performed on 26 March 1998, and it represents the third test of this bridge by the research team.

3.3.1 Loading Vehicle

The two loading vehicles used for the diagnostic load test were provided by the TxDOT maintenance office in San Marcos, Texas. The trucks were ten-cubic-yard dump trucks filled with roadway base material and weighed approximately 43 kips each. Figure 3.16 shows a view of one of the trucks, and Figures 3.17 and 3.18 show the dimensions and axle weights of the two vehicles.

Figure 3.16 TxDOT Loading Vehicle

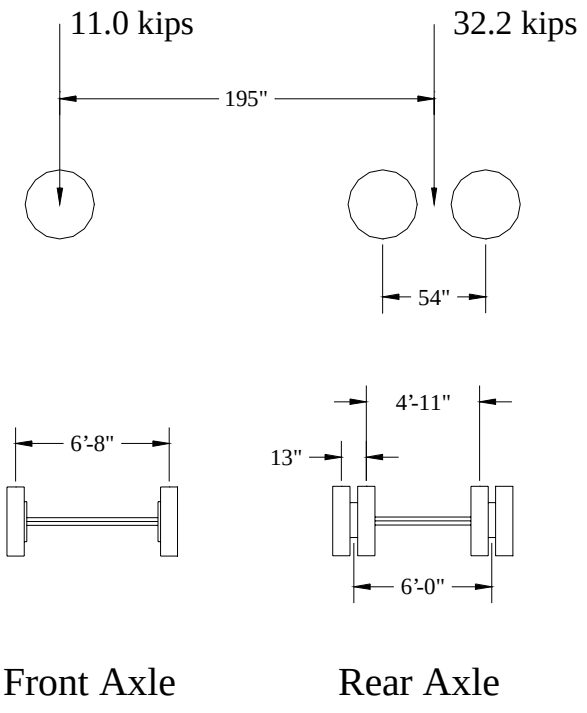

Figure 3.17 Sketch of Configuration of Truck 1

In order to determine the distribution of load among the girders, the loading vehicles were driven across the bridge in five transverse positions (Figure 3.19). The nominal wheelbase of the trucks was six feet, which corresponds to the distance between alternate girders. Five truck positions corresponded to the placement of the wheel lines directly over the girders. When a single loading vehicle, Truck 1, was used, it was located adjacent to the north curb in truck location 1. The transverse location of a single loading vehicle was shifted south by three feet in subsequent positions.

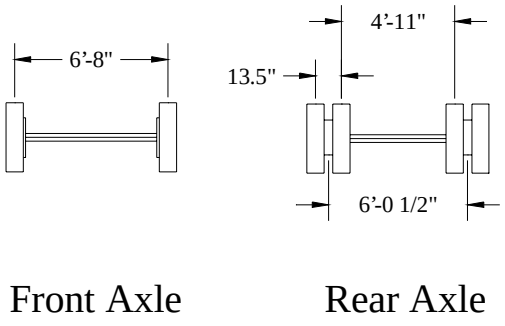

Figure 3.18 Sketch of Configuration of Truck 2

The bridge was loaded with the loading vehicle traveling at two speeds. In the first three test series, the truck speed was approximately five miles per hour. This speed was selected to minimize the influence of impact on the measured response of the bridge. The last two test series were conducted at a speed of approximately thirty miles per hour. This speed was selected to observe the influence of impact on the bridge and evaluate any dynamic amplification that may occur.

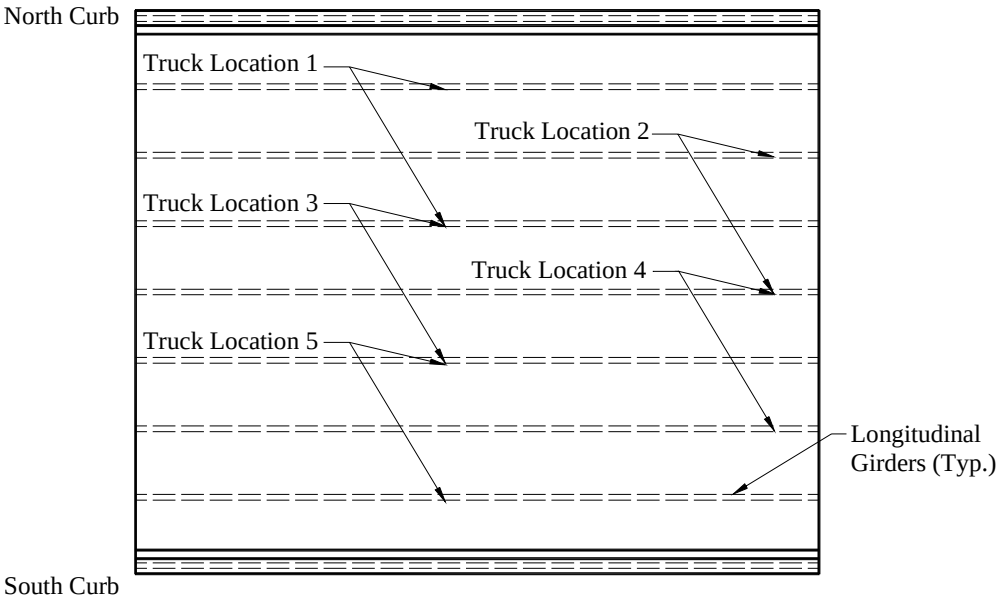

Figure 3.19 Transverse Positioning of Loading Vehicle

3.3.2 Test Series

The measured data were organized in five test series. The primary test parameters included the transverse truck position, the number of loading vehicles, and the speed of the loading vehicles. Table 3.2 lists the five test series and the corresponding testing parameters. Two trucks were used during Test Series 1. Data from Test Series 1 were used to determine if the bridge responded symmetrically to a symmetric loading condition. In addition, data from subsequent tests with a single truck, Truck 1, could be compared with data from Test Series 1 to determine if superposition was applicable. A single truck was used in Test Series 2 through 5. The trucks traveled westward across the instrumented span in Test Series 1, 2, 4, and 5 and eastward in Test Series 3. Vehicle speeds were 5 mph in Test Series 1, 2, and 3, and data from all 50 instruments were recorded. Truck 1 traveled at 30 mph in Test Series 4 and 5, and only five instruments were monitored in these tests. A smaller number of channels were monitored in the higher-speed tests to allow a sampling frequency of 100 Hz. The truck crossed the bridge two times in each transverse location in order to evaluate the repeatability of the measured data.

Table 3.2 Description of Test Series

Test Series	# of Loading Vehicles	Speed mph	Instruments	Direction of Travel	Truck Locations	# of Passes
1	2	5	All	Westbound	1, 5	2
2	1	5	All	Westbound	1, 2, 3, 4, 5	2
3	1	5	All	Eastbound	1, 2, 3, 4, 5	2
4	1	30	R1,R2,R3 R4, RB1	Westbound	1, 2, 3, 4, 5	2
5	1	30	RB3, RB4 RB5, C3,C4	Westbound	1, 2, 3, 4, 5	2

3.3.3 Test Procedure

The load test was conducted on 26 March 1998. Six researchers arrived around 8:00 a.m. to set up all of the instruments. The first task to be completed was to connect the forty-five completion boxes to the strain gages. A scaffold was used to make the connections underneath the bridge. While a couple of researchers were making these connections, others were mounting the displacement transducers. Once all of the instrumentation was connected and the TxDOT assistants arrived, the top of the bridge deck was marked so that the wheel lines of the loading vehicle were directly over the girders. In order to mark the bridge, traffic control was necessary and was controlled by two team members with traffic control flags. One was situated on the west end of the bridge, and the other was on the east end of the bridge. Once traffic was stopped, the roadway was marked with an inverted marker. Five lines were marked as the five transverse loading positions required for determining the distribution of load. Additionally, these lines were marked over a one-hundred-foot length. After about three hours, everything was connected and marked, and the load test was ready to begin.

Prior to starting the test, the bridge had to be cleared of all traffic, and thus required the assistance of traffic controllers, as shown in Figure 3.20. Traffic was free to flow once the rear axle of the loading vehicles exited the testing region. This region was composed of three spans and was approximately one hundred feet long. Figure 3.21 shows the distance and spans over which measurements were taken. The test was started when the front axle of the loading vehicle was a few feet east of Span 1 and was stopped when the rear axle exited Span 3. The loading vehicle would then travel about 250 ft. to turn around. Figure 3.22 shows the two loading vehicles in position for Test Series 1, while Figure 3.23 shows the loading vehicle traveling eastbound in Test Series 3. The average time for each run was two minutes, while the average time for each test series was 30 minutes.

Figure 3.20 Traffic Control during Test

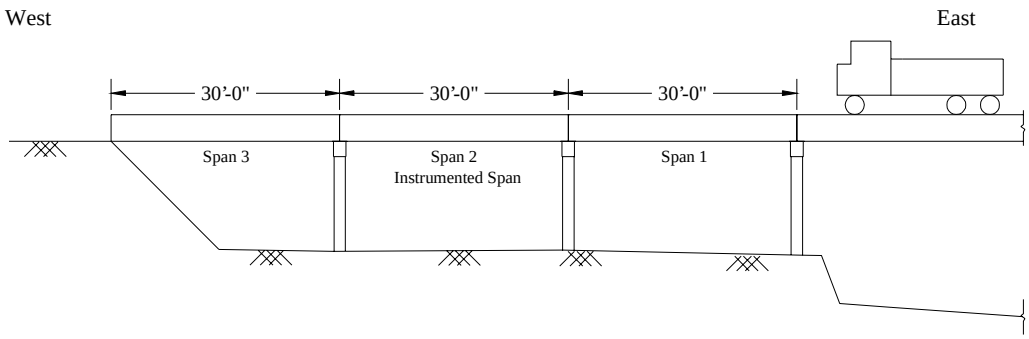

Figure 3.21 Distance Traveled during Test

Figure 3.22 Loading Vehicles in Test Series 1

Figure 3.23 Test Series 3 in Progress

3.3.4 Problems Encountered during Testing

Only one problem was encountered during testing. The problem was the traffic because the test could not be started until the bridge traffic was cleared. Other than the traffic, the test proceeded rather quickly because of the new data acquisition system. The test took about 2.5 hours to complete; a significant reduction in time compared with previous tests using the old data acquisition system. The new data acquisition system saved about eight hours.

CHAPTER 4: MEASURED RESPONSE OF BRIDGE

This chapter presents the measured response of the pan-girder bridge during a diagnostic load test conducted on 26 March 1998. A total of three load tests were conducted on this bridge. Table 4.1 shows the date, the data acquisition system used, and the number of strain gages and displacement gages used during the three load tests. Emphasis is placed on the instrumentation and results from Load Test 3 because of problems encountered during Load Tests 1 and 2.

Table 4.1 Summary of Diagnostic Load Tests Performed on Pan-Girder Bridge

Test	Date	Data Acquisition System	Number of Instruments				
			Foil Strain Gages*	Wire Strain Gages**	Linear Pots	String Pots	DCDTs
1	7/1/97	21X	11	15	5	5	0
2	9/8/97	21X	4	16	0	0	0
3	3/26/98	CR9000	18	27	0	0	5

* Attached to Surface of Reinforcing Bars
** Attached to Surface of Concrete

The measured response of the bridge is divided into four groups based on the type and the location of the instrument. Each group contains data taken at midspan and at one-quarter of the span. The first group summarizes the results obtained from foil strain gages attached to the longitudinal reinforcing bars located near the bottom of the girders. The second group is the measured response of wire strain gages attached to the concrete surface of the curb and directly underneath the curb. The third and fourth groups present the measured response from wire strain gages attached to the crowns and DCDTs connected to the bottom of the girders, respectively. The complete response histories of all instruments obtained during Load Test 3 are presented in Appendices A through G. The data represent live-load effects.

All response histories are plotted as a function of the centroid of the rear axles. In order to find the location of the centroid, the truck driver made an attempt to traverse the bridge at a constant velocity so that the position of the centroid could be interpolated from two measured data points. Data collection for Test Series 1, 2, 4, and 5 started when the front axle was approximately fifteen feet east of Span 1 and ended when the rear axle exited Span 3 (Figure 4.1). The direction of the truck was reversed in Test Series 3. Therefore, data collection began when the truck was approximately fifteen feet west of Span 3 and ended when the truck exited Span 1.

The location of the centroid of the rear axles shown in the response histories corresponds to 20 ft. before entering the instrumented span from and 10 ft. after exiting the instrumented span. The reason for selecting this range of positions for plotting was that the measured response was essentially zero when the truck was outside this range. Therefore, the centroid of the rear axles was within the instrumented span when the centroid was positioned between 0 and 30 ft.

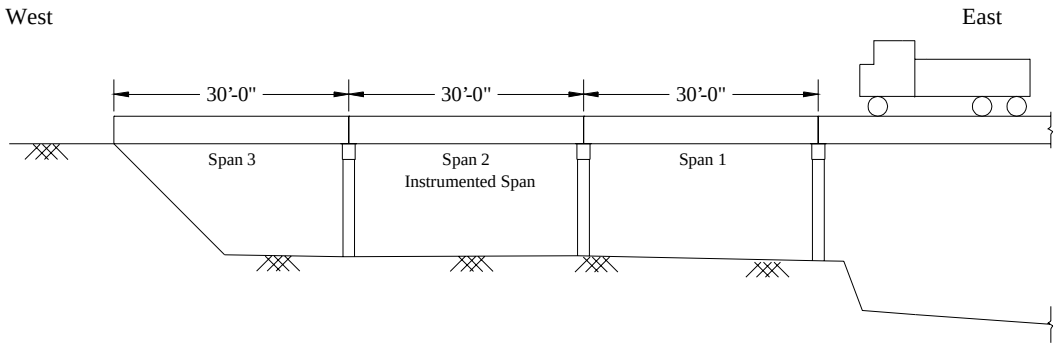

Figure 4.1 Distance Traveled during Test

4.1 DATA REDUCTION

Throughout this report, tensile strains and upward displacements are considered to be positive. The following sections discuss trends observed in the response histories of the gages and the procedure by which readings were considered reliable or unreliable.

4.1.1 Ambient Effect on Gages

In Load Tests 1 and 2, the data collected during each pass were set to zero immediately before the truck entered the test area. For Load Test 3, zero readings were established at the beginning of the first run, and the readings for subsequent runs were not adjusted during the tests. Zeroing of the readings is done so that all response histories can be compared directly with one another.

The readings in Load Test 3 were not zeroed in order to assess the influence of temperature and/or long-term drift on the behavior of the gages. In assessing the ambient effect on the gages, measurements from four gages, R2, R8, RB1, and DCDT 1, were plotted as a function of time. Figures 4.2 through 4.5 show how each gage drifted throughout the day. These figures are representative of other gages in similar locations on the span. The x-axis represents the actual clock time when the readings were taken, which shows that the gages were read intermittently for about 1-½ hours. The y-axis represents the range throughout which strain readings were obtained. Figures 4.2 through 4.4 have the same strain range in order to compare the degree of drift between the three gages. The long thin peaks shown in the plots are the maximum strains for each reading, and emphasis should be placed at the strain level where each gage initially begins. Figure 4.2 shows the readings from strain gage R2. Strain gage R2 is located on the outside face of the south curb, i.e. facing the sun, while strain gage R8 is located on the outside face of the north curb, i.e. in the shade. As shown, there is a large variation in the degree of drift when comparing the behavior of the two gages. The figures indicate that gages exposed to direct sunlight experienced more drift than gages in the shade. A possible explanation for the cause of the significant drift is the combination of the variation of the restraint at the supports and the temperature variations. Because the supports of the instrumented span are restrained by the adjacent spans, temperature contributes to the elongation or contraction of the strain gage, and thus possibly the cause in the drifting of the gages. The oscillating nature of the two plots could be due to sporadic cloud cover during the day.

Strain gage RB1 was located on a reinforcing bar under the bridge. Figure 4.4 shows minimal drifting in the gage readings. Figure 4.5 shows the displacement readings from a DCDT located underneath gage RB1. This figure shows that all readings begin near zero.

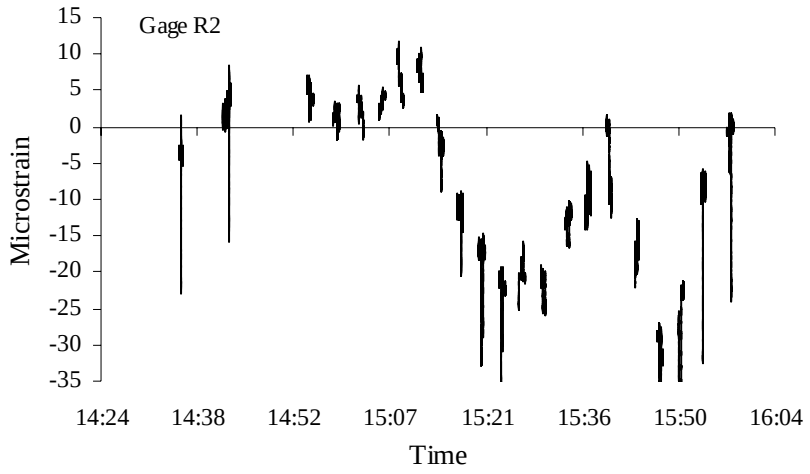

Figure 4.2 Drift in Wire Strain Gage Exposed to Sunlight, Test Series 1 through 3

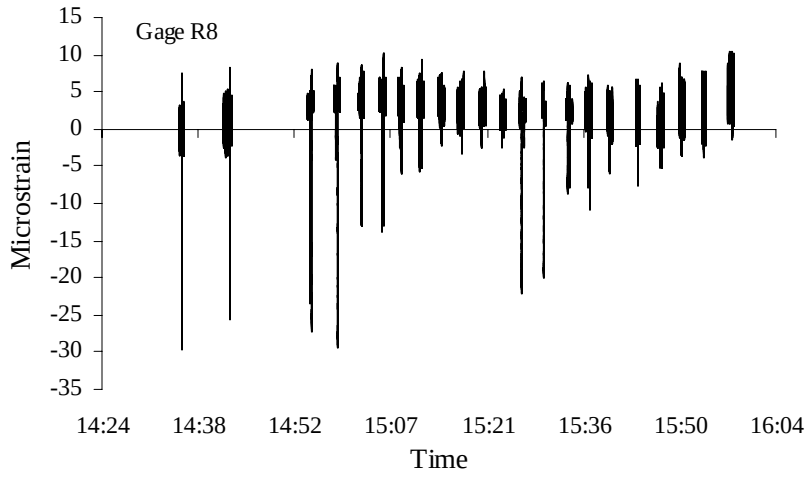

Figure 4.3 Drift in Wire Strain Gage not Exposed to Sunlight, Test Series 1 through 3

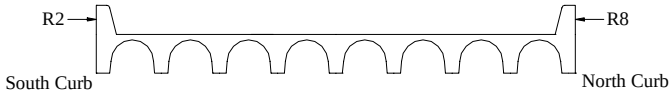

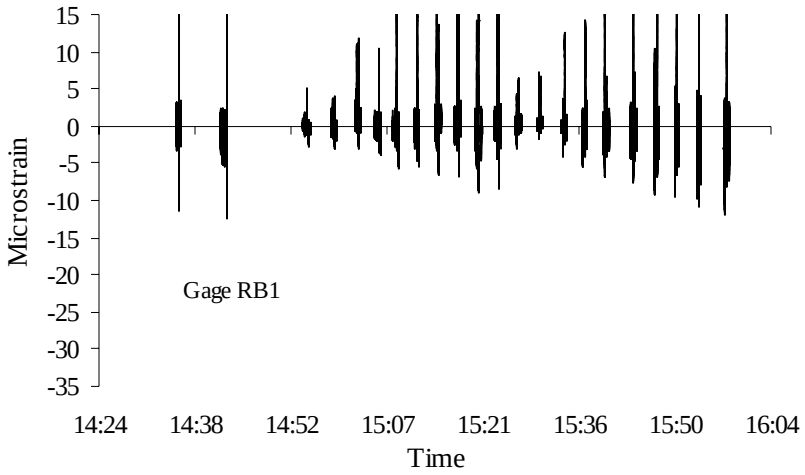

Figure 4.4 Drift in Foil Strain Gage, Test Series 1 through 3

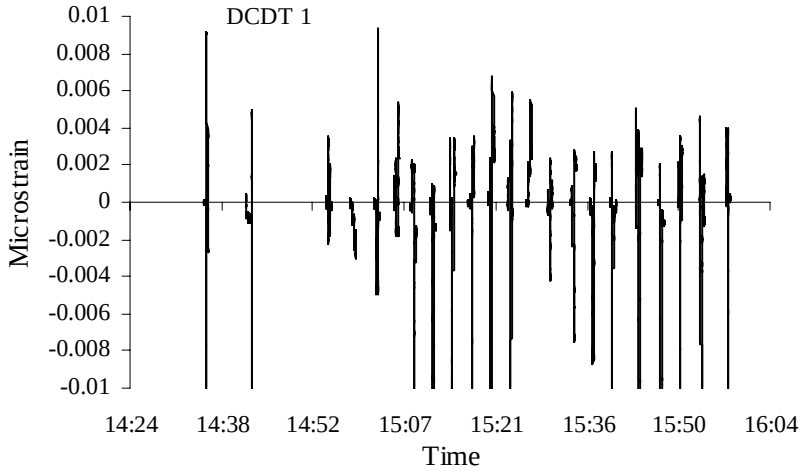

Figure 4.5 Drift in DCDT, Test Series 1 through 3

Each response history for each gage was plotted and adjusted so the readings began at zero. The data were shifted by a constant value so the initial data points began at zero. For example, Figure 4.6 shows the unadjusted response history for gage RB1 obtained during pass 1 of truck location 4 in Test Series 2. The figure shows the data to begin at approximately –8 microstrains. Therefore, adding 8 microstrains to all values shifts all data points so the initial data points begin at zero. Figure 4.7 shows the adjusted response history.

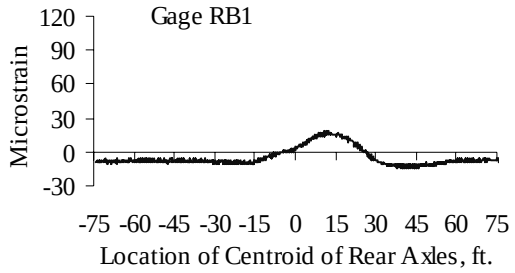

Figure 4.6 Unadjusted Response History for Gage RB1

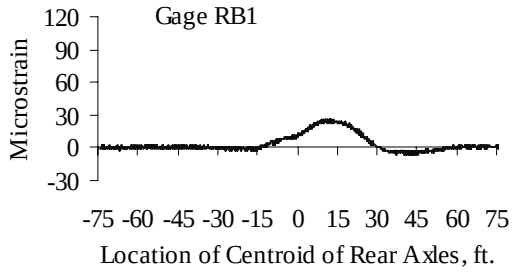

Figure 4.7 Adjusted Response History for Gage RB1

4.1.2 Reliability of Readings

Once this shift was performed on all readings, the behavior of each instrument as a function of rear axle location was analyzed to determine the reliability of the data. Two approaches were used to identify reliable data. A response history in which the initial and final values were the same two satisfied the first approach. Figure 4.8 shows a reading for gage R1. As shown, the final strain data values at a location of 75 ft. are very close to the initial strain data values located at –75 ft. This response history is considered reliable and used to compare with other readings.

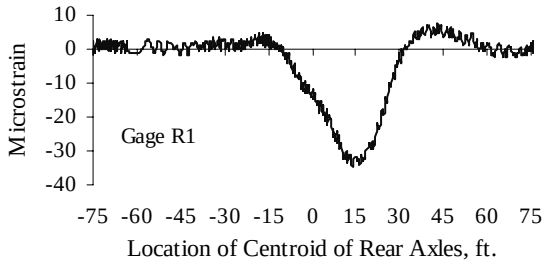

Figure 4.8 Response History for Gage R1 during Test Series 2, Truck Location 5, Pass 1

Response histories which tended to drift linearly with time were not considered to be ideal but appeared to be reliable. Figure 4.9 depicts the response history of gage R1 during a different run. The strain data at the end of the test display a permanent offset of approximately –5 microstrain. If all the points in the response history were adjusted by an equation that was a function of longitudinal truck location, then the adjusted response history would resemble the behavior of Figure 4.8. Therefore, this response history

was considered reliable. In addition, the downward shift of the response history overestimated the maximum compression strain readings, which should lead to conservative results.

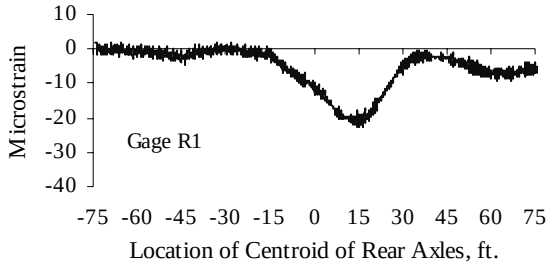

Figure 4.9 Response History for Gage R1 during Test Series 2, Truck Location 4, Pass 1

An example of a response history considered to be unreliable is shown in Figure 4.10. This figure shows how the response history of gage R1 does not resemble the other two histories. Readings similar to this one, as well as those that produced unconservative results were considered unreliable; and therefore, were not used in the analysis of the bridge behavior.

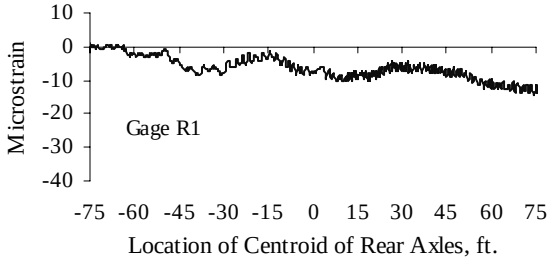

Figure 4.10 Response History for Gage R1 during Test Series 2, Truck Location 2, Pass 1

All data are presented in the following sections, and the data have been adjusted according to the procedures presented above.

4.2 STRAINS MEASURED ON THE SURFACE OF REINFORCING BARS

A total of 18 foil strain gages were placed on the #11 longitudinal reinforcing bars. Each bar contained two strain gages: one at midspan and the other at one quarter of the span. The data collected from strain gages located at midspan are presented first, followed by data collected from strain gages located at quarter-span. The strains were measured and are presented in microstrains.

4.2.1 Foil Strain Gages Located at Midspan

Nine gages were attached to the reinforcing bars at midspan. The complete response histories for foil strain gages located at midspan are presented in Reference 11. All nine gages were monitored during Test Series 1 through 3, and their maximum strains are reported in Table 4.2. Strain gage RB1 was also monitored during Test Series 4, and strain gages RB3, RB4, and RB5 were monitored in Test Series 5. Test Series 1 through 3 were conducted at a truck speed of 5 miles per hour, whereas Test Series 4 and 5 were conducted at a speed of 30 miles per hour. The maximum strains for Test Series 4 and 5 are presented in Table 4.3.

Table 4.2 Maximum Strains Measured on the Surface of Reinforcing Bars at Midspan for Test Series 1 through 3, Microstrain

Test Series	Truck Location	Pass	Gage Identification								
			RB1	RB2	RB3	RB4	RB5	RB6	RB7	RB8	RB9
1	1 & 5	1	59	92	104	142	145	137	129	109	52
		2	55	90	146	146	159	137	128	106	50
2	1	1	5	6	8	17	43	80	101	87	52
		2	4	5	8	15	37	71	102	88	55
	2	1	12	11	16	39	84	93	105	76	32
		2	10	11	16	39	81	94	102	74	31
	3	1	17	20	33	84	100	90	82	37	20
		2	17	21	33	83	100	91	84	37	20
	4	1	27	43	71	112	101	71	40	20	13
		2	28	43	73	113	102	72	38	20	14
	5	1	45	78	88	106	77	30	17	11	8
		2	45	78	91	106	77	30	17	11	7
3	1	1	7	7	10	23	59	91	100	86	40
		2	7	8	11	25	62	92	101	88	39
	2	1	13	15	22	63	99	93	96	46	22
		2	14	17	24	65	101	93	95	47	22
	3	1	21	31	57	108	100	83	50	24	14
		2	21	31	54	106	100	84	52	26	14
	4	1	34	62	86	104	98	46	24	14	9
		2	33	63	88	105	96	45	24	15	9
	5	1	63	91	87	104	52	19	12	9	5
		2	61	92	88	107	55	20	12	9	4

Table 4.3 Maximum Strains Measured on the Surface of Reinforcing Bars at Midspan for Test Series 4 and 5, Microstrain

Test Series	Truck Location	Pass	Gage Identification			
			RB1	RB3	RB4	RB5
4	1	1	9			
		2	8			
	2	1	14			
		2	16			
	3	1	25			
		2	27			
	4	1	32			
		2	33			
	5	1	56			
		2	56			
5	1	1		12	24	55
		2		11	24	53
	2	1		20	48	94
		2		22	51	91
	3	1		48	106	113
		2		48	106	111
	4	1		79	114	98
		2		80	111	97
	5	1		87	109	66
		2		89	114	61

Strain data recorded during the first pass of truck location 1 for Test Series 2 are shown in Figure 4.11. These strain data are representative of the response obtained for all foil strain gages monitored during all test series. The response histories show the influence of the truck position on the strain data. As shown in Figure 4.11, most of the reinforcing bar response histories are characterized by two peaks corresponding to when the front axle is located at midspan and when the centroid of the rear axles is at midspan. The peaks are more pronounced in girders directly below wheels. These peaks are not observed in strain gages RB1 and RB9, which are located underneath the curbs. The response histories also indicate tensile strains in the reinforcing bars while the truck is located on the instrumented span, but when the truck is on an adjacent span, a reversal in strain is observed. This strain reversal indicates some transfer of load between adjacent spans and thus continuity at the supports.

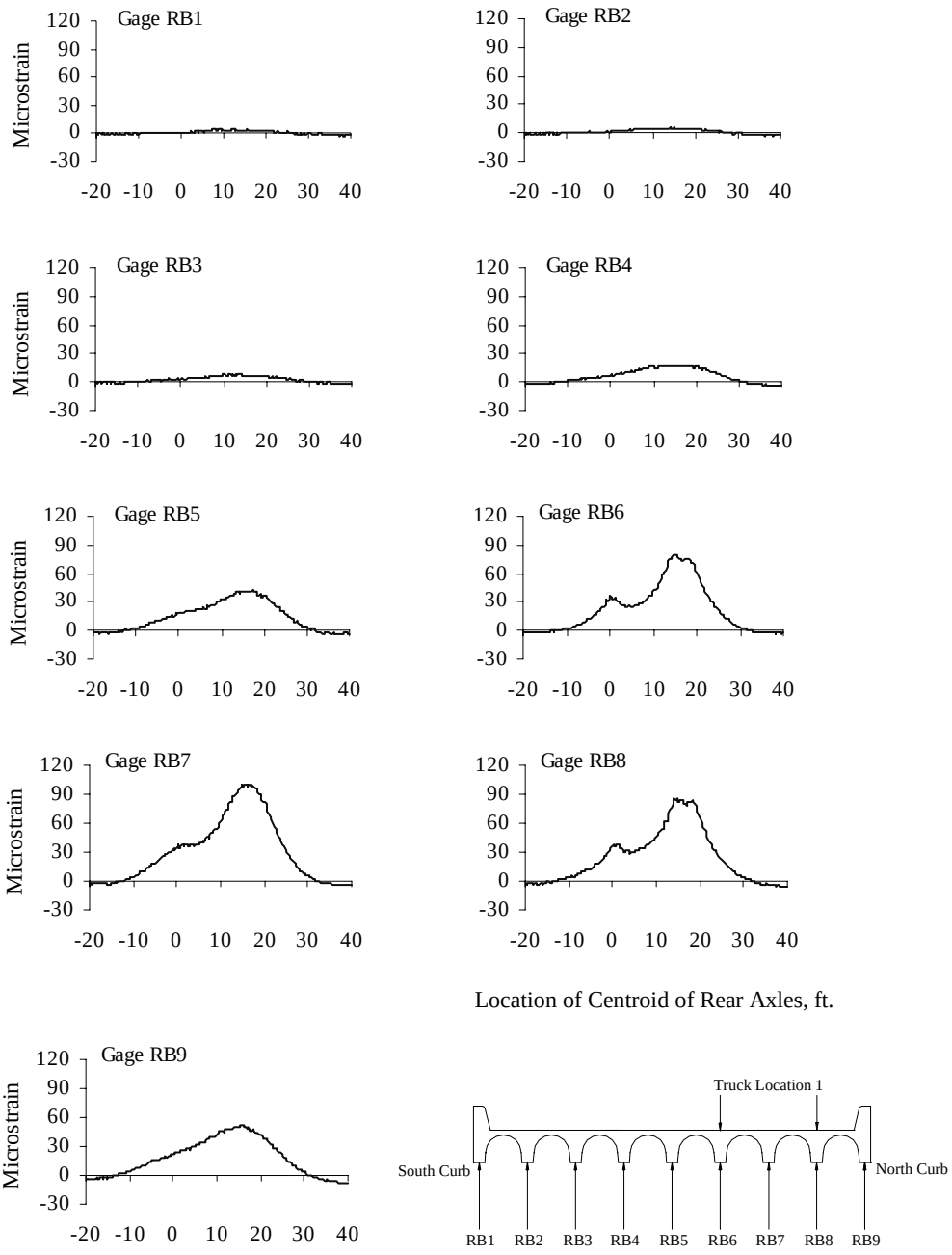

Figure 4.11 Reinforcing Bar Strains at Midspan, Test Series 2, Truck Location 1, Pass 1

Profiles of the maximum strains recorded for the five transverse positions in Test Series 1, 2, and 3 are shown in Figures 4.12, 4.13, and 4.14, respectively. These figures show how the distribution of strains corresponds to the truck location. The profiles from Test Series 2 and 3 have similar patterns, but the peaks of one test series do not always correspond with the peaks of the other.

Figure 4.15 shows the profiles of the maximum strains recorded during Test Series 4 and 5. The maximum strain occurs when the wheel lines are centered around the strain gage. For example, strain gage RB3 has a maximum strain during truck location 5, which corresponds to a wheel line on each girder

adjacent to strain, gage RB3. The maximum strains from the runs conducted at 30 mph are compared with those runs conducted at 5 mph in Figure 4.16. The increase in strain due to dynamic loading conditions on the bridge was found to be equal to or 10% greater than strains measured from the semistatic loading conditions for the majority of the loading cases.

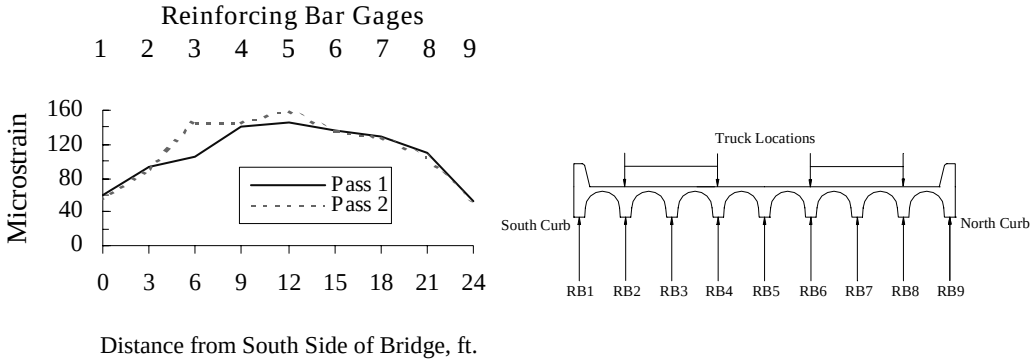

Figure 4.12 Profile of Maximum Reinforcing Bar Strains at Midspan for Test Series 1

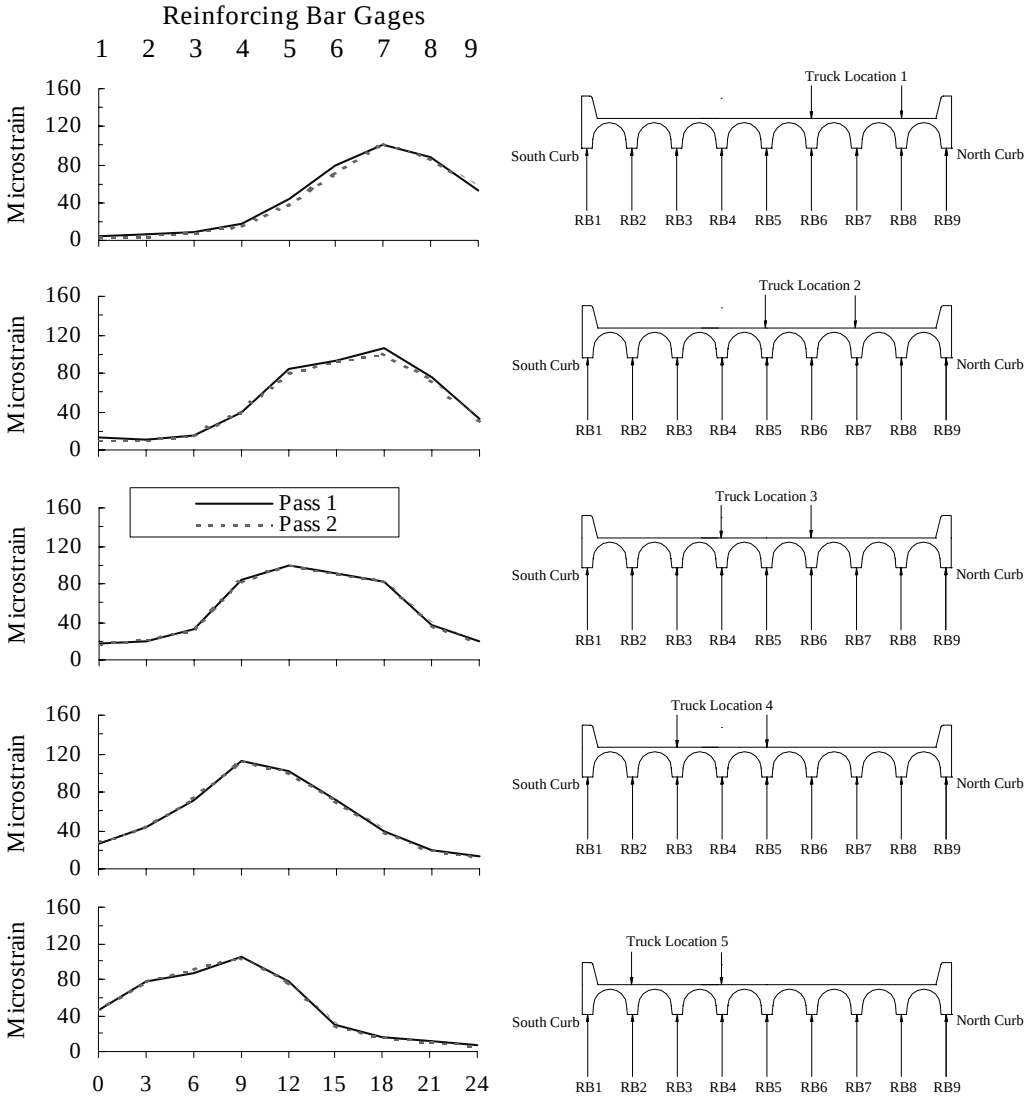

Figure 4.13 Profiles of Maximum Reinforcing Bar Strains at Midspan for Test Series 2

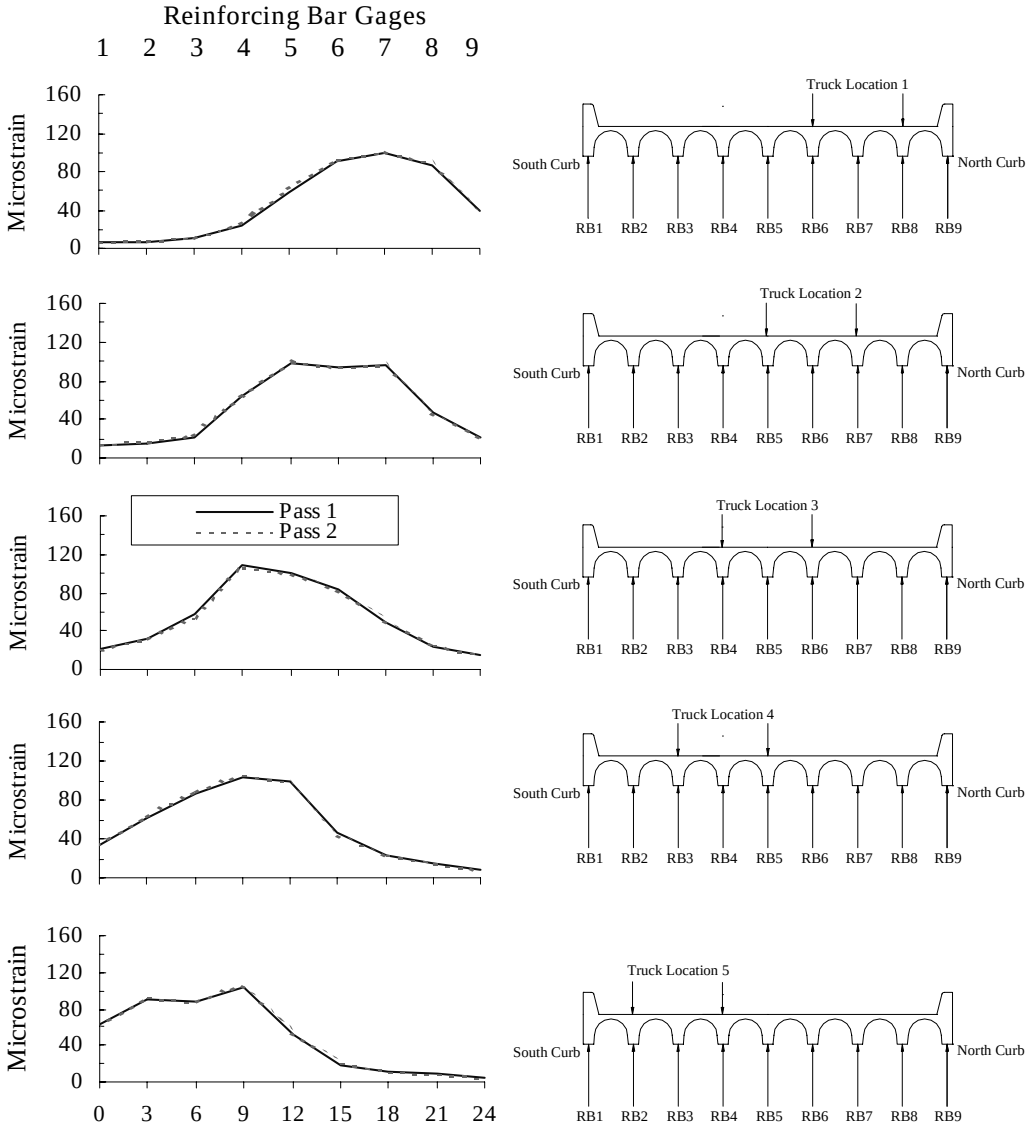

Figure 4.14 Profiles of Maximum Reinforcing Bar Strains at Midspan for Test Series 3

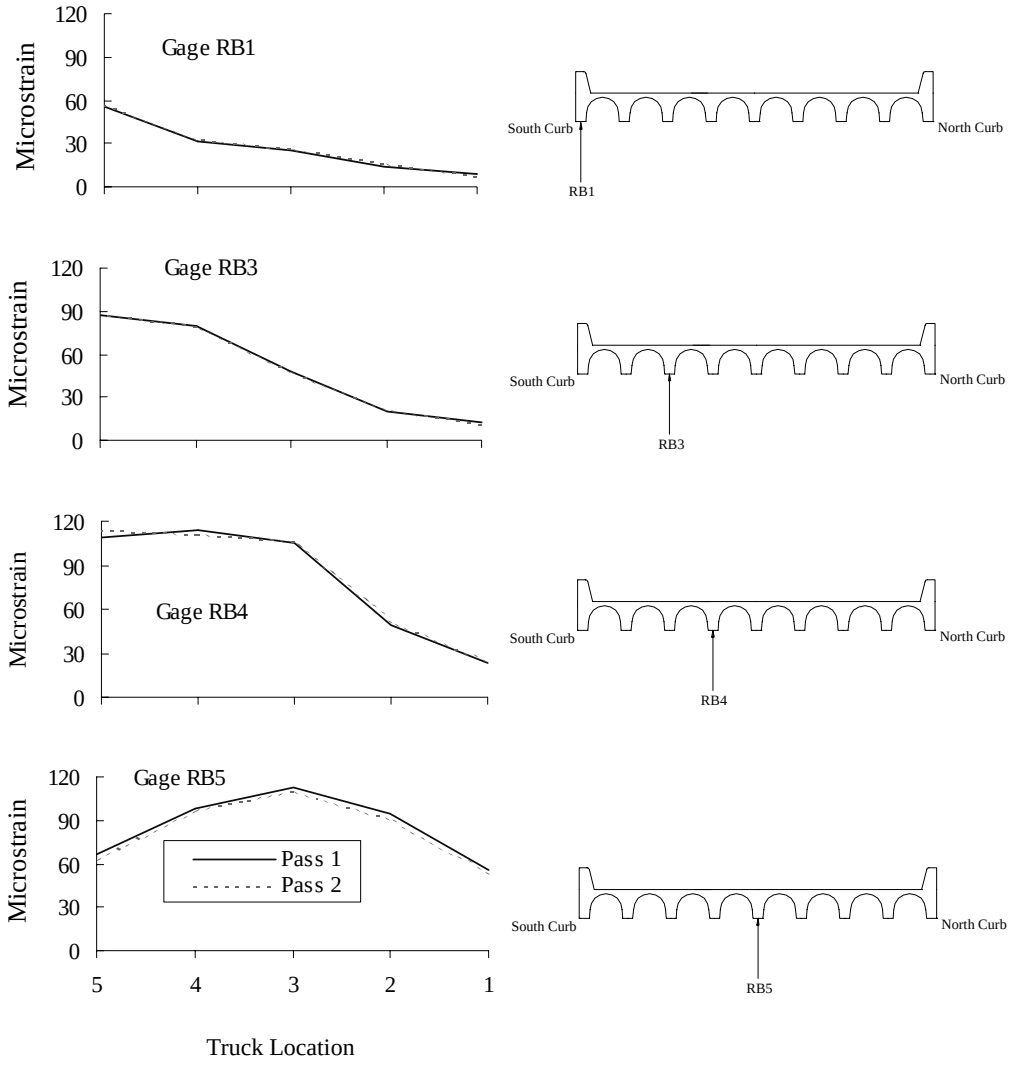

Figure 4.15 Profiles of Maximum Reinforcing Bar Strains at Midspan for Test Series 4 and 5

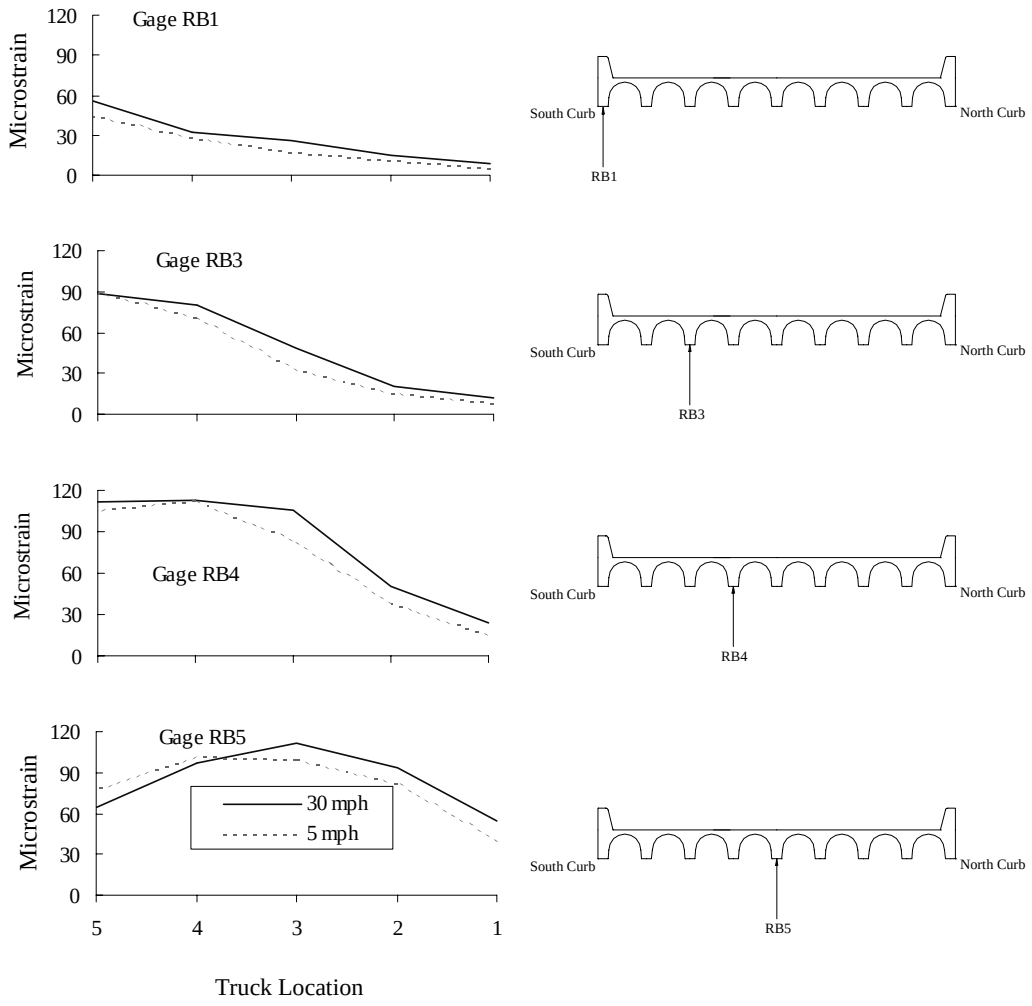

Figure 4.16 Comparison of Maximum Strains at Midspan for 30 mph and 5 mph Runs

4.2.2 Foil Strain Gages Located at Quarter-Span

Nine additional foil strain gages were placed on the same reinforcing bars but at their quarter point. The complete response histories for these foil strain gages are presented in Reference 11. All nine gages were monitored during Test Series 1 through 3, and their maximum strains are reported in Table 4.4. As indicated by an asterisk in the table, strain gage RB7Q was considered to be unreliable throughout the entire test.

Table 4.4 Maximum Strains Measured on the Surface of Reinforcing Bars at Quarter-Span for Test Series 1 through 3, Microstrain

Test Series	Truck Location	Pass	Gage Identification								
			RB1Q	RB2Q	RB3Q	RB4Q	RB5Q	RB6Q	RB7Q	RB8Q	RB9Q
1	1 & 5	1	52	88	108	119	139	137	113	130	54
		2	49	86	114	119	149	134	*	124	52
2	1	1	2	7	15	22	38	86	*	97	50
		2	2	7	13	20	34	80	*	97	54
	2	1	8	15	26	41	77	95	*	87	36
		2	8	14	25	40	75	93	*	87	34
	3	1	15	24	42	72	99	93	*	48	24
		2	16	24	43	71	101	95	*	50	24
	4	1	25	41	81	86	94	76	*	30	16
		2	26	42	83	89	95	77	*	31	16
	5	1	38	70	91	79	91	35	*	17	9
		2	38	70	92	80	94	35	*	17	9
3	1	1	4	9	17	25	46	92	*	96	38
		2	5	10	18	26	48	91	*	96	37
	2	1	10	17	29	52	96	86	*	52	24
		2	11	20	30	54	95	87	*	52	25
	3	1	18	26	62	83	83	85	*	32	17
		2	17	29	60	81	83	88	*	33	18
	4	1	26	51	89	73	99	45	*	21	12
		2	26	52	91	74	100	46	*	20	12
	5	1	42	74	77	76	56	22	*	11	6
		2	42	73	79	77	59	23	*	11	7

* Denotes unreliable data

Strain data recorded during the first pass of truck location 1 for Test Series 2 are shown in Figure 4.17. Similarly to the reinforcing bar gages at midspan, the response histories indicate tensile strains in the reinforcing bars while the truck is located on the instrumented span and compressive strains when it is on adjacent spans.

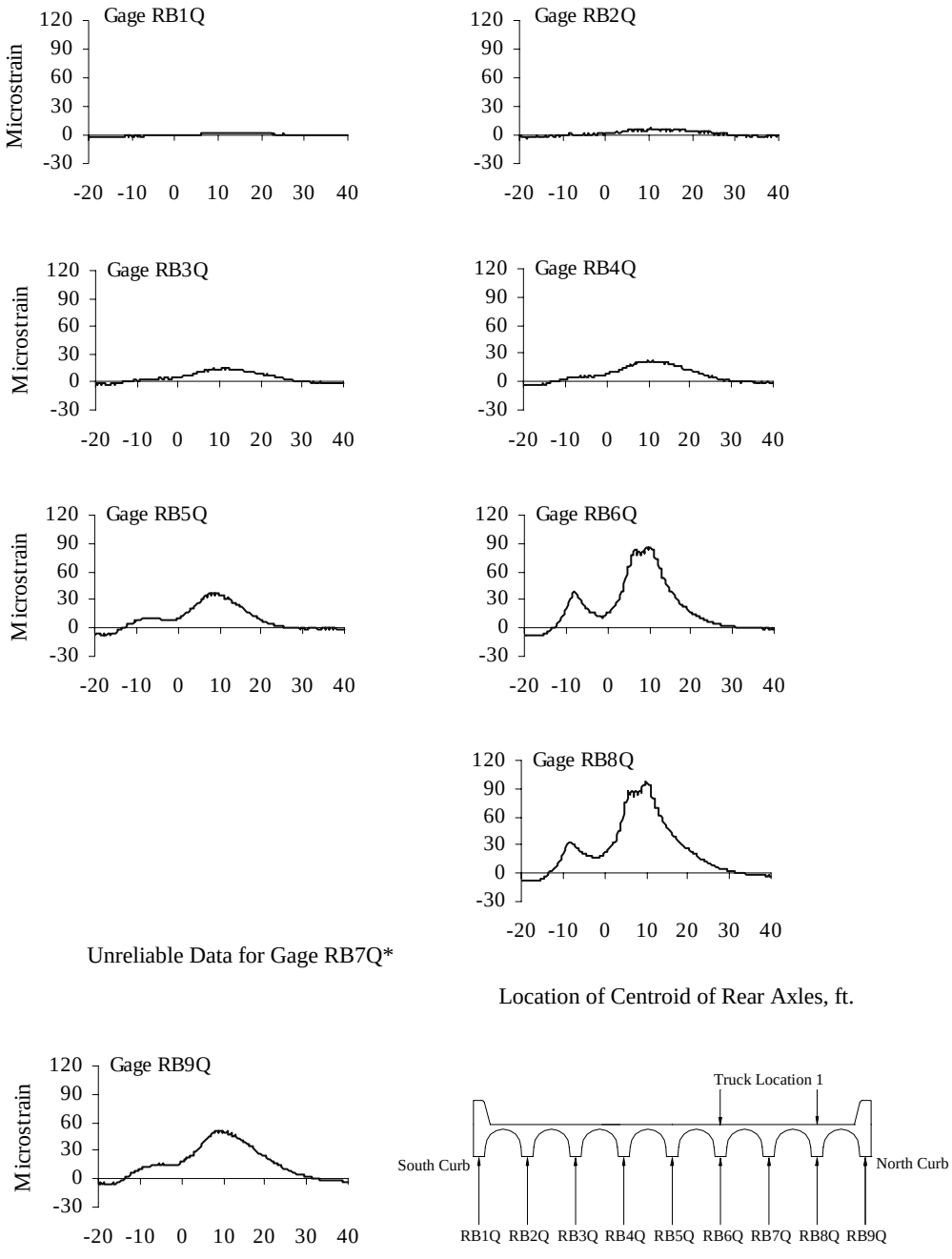

* Gage RB7Q produced a response history unfamiliar and unlike others

Figure 4.17 Reinforcing Bar Strains at Quarter-Span, Test Series 2, Truck Location 1, Pass 1

Assessing the distribution of strain across the bridge cross section was not possible because strain gage RB7Q provided unreliable data. For this reason the profiles of maximum strains recorded for the five transverse positions in Test Series 1, 2, and 3 are shown to be incomplete in Figures 4.18, 4.19, and 4.20, respectively. In comparing the profiles of Test Series 2 with those of Test Series 3, similar trends are observed as the truck location changes, but the peaks in some strain gages did not correspond in the two test series.

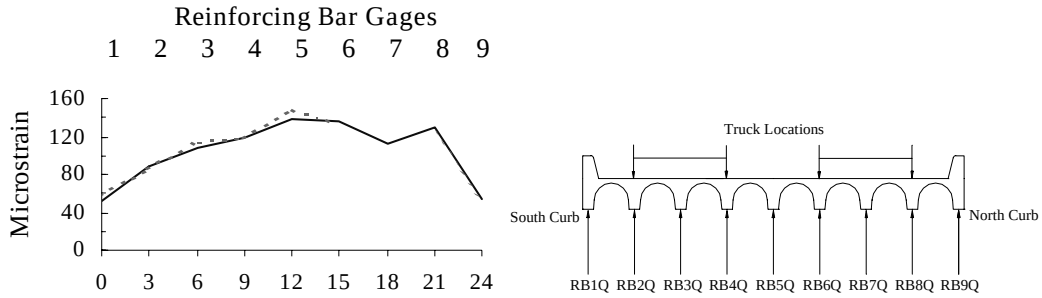

Distance from South Side of Bridge, ft

Figure 4.18 Profile of Maximum Reinforcing Bar Strains at Quarter-Span for Test Series 1

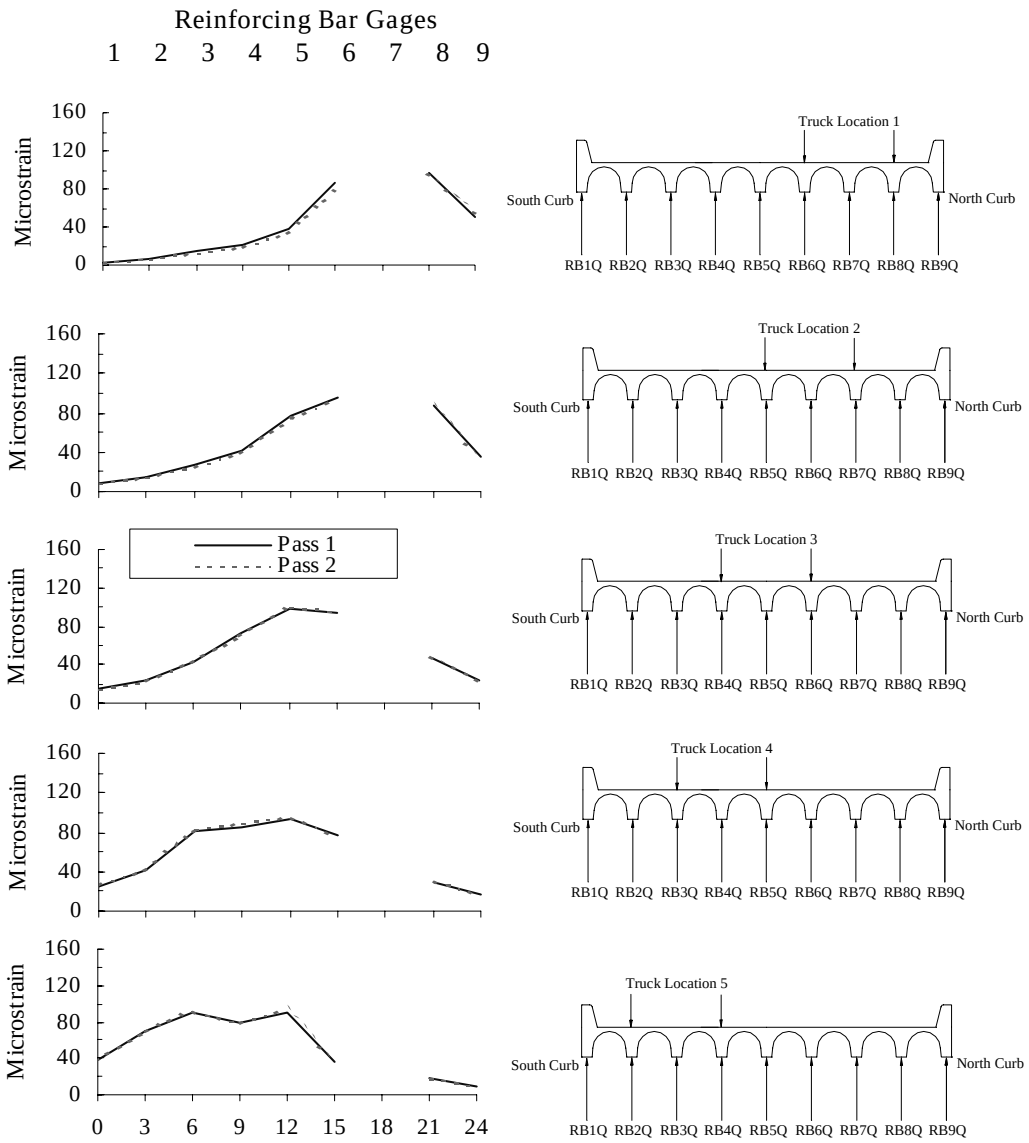

Figure 4.19 Profiles of Maximum Reinforcing Bar Strains at Quarter-Span for Test Series 2

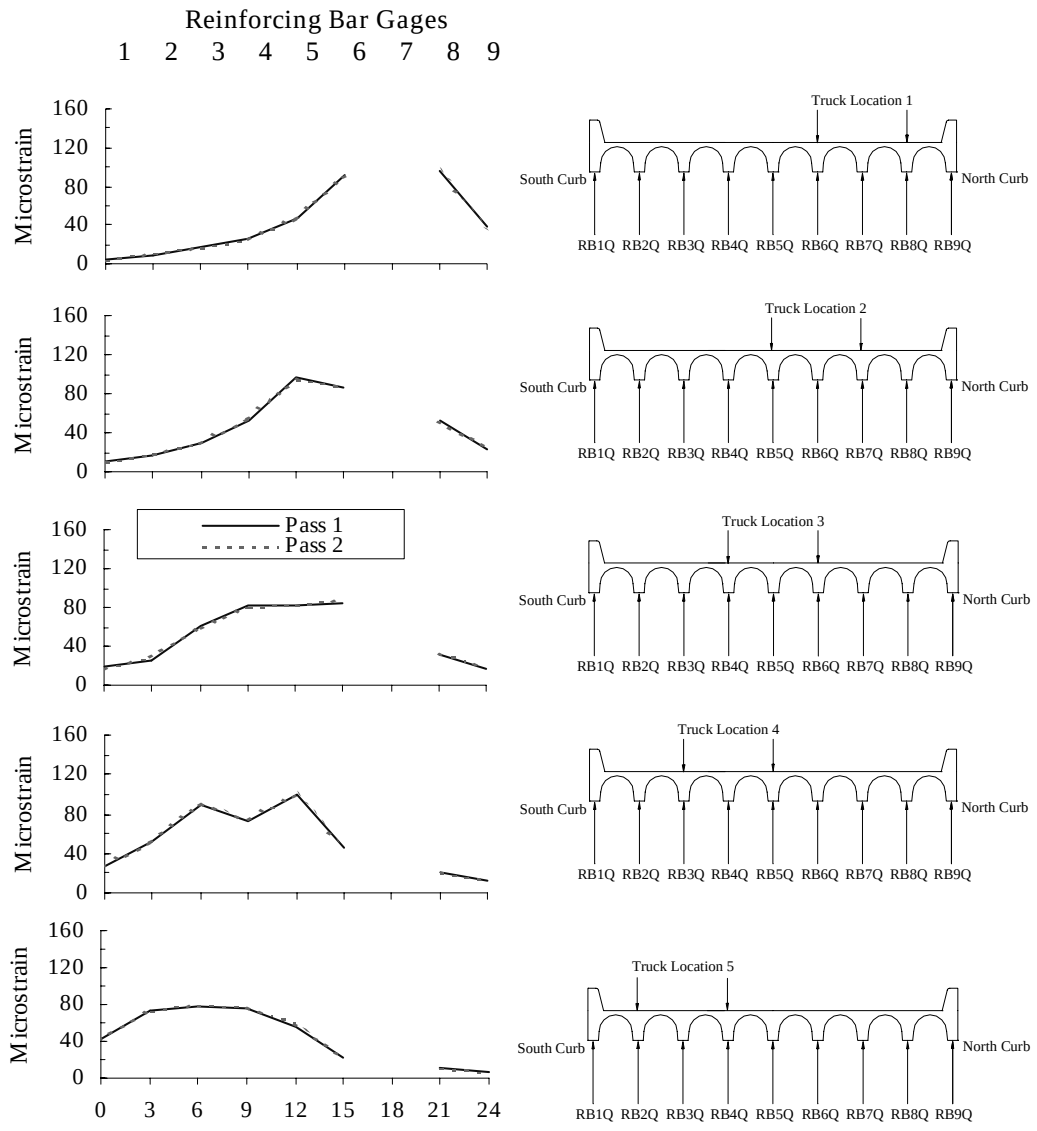

Figure 4.20 Profiles of Maximum Reinforcing Bar Strains at Quarter-Span for Test Series 3

4.2.3 Repeatability of Strain Measurements

As indicated in all of the tables and figures presented, two passes were made at each transverse position during each test series. This was done to obtain information on the repeatability of the data. Slight variations in the data obtained for each pass were observed and are attributed to the variations in the truck position. Many times the truck was positioned a few inches to the right or left of the line marker. Figure 4.21 compares the maximum strains for all reinforcing bar gages during all runs. As shown in the figure, all the data points fall within a ±10% range.

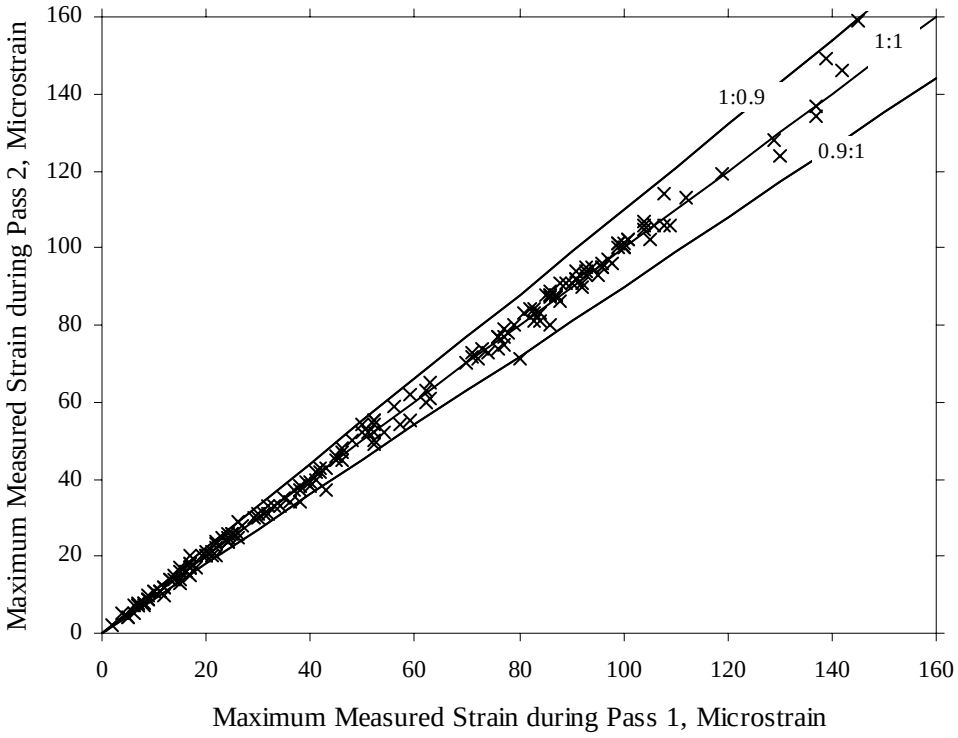

Figure 4.21 Repeatability of Maximum Reinforcing Bar Strains at Midspan and Quarter-Span

4.3 STRAINS MEASURED ON THE SURFACE OF CONCRETE AT THE CURB

A total of 11 wire strain gages were used to measure strains on the surface of the curbs. The gages were mounted on the top and both the inside and outside faces of the curb.

4.3.1 Wire Strain Gages Located at Midspan

Eight wire strain gages were attached to the surface of the south and north curbs at midspan; six were located on the south curb and two on the north curb. The complete response histories for these wire strain gages are presented in Reference 11. All eight wire strain gages were monitored during Test Series 1 through 3, and their maximum strains are reported in Table 4.5. Strain gages R1 through R4 were also monitored during Test Series 4. The maximum strains for Test Series 4 are also presented in Table 4.5. The strains presented in Table 4.5 show positive and negative values. The signs indicate whether tensile or compressive strains dominated the response of the gage. Gages R5 and R6 were placed in locations where tensile forces were expected, and therefore, their behavior was controlled by tensile strains. Many gages provided unreliable data, as denoted by an asterisk in Table 4.5.

Strain data recorded during the first pass of truck location 1 for Test Series 2 are shown in Figure 4.22. These strain data are representative of the response obtained for wire strain gages on the curb monitored during all test series. The majority of the gages are in compression. The only two strain gages that are never in compression are gages R5 and R6. The reason is that these gages are located just five inches above the gaged, longitudinal reinforcing bars; therefore, the gages are in a tension region and experience elongation. The two peaks observed in the reinforcing bar gages are not distinct in the curb gages under compression, but they are noticeable in strain gages R5 and R6. This trend is not shown in Figure 4.22, but it is found in the response histories in Reference 11. The only peak observed on the curb gages in compression is when the centroid of the rear axles is directly over the gages; i.e. location of maximum strain. All gages experienced a reversal in strain when the truck was located on an adjacent span.

Table 4.5 Maximum Strains Measured on the Surface of the Curb at Midspan, Microstrain

Test Series	Truck Location	Pass	Gage Identification							
			R1	R2	R3	R4	R5	R6	R7	R8
1	1 & 5	1	-48	-20	-1	-16	17	25	-43	-30
		2	-43	-17	-1	-15	17	24	-45	-26
2	1	1	-9	*	-1	-2	2	2	-43	-30
		2	*	*	-1	*	2	2	*	-33
	2	1	*	*	-1	*	3	4	*	-16
		2	*	*	-1	-2	4	4	*	-18
	3	1	*	*	-1	-4	6	7	*	-10
		2	*	*	-1	-4	6	7	*	-10
	4	1	-23	-10	-1	-6	8	12	*	-6
		2	-21	-9	-1	-7	7	12	-11	-6
	5	1	-35	-16	-1	-11	12	21	*	-5
		2	-35	-15	-1	-11	12	22	-6	-5
3	1	1	*	*	*	-1	2	3	*	-24
		2	*	*	-1	-2	2	3	-32	-23
	2	1	-8	*	-1	-2	4	5	*	-11
		2	*	*	-1	-3	4	5	*	-13
	3	1	*	*	-1	-7	6	9	-19	-8
		2	*	*	-1	-7	7	9	*	-9
	4	1	-29	-11	-1	-10	11	16	-11	-5
		2	*	*	-1	-11	9	16	*	-6
	5	1	-51	-22	-1	-21	17	21	*	-6
		2	-50	-23	-1	-19	17	20	*	*
4	1	1	-8	-4	-4	-1				
		2	-6	*	-1	-4				
	2	1	-12	*	-1	-6				
		2	*	*	-1	-5				
	3	1	-16	*	-1	-5				
		2	-17	*	-1	-7				
	4	1	-27	-12	-1	-10				
		2	-30	-15	-1	-10				
	5	1	-47	-22	-1	-17				
		2	-46	-22	-1	-17				

* denotes unreliable data

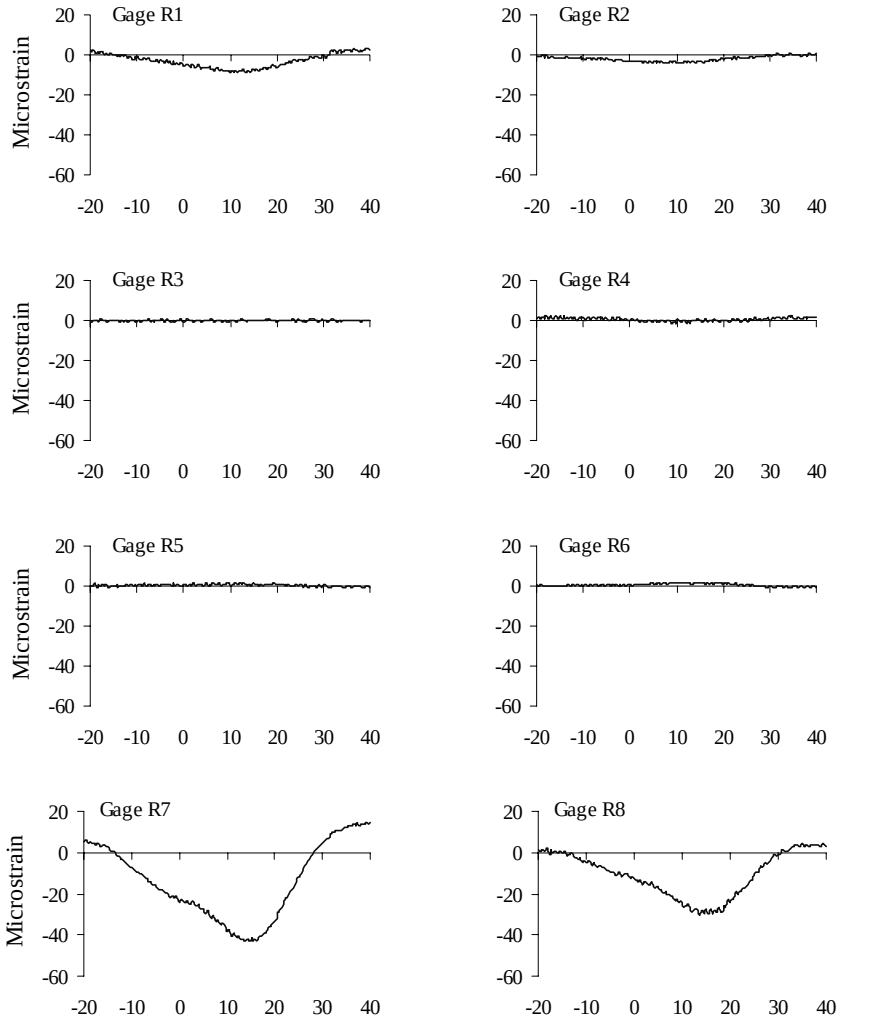

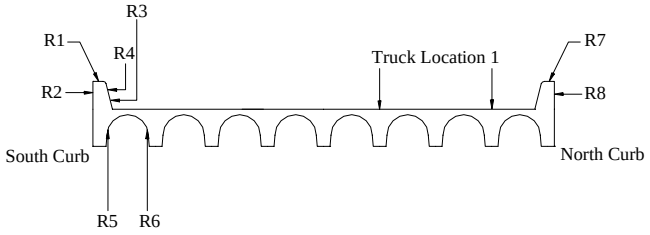

Figure 4.22 Curb Strains at Midspan, Test Series 2, Truck Location 1, Pass 1

4.3.2 Wire Strain Gages Located at Quarter-Span

Three wire strain gages were attached to the surface of the north and south curbs at quarter-span; two were located on the south curb and one on the north curb. The complete response histories for these wire strain gages are presented in Reference 11. All three wire strain gages were monitored during Test Series 1 through 3, and their maximum strains are reported in Table 4.6.

Table 4.6 Maximum Strains Measured on the Surface of the Curb at Quarter-Span, Microstrain

Test Series	Truck Location	Pass	Gage Identification		
			R1Q	R2Q	R7Q
1	1 & 5	1	-44	-14	-38
		2	-41	-14	-41
2	1	1	-8	-9	-37
		2	*	*	-40
	2	1	*	*	*
		2	*	*	*
	3	1	*	*	-23
		2	*	*	*
	4	1	-21	*	-15
		2	-21	-8	-11
	5	1	-34	-13	-7
		2	-32	-11	-8
3	1	1	*	*	*
		2	*	*	-29
	2	1	*	*	-16
		2	*	*	*
	3	1	-20	*	*
		2	*	*	*
	4	1	-25	-9	*
		2	*	*	*
	5	1	-41	-17	*
		2	-42	-17	*

* denotes unreliable data

Strain data recorded during the first pass of truck location 1 for Test Series 2 are shown in Figure 4.23. These strain data are representative of most of the response histories obtained for wire strain gages on the curb monitored during all test series. All of the gages are in compression because these strain gages are located within the top ten inches of the curb. Strain gage R7Q in Figure 4.23 is shown drifting at rear axle locations –20 and 40 ft. As mentioned, this trend is observed in many of the gages located on the curb and exposed to the sunlight. On the otherhand, some response histories for strain gage R7Q are reliable and are used in the analysis of the bridge behavior. All gages experienced a reversal in strain when the truck was located on an adjacent span.

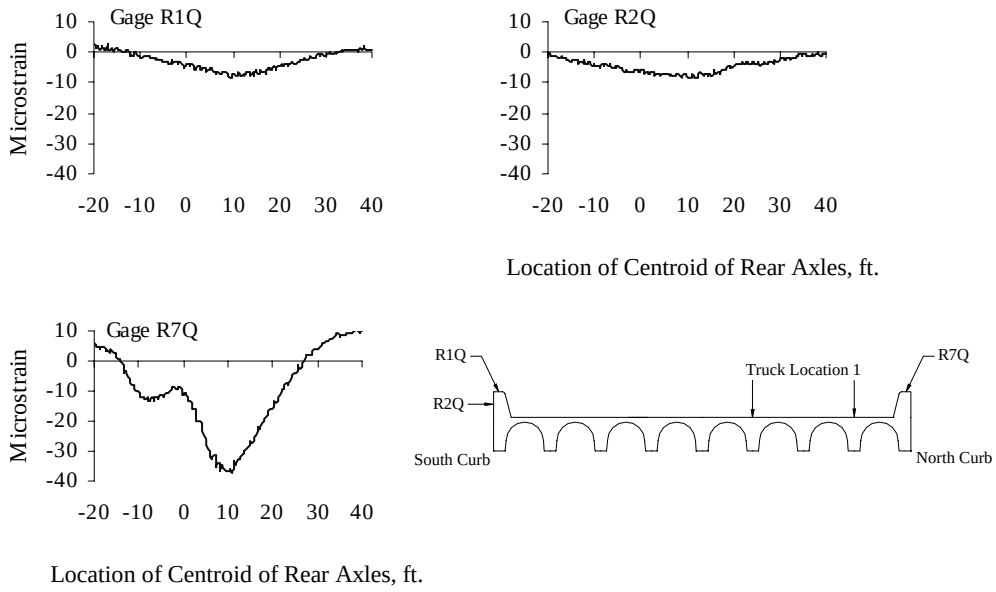

Figure 4.23 Curb Strains at Quarter-Span, Test Series 2, Truck Location 1, Pass 1

4.3.3 Repeatability of Strain Measurements

Figure 4.24 compares the maximum compressive and tensile strains measured on the surface of the curb for gages at midspan and quarter-span. The figure depicts the repeatability of the data. The majority of the data points fall within a ±25% range. The curb gages were more sensitive to the position of the truck than the reinforcing bar gages.

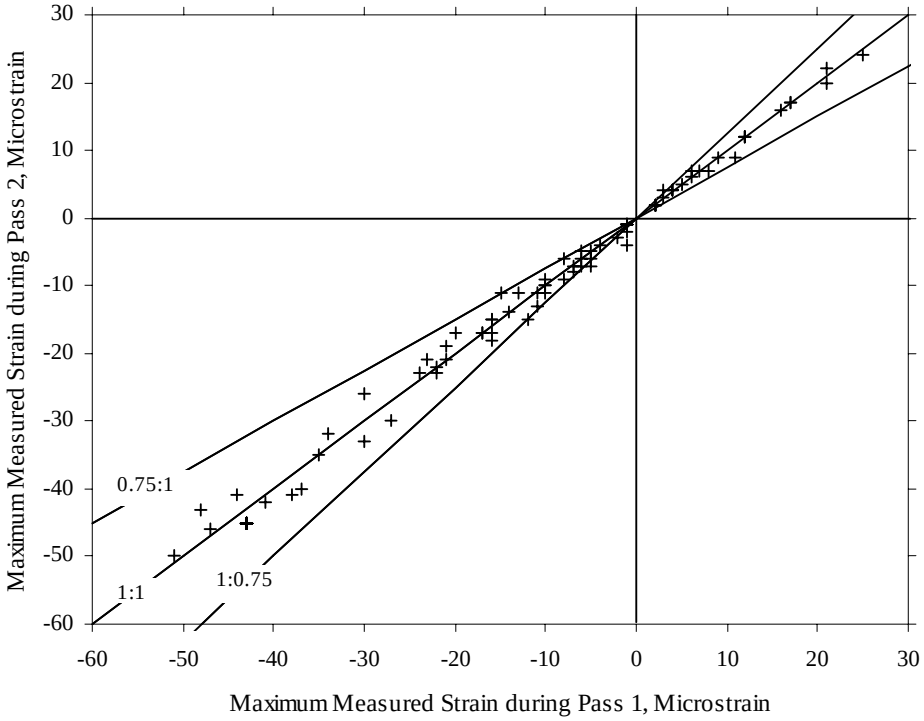

Figure 4.24 Repeatability of Maximum Strains on Surface of Curbs at Midspan and Quarter-Span

4.4 STRAINS MEASURED ON THE SURFACE OF CONCRETE AT THE CROWNS

A total of 16 wire strain gages were used to measure strains on the surface of the concrete at the crowns. The gages were mounted at the top of the crown, slightly to the left or right of longitudinal cracks. The data collected from strain gages located at midspan are presented first, followed by data collected from strain gages located at quarter-span.

4.4.1 Wire Strain Gages Located at Midspan

Eight wire strain gages were attached to the surface of the crowns at midspan. The complete response histories for these wire strain gages are presented in Reference 11. Some response histories in the appendix are not representative of the behavior expected. Although the response histories provided unreliable data, they were plotted to show their odd behavior. These unreliable response histories are denoted by an asterisk in the tables presented. All eight wire strain gages were monitored during Test Series 1 through 3, and their maximum strains are reported in Table 4.7. Strain gages C3 and C4 were also monitored during Test Series 5. The maximum strains for Test Series 5 are also presented in Table 4.7. Similarly to the gages located on the curb, the strains presented in Table 4.7 show positive and negative values. The signs indicate whether tensile or compressive strains dominated the response of the gage. Gages C1, C4, and C8 were controlled by tensile strains during certain truck locations; for this reason positive maximum values are presented.

Strain data recorded during the first pass of truck location 2 for Test Series 2 are shown in Figure 4.25. These strain data are representative of the response obtained from wire strain gages on the crowns monitored during all test series. As shown in Figure 4.25, gage C2 was not working correctly, and it was not replaced because of time constraints. Response histories for gages C1 and C4 were considered unreliable and are not presented in the figure. The figure shows that the majority of the gages are in compression. Gage C8 is shown to alternate between tensile and compressive strains, experiencing almost no strain. Gages C5 and C7 show abrupt changes in the amplitude of strains at three locations.

These jumps occur in all crown gages when the wheels of the truck pass directly over the location of the gage or directly over the holes that are adjacent to the gages. The values shown in Table 4.7 correspond to the maximum negative strains obtained from these jumps because the gage was acting in compression. The response histories for the crown strain gages also indicate considerable noise. The level of noise becomes more significant when small strains are measured. Similarly to all other gages, the reliable crown gages experienced a reversal in strain when the truck was positioned on an adjacent span. Overall, the crown strain gages located at midspan were the most sensitive and least reliable.

Table 4.7 Maximum Strains Measured on the Surface of the Crowns at Midspan, Microstrain

Test Series	Truck Location	Pass	Gage Identification							
			C1	C2	C3	C4	C5	C6	C7	C8
1	1 & 5	1	5	*	-15	-23	-16	-13	-21	-2
		2	4	*	-16	-27	-19	-13	-15	-3
2	1	1	1	*	-2	*	*	-21	*	-4
		2	*	*	*	*	*	-24	*	*
	2	1	*	*	-6	*	-17	-9	-13	-2
		2	*	*	*	*	*	-7	*	-1
	3	1	*	*	-9	*	*	-26	*	3
		2	2	*	-9	*	-13	-24	*	3
	4	1	2	*	-19	*	*	-9	*	3
		2	*	*	-20	*	*	-8	*	3
	5	1	3	*	-12	*	-10	-4	*	*
		2	*	*	-12	*	*	-5	*	-2
3	1	1	*	*	*	4	*	-12	*	-1
		2	*	*	*	*	-17	-11	*	*
	2	1	2	*	-6	-16	*	*	*	*
		2	3	*	-7	*	-11	-20	*	-3
	3	1	*	*	-21	*	*	-14	*	-2
		2	*	*	-18	*	-19	-15	*	-3
	4	1	-2	*	-13	*	-10	-6	*	3
		2	*	*	-12	*	*	-6	*	3
	5	1	*	*	-16	-12	*	-4	*	-3
		2	*	*	-16	-12	-8	-4	*	-2
5	1	1			-3	3				
		2			-3	*				
	2	1			-5	*				
		2			-5	-4				
	3	1			-12	-24				
		2			-13	-19				
	4	1			-18	*				
		2			-16	*				
	5	1			-13	*				
		2			-12	*				

* denotes unreliable data

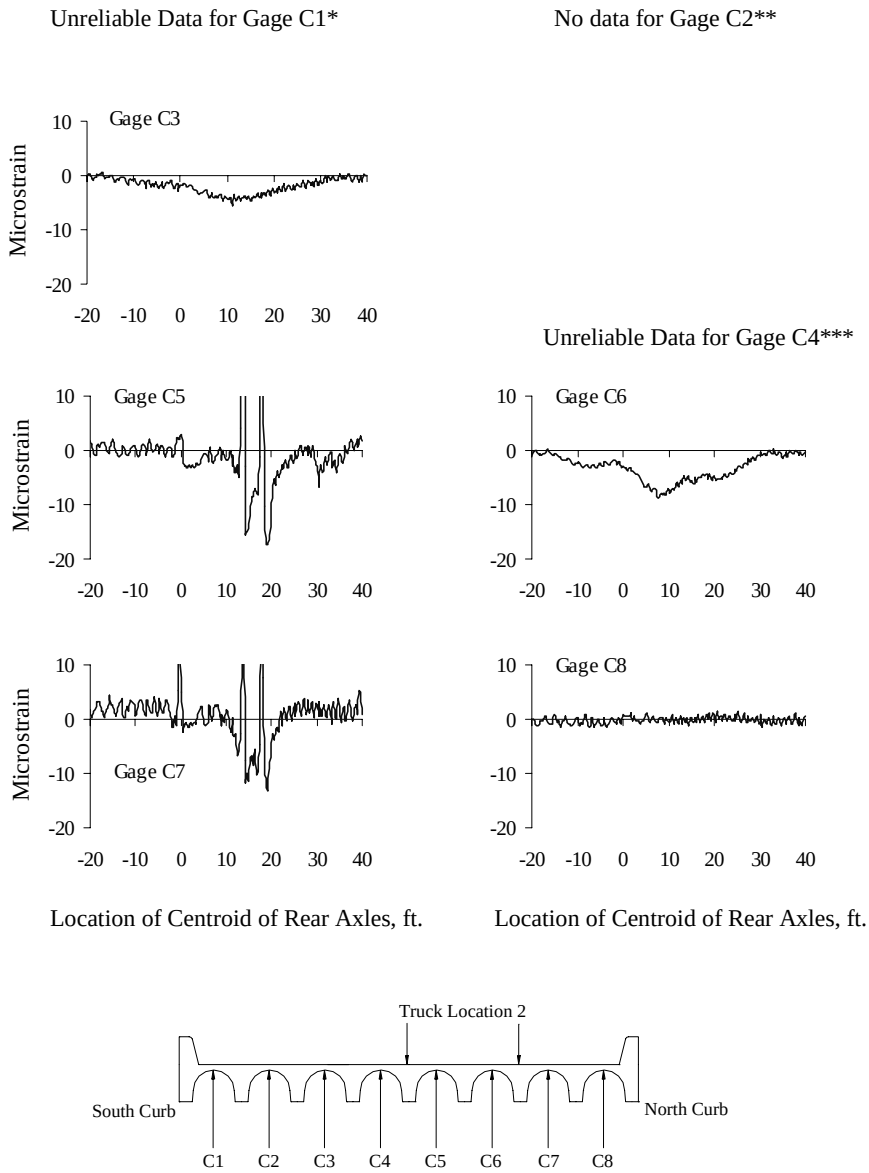

* Gage C1 produced unconservative maximum strains after data points were shifted by a constant value
** Gage C2 did not provide any readings
*** Gage C4 produced a response history unfamiliar and unlike others

Figure 4.25 Crown Strains at Midspan, Test Series 2, Truck Location 2, Pass 1

4.4.2 Wire Strain Gages Located at Quarter-Span

Similarly to the crowns at midspan, eight wire strain gages were attached to the surface of the crowns located at quarter-span. The complete response histories for these wire strain gages are presented in Reference 11. All eight wire strain gages were monitored during Test Series 1 through 3, and their maximum strains are reported in Table 4.8. The strains presented in Table 4.8 show positive and negative values. As mentioned, the signs indicate whether tensile or compressive strains dominated the response of the gage. Gages C1Q, C2Q, and C8Q were controlled by tensile strains during certain truck locations; for this reason positive maximum values are presented.

Strain data recorded during the first pass of truck location 3 for Test Series 2 are shown in Figure 4.26. These strain data are representative of the response obtained for gages located on the crowns that were monitored during the three test series. Similarly to midspan, the two gages located adjacent to the curbs, C1Q and C8Q, experience tensile strains throughout their readings. The only exception is truck location 5 of Test Series 3 where strain gage C1Q is in compression. Abrupt changes in the amplitude of strains are once again evident in the response histories of some of the gages. The gages also show the two peaks that indicate when an axle is located over the strain gages.

In comparing the quarter-span crown gages with those at midspan, the majority of the data from the gages at quarter-span were more reliable than those at midspan. A possible cause of this reduced reliability is the cracking is more pronounced at midspan, and this cracking could have affected the gages located right next to the cracks.

Table 4.8 Maximum Strains Measured on the Surface of Crowns at Quarter-Span, Microstrain

Test Series	Truck Location	Pass	Gage Identification							
			C1Q	C2Q	C3Q	C4Q	C5Q	C6Q	C7Q	C8Q
1	1 & 5	1	5	-10	-13	-8	-16	-10	-17	6
		2	5	-15	-18	-16	-19	-10	-19	7
2	1	1	*	*	*	*	-4	-17	-8	*
		2	*	*	*	*	-3	*	-8	-9
	2	1	*	*	-15	-9	-19	*	-20	6
		2	4	*	-15	-8	-18	-8	-19	5
	3	1	4	9	-14	-16	-9	*	-8	*
		2	5	*	-14	*	-8	-10	-8	5
	4	1	*	*	*	-11	*	*	-2	5
		2	5	*	-13	-12	-17	*	-3	4
	5	1	*	*	-11	*	-6	*	-2	3
		2	3	*	*	-12	-6	*	-2	2
3	1	1	*	*	-9	*	-9	-10	-13	*
		2	*	*	-10	*	-11	*	-15	5
	2	1	4	*	-22	-17	*	*	-10	5
		2	*	7	-21	*	*	*	-10	5
	3	1	5	10	-13	-9	-15	*	-4	4
		2	*	13	-12	-9	-12	*	-4	4
	4	1	5	-15	-13	-20	*	*	*	2
		2	4	*	-12	-19	*	*	-3	3
	5	1	-10	*	-12	*	-4	-3	-3	*
		2	-8	*	-12	*	-4	*	-2	*

* denotes unreliable data

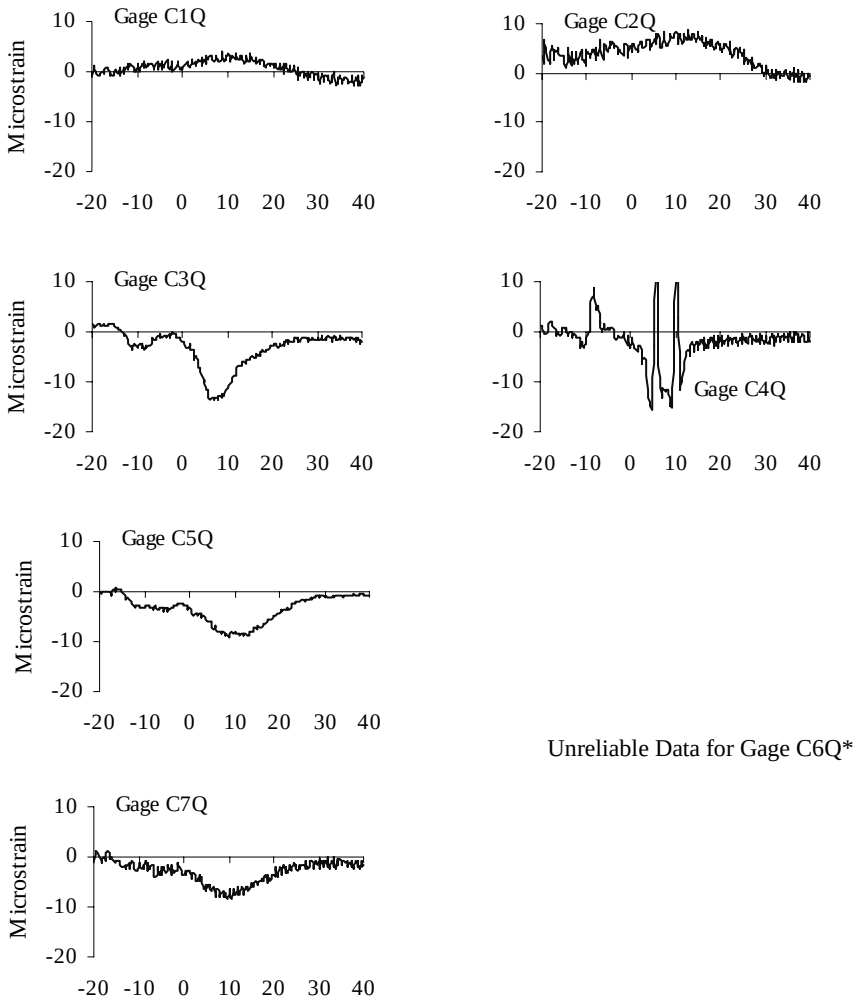

* Gage C6Q produced a response history unlike other response histories
** Gage C8Q procuded unconservative maximum strains after data points were shifted by a constant value

Figure 4.26 Crown Strains at Quarter-Span, Test Series 2, Truck Location 3, Pass 1

4.4.3 Repeatability of Strain Measurements

The repeatability of the data for the gages located on the crowns is presented in Figure 4.27. As shown, significant scatter is observed in all of the gages. This scatter indicates that the gages are sensitive to any slight change in the positioning of the truck. Such behavior is most likely due to the small readings measured by the gages, and thus variations within a ±25% range are shown in the figure.

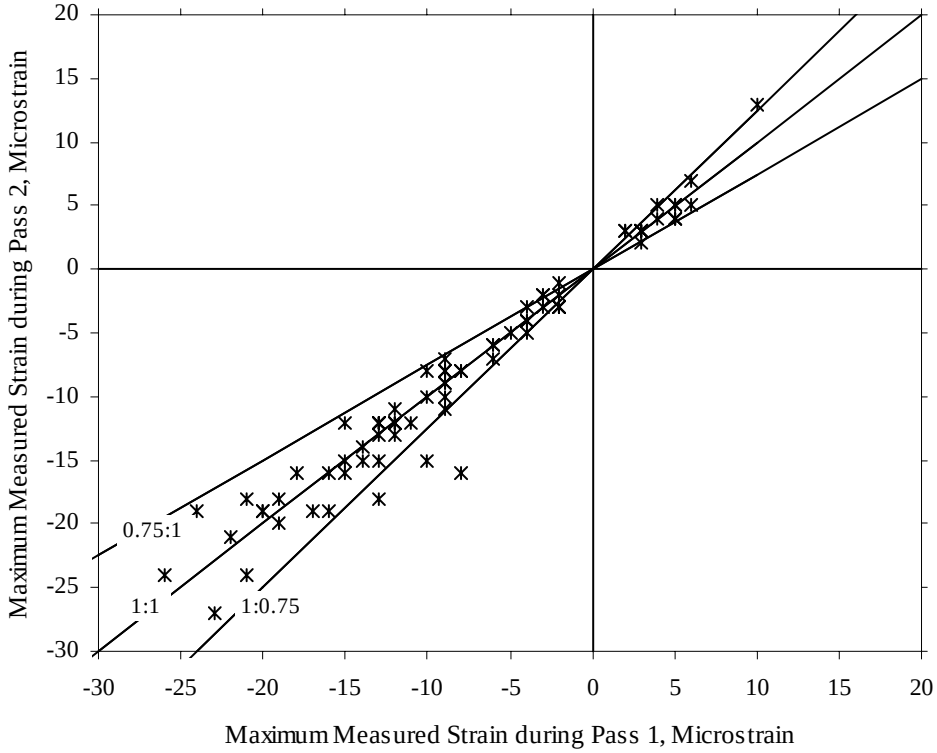

Figure 4.27 Repeatability of Maximum Strains on Surface of Crowns at Midspan and Quarter-Span

4.5 STRAIN GRADIENTS WITHIN CURBS

Strains gradients within the south and north curbs were obtained at two locations. The gradients were developed using the gages located on the surface of the curb and the girder directly underneath the curb. Strain gradients within the curbs at midspan are presented first, followed by strain gradients at quarter-span.

4.5.1 Midspan

Strain gradients within the south and north curbs at midspan for each truck location of Test Series 2 are presented in Figures 4.28 and 4.29, respectively. Maximum strain data from six curb gages, one reinforcing bar gage, and one crown gage were used to develop the strain gradients for the south curb. A best-fit line through the measured maximum strain data was plotted to approximate the location of the neutral axis. The plots show that the strains do not vary linearly with depth. In Figure 4.28, some variation appears in the response between gages located on the inside and outside faces of the curb. Gages located on the inside face of the curb do not appear to fall near the best-fit line. For the north curb, two curb gages, one reinforcing bar gage, and one crown gage were used to develop the strain gradients. Figure 4.29 shows that the strains vary linearly with depth within the north curb, unlike those plots in Figure 4.28.

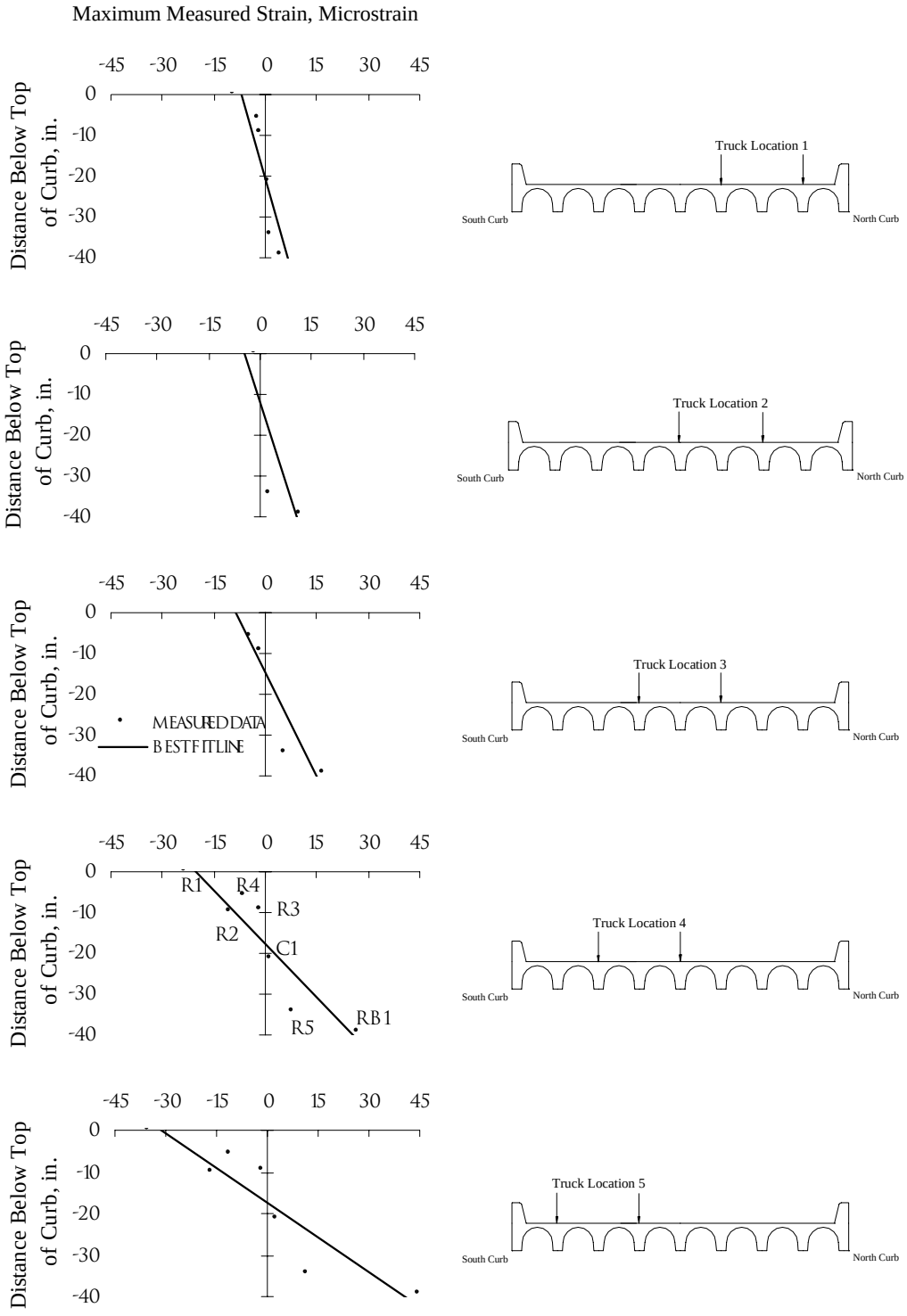

Figure 4.28 Measured Strain Gradients within South Curb at Midspan

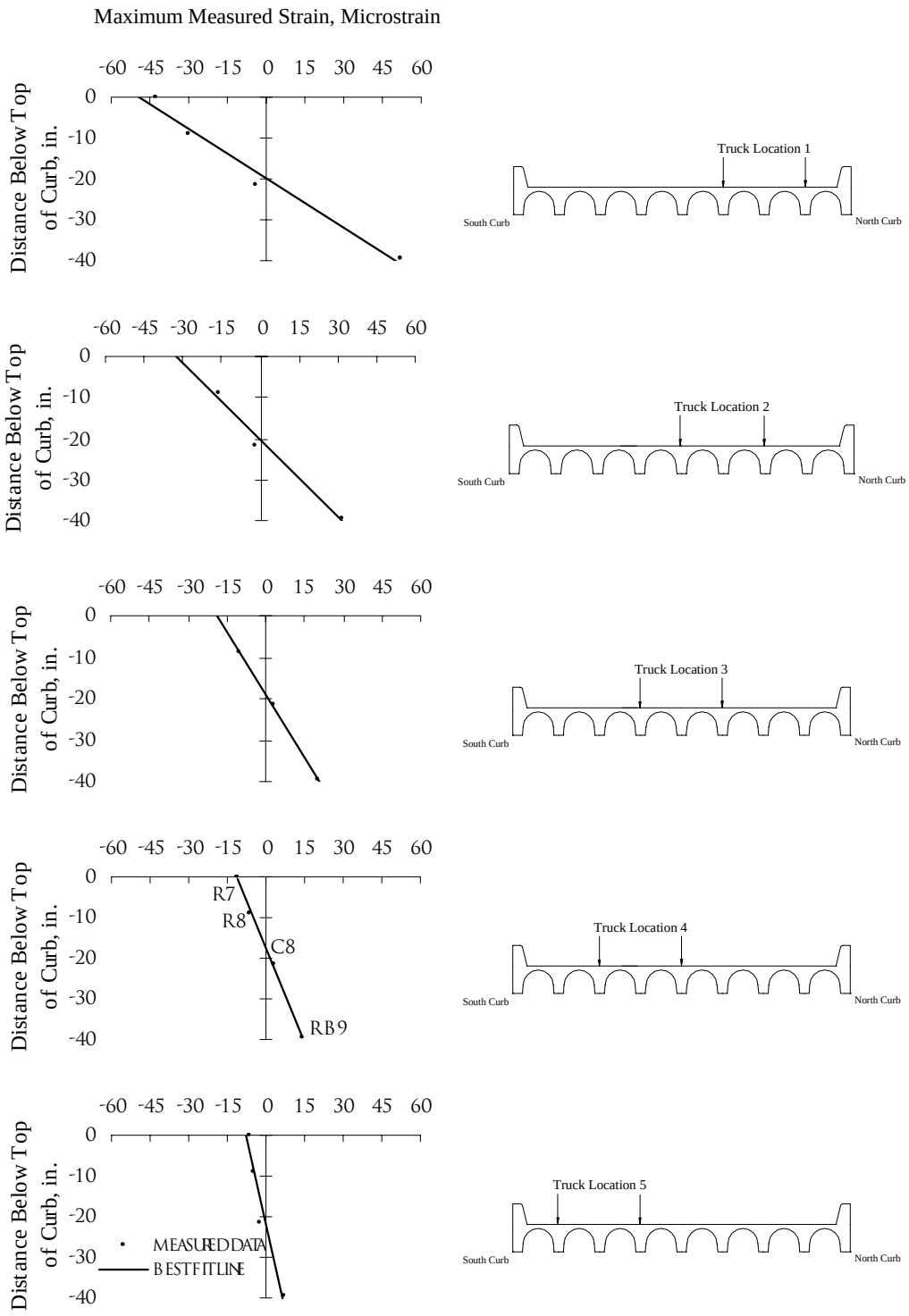

Figure 4.29 Measured Strain Gradients within North Curb at Midspan

4.5.2 Quarter-Span

Strain gradients within the south curb at quarter-span for truck locations 1, 4 and 5 of Test Series 2 are presented in Figure 4.30. For the north curb, strain gradients for truck locations 1, 3, 4 and 5 of Test Series 2 are presented in Figure 4.31. Maximum strain data from two curb gages, one reinforcing bar

gage, and one crown gage were used to develop the strain gradients of Figure 4.30. Maximum strain data from one curb gage, one reinforcing bar gage, and one crown gage were used to develop the strain gradients of Figure 4.31. As in other strain gradient plots, a best-fit line through the measured maximum strain data was plotted to approximate the location of the neutral axis. These plots show that the strains vary linearly with depth within the curbs. Figures 4.30 and 4.31 produce similar neutral axis depths.

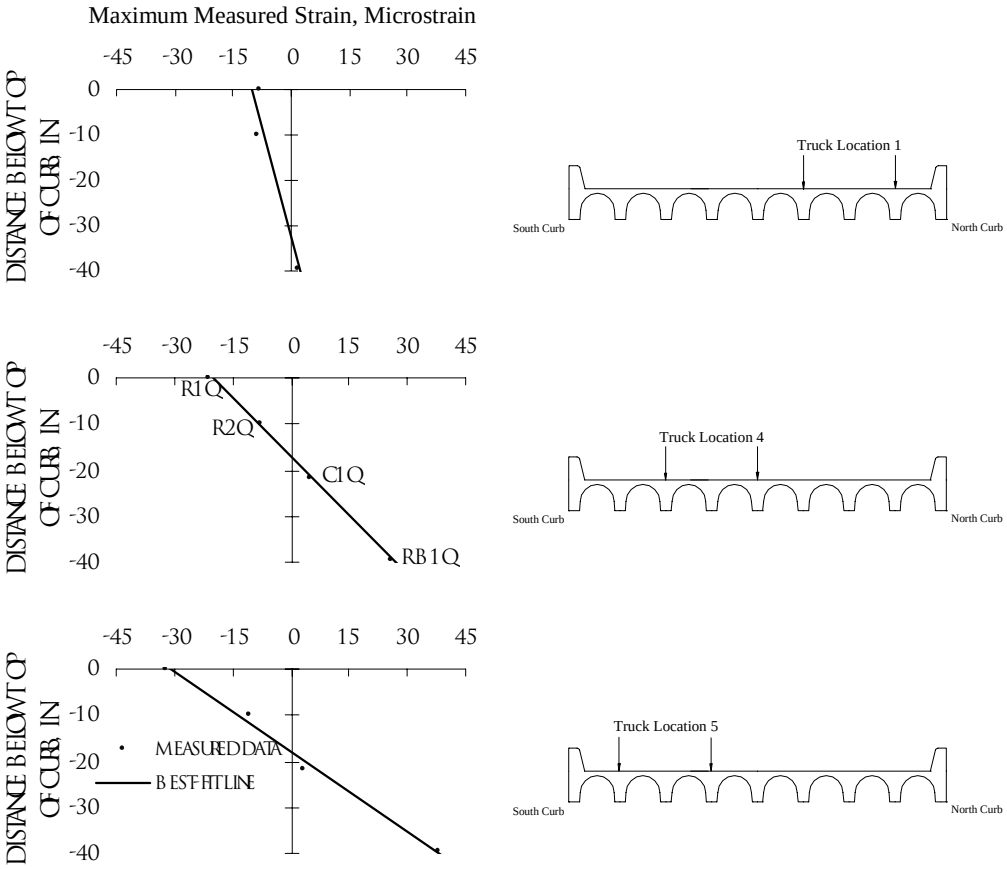

Figure 4.30 Measured Strain Gradients within South Curb at Quarter-Span

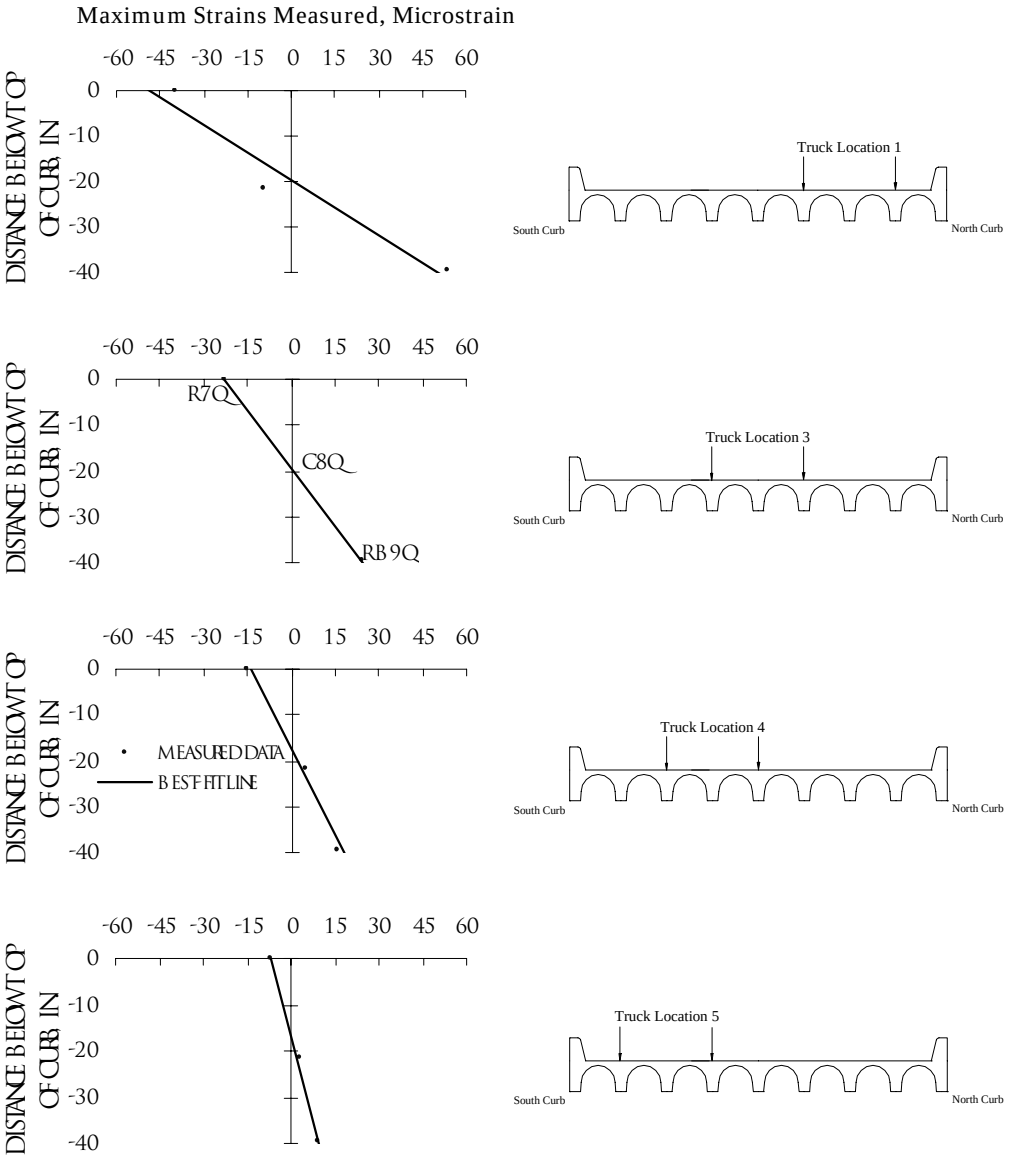

Figure 4.31 Measured Strain Gradients within North Curb at Quarter-Span

4.6 VERTICAL DEFLECTIONS

A total of five displacement transducers were placed at the midspan of five longitudinal girders. The instruments used to measure the vertical deflection of the bridge were Direct Current Differential Transformers, known as DCDTs. The DCDTs were used because string and linear potentiometers used in Load Test 1 were not sensitive enough to measure the vertical deflection of the bridge. All five DCDTs were monitored during Test Series 1 through 3. The complete response histories for the DCDTs are presented in Reference 11, and their maximum vertical deflections are reported in Table 4.9.

Table 4.9 Maximum Vertical Displacements of Girders, in.

Test Series	Truck Location	Pass	Gage Identification				
			DCDT1	DCDT2	DCDT3	DCDT4	DCDT5
1		1	-0.060	-0.153	-0.208	-0.149	-0.055
		2	-0.061	-0.161	-0.219	-0.151	-0.056
2	1	1	-0.002	-0.019	-0.076	-0.100	-0.057
		2	-0.003	-0.017	-0.069	-0.099	-0.062
	2	1	-0.005	-0.037	-0.124	-0.107	-0.034
		2	-0.002	-0.035	-0.123	-0.103	-0.033
	3	1	-0.014	-0.067	-0.139	-0.083	-0.016
		2	-0.013	-0.065	-0.139	-0.081	-0.017
	4	1	-0.024	-0.111	-0.139	-0.040	-0.007
		2	-0.025	-0.111	-0.138	-0.045	-0.008
	5	1	-0.045	-0.121	-0.103	-0.017	-0.003
		2	-0.047	-0.120	-0.104	-0.016	-0.002
3	1	1	0	-0.020	-0.093	-0.098	-0.043
		2	-0.004	-0.025	-0.099	-0.103	-0.045
	2	1	-0.007	-0.047	-0.133	-0.094	-0.023
		2	-0.009	-0.050	-0.134	-0.091	-0.019
	3	1	-0.021	-0.094	-0.136	-0.054	-0.012
		2	-0.019	-0.091	-0.136	-0.056	-0.013
	4	1	-0.034	-0.119	-0.122	-0.022	-0.003
		2	-0.033	-0.117	-0.120	-0.020	-0.004
	5	1	-0.061	-0.117	-0.071	-0.004	-0.001
		2	-0.060	-0.119	-0.075	-0.004	0

Displacement data recorded during the first pass of truck location 1 for Test Series 2 are shown in Figure 4.32. These displacement data are representative of the response obtained from the DCDTs during the three test series. As observed in the figure, the readings tend to flatten out at the location where maximum displacement is expected. Such response is usually attributed to the flexibility in the connection between the wire and the DCDT. Shown in Figure 4.32, a change in displacements from downward to upward as the truck moves onto the adjacent span is observed. The response was dominated when the centroid of the rear axles was located at midspan.

Profiles of the maximum vertical deflections for the five transverse positions for Test Series 1, 2, and 3 are shown in Figures 4.33, 4.34, and 4.35, respectively. These figures show the vertical displacement of the bridge. The profiles for Test Series 2 and 3 are very similar in that the peaks of one test series coincide with the peaks of the other test series.

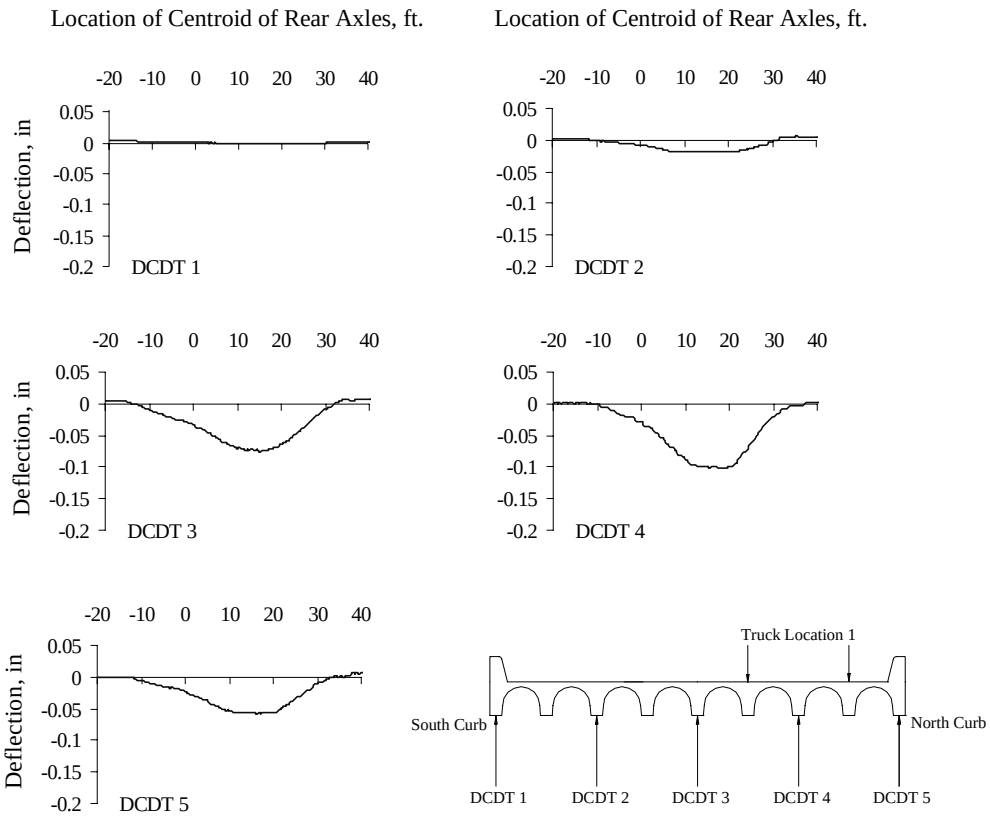

Figure 4.32 Vertical Deflections Measured at Midspan, Test Series 2, Truck Location 1, Pass 1

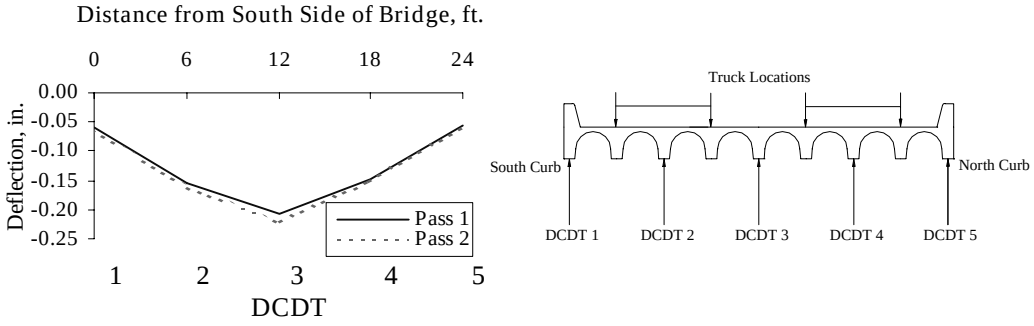

Figure 4.33 Profile of Maximum Vertical Deflections at Midspan for Test Series 1

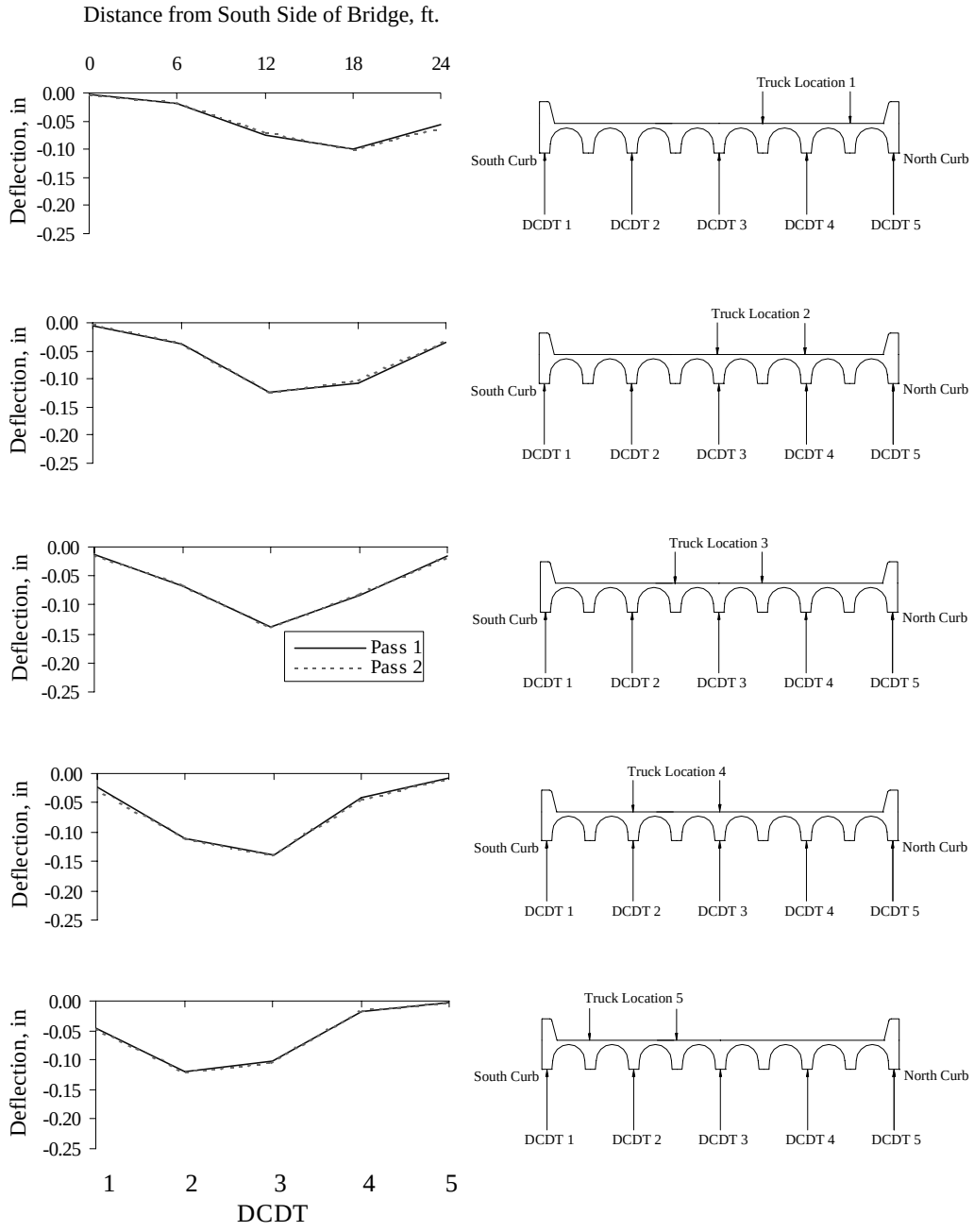

Figure 4.34 Profiles of Maximum Vertical Deflections at Midspan for Test Series 2

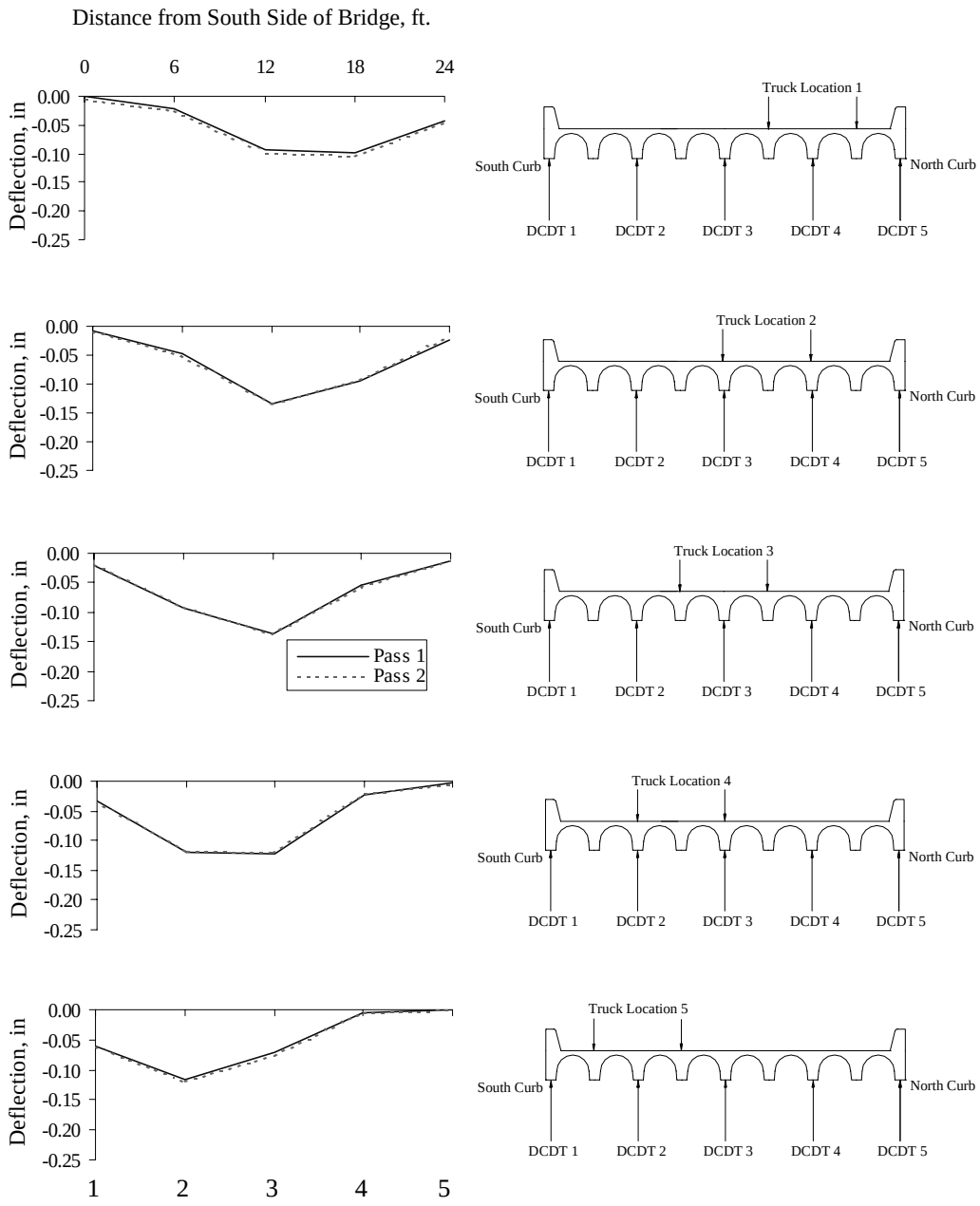

Figure 4.35 Profiles of Maximum Vertical Deflections at Midspan for Test Series 3

4.6.1 Repeatability of Deflection Measurements

Figure 4.36 compares the maximum deflections obtained from pass 1 with those from pass 2. Very small differences are observed which indicate that the deflection readings are not sensitive to slight changes in the position of the truck during pass 2. The data fall within a range of ±10%, probably even within a ±5% range.

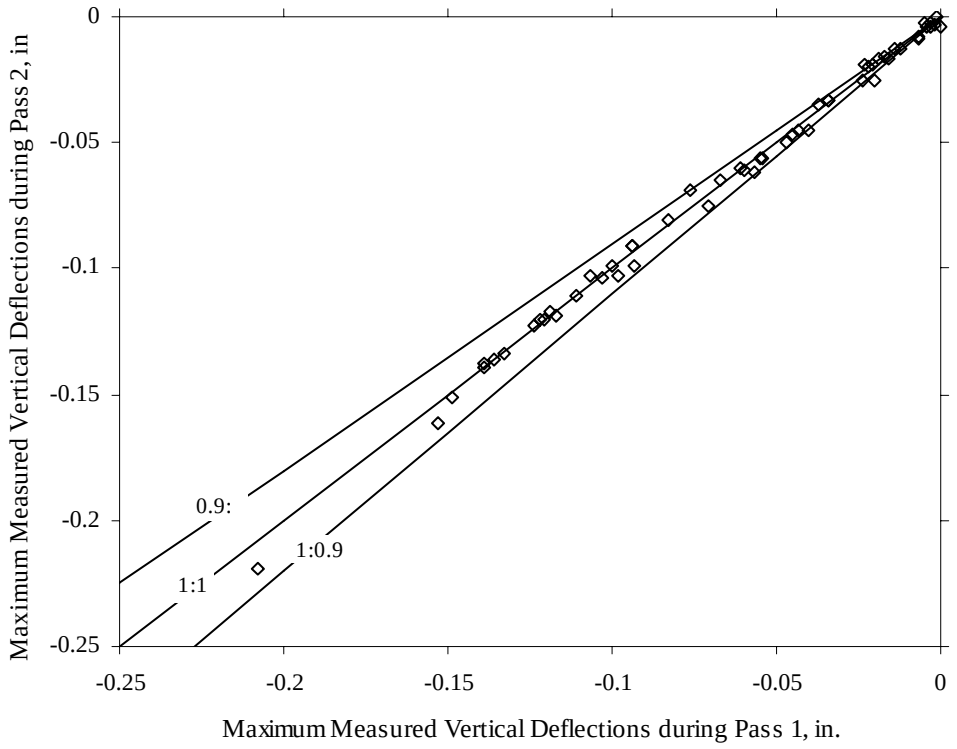

Figure 4.36 Repeatability of Maximum Vertical Deflections at Midspan

4.7 SUMMARY

In general, the readings obtained from the foil strain gages provided repeatable data and were more reliable than the wire strain gages. Wire strain gages located on the surface of the curb provided some reliable readings. The only problem with the gages located on the curbs was the ambient effect on the drift. The wire strain gages located on the surface of the crowns provided data that were the least reliable of the four groups. The problems observed with these gages were the abrupt jumps in strain when the wheels of the truck traveled above a gage and the possibility of placing a gage across a crack. The deflection transducers provided repeatable, flattened peaks. The data were unconservative because of the flattening of the response at the location where maximum displacements were expected. This problem is most likely due to the frictional resistance of the DCDT core. Most of the data do indicate that some continuity exists at the supports. This is based on the reversal of strains and deflections when the truck moves onto an adjacent span. The measured response is evaluated in Chapter 5.

CHAPTER 5: EVALUATION OF MEASURED RESPONSE

This chapter interprets the measured response obtained from a diagnostic load test. Before the measured data are presented, line-girder analyses of a simply-supported and a continuous beam are presented and are compared with the experimental results in a later section.

5.1 LINE-GIRDER ANALYSIS

A line girder analysis was performed to serve as a frame of reference for interpreting the measured response of the pan-girder bridge. The analysis was based on loads similar to one of the test vehicles. Two idealized support conditions were modeled: simply-supported and continuous. The simple-supported span was modelled with a span length of 29 ft. The continuous system was modelled with eleven spans with a span length of 30 ft. Figures 5.1 and 5.2 show the moment at midspan and quarter-span for simply-supported conditions as a function of the rear axle centroid for the test vehicle, respectively. Figures 5.3 through 5.6 show similar moment lines at midspan, quarter-span, the east support, and the west support for the continuous beam, respectively. The figures are discussed and compared with the experimental results later in this chapter.

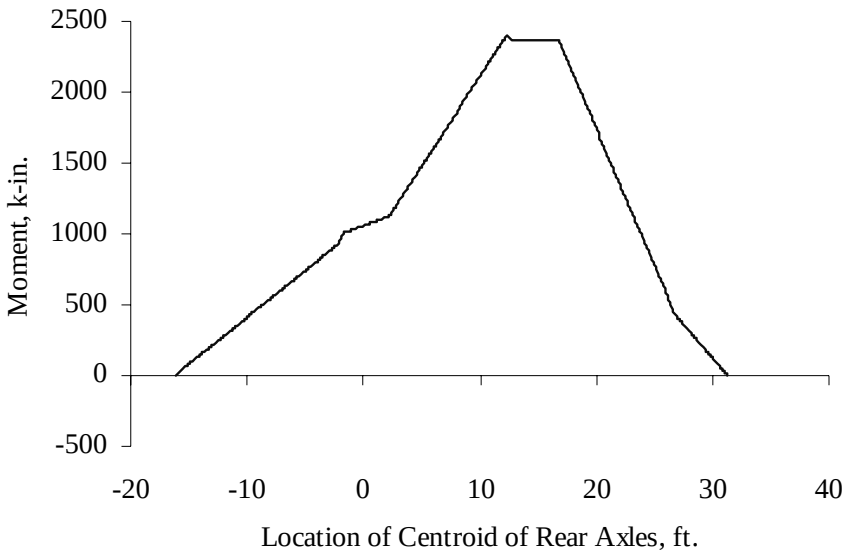

Figure 5.1 Moment Line at Midspan for a Simply-supported Beam

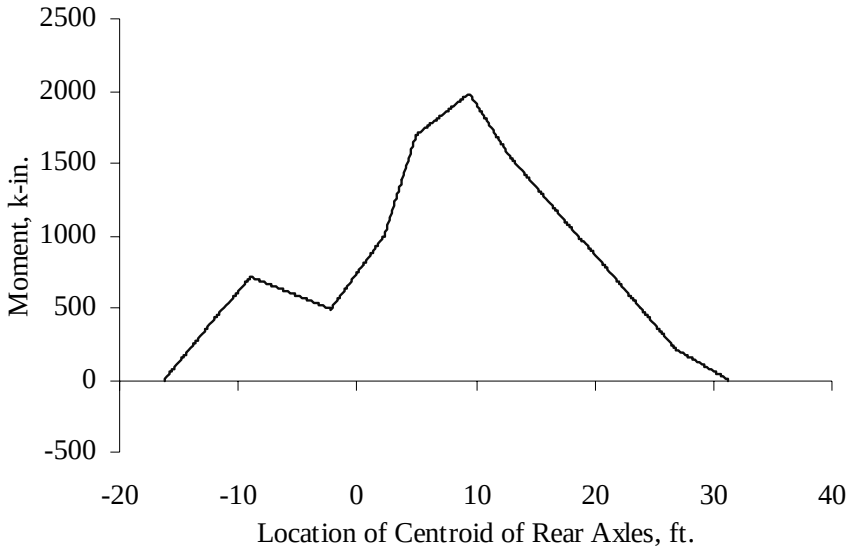

Figure 5.2 Moment Line at Quarter-Span for a Simply supported Beam

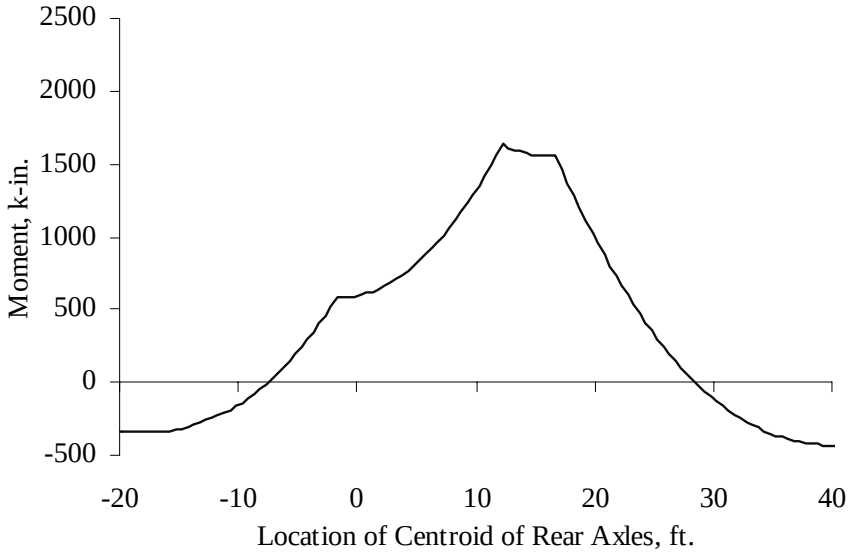

Figure 5.3 Moment Line at Midspan for a Continuous Beam

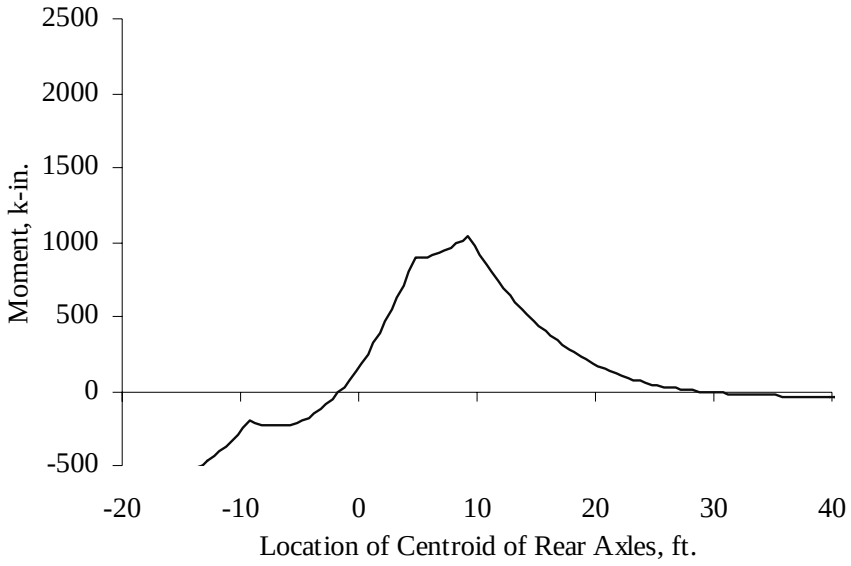

Figure 5.4 Moment Line at Quarter-Span for a Continuous Beam

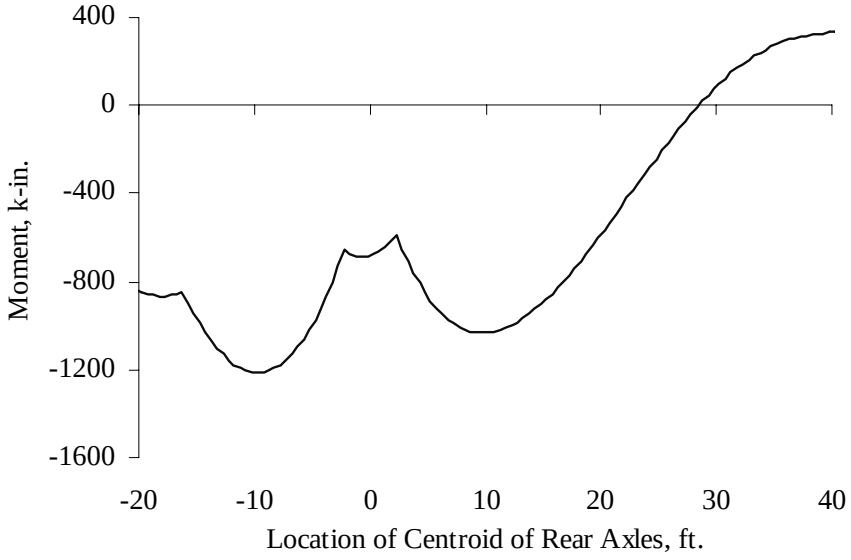

Figure 5.5 Moment Line at East Support for a Continuous Beam

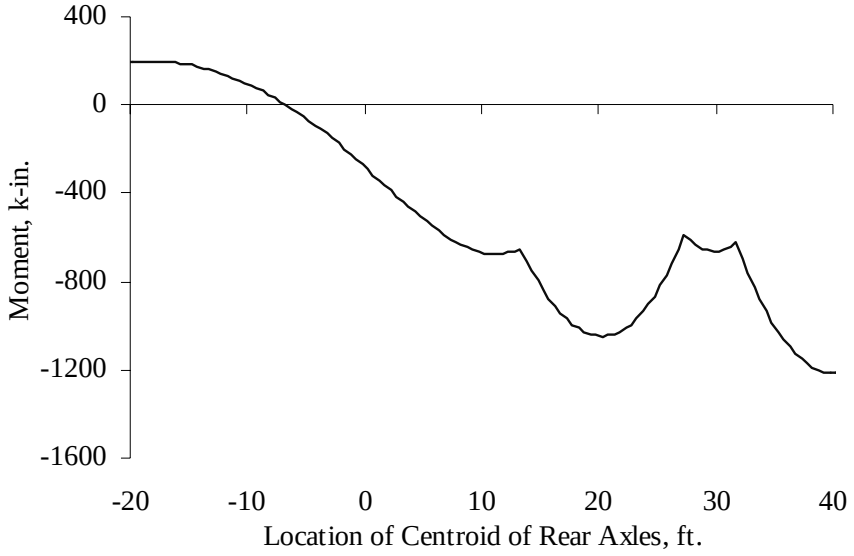

Figure 5.6 Moment Line at West Support for a Continuous Beam

5.2 EVALUATION OF MEASURED RESPONSE

The measured response was evaluated and used to study the behavior of the pan-girder bridge during the diagnostic load tests. Emphasis was placed on determining the distribution of loads among the girders and the degree of continuity provided at the supports. To assess these quantities, the moments in each girder must be calculated. Therefore, obtaining the neutral axis depth for the two typical cross sections presented in Chapter 2 was required. Neutral axis depths from the measured data were calculated and compared with those obtained from analysis. Because the data recorded during the two passes of the truck were nominally identical, strain readings obtained during pass 1 were used for all analyses, except calculation of the maximum moments in the girders, where strains from both passes were averaged.

5.2.1 Neutral Axis Depths

The neutral axis depths in the girders under service-load conditions were calculated from the measured strains in the reinforcing bars and on the surface of the concrete. A linear variation of strain with depth was assumed for all girders. Because the measured strains varied from the assumed distribution, a best-fit line was used to estimate the neutral axis depths (Figures 5.7 and 5.8).

Under ideal conditions, the strain gages used for neutral axis depth of an interior girder cross section consisted of one reinforcing bar gage and one concrete gage on each of the adjacent crowns. The strain readings from the two crown gages located at the same depth were averaged and this strain was used in the neutral axis depth calculation. The neutral axis depth for the exterior girder cross sections consisted of one reinforcing bar gage and multiple concrete gages located on the surface of the curb.

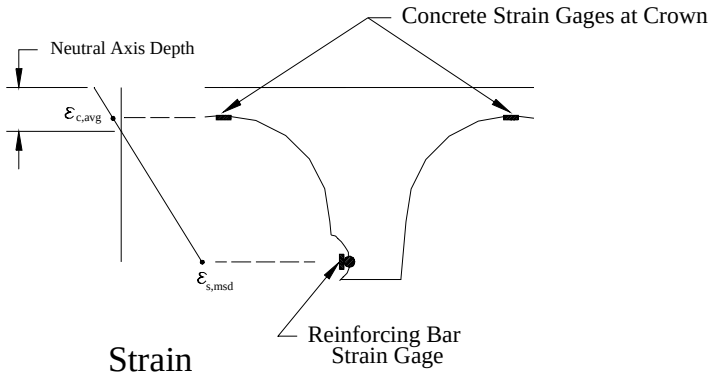

Figure 5.7 Calculation of Neutral Axis Depth for an Interior Girder Using Measured Strain Data

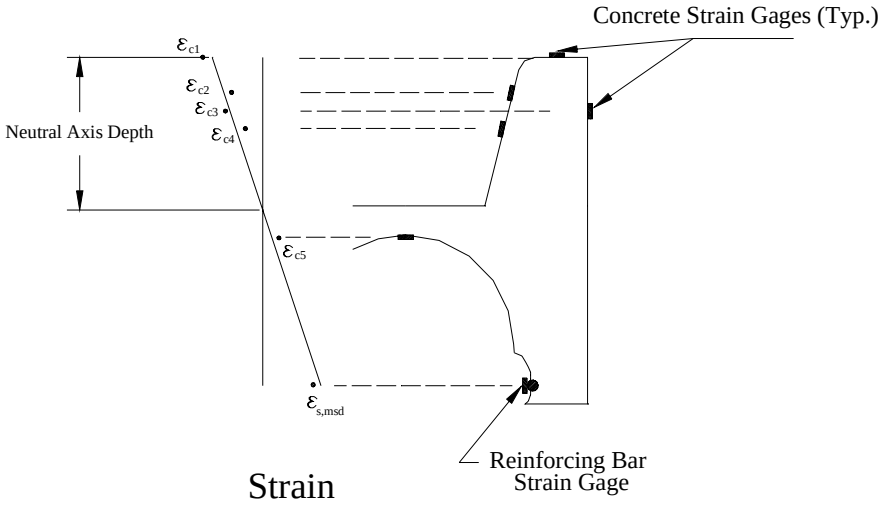

Figure 5.8 Calculation of Neutral Axis Depth for an Exterior Girder Using Measured Strain Data

The neutral axis depth as a function of longitudinal truck location was obtained for each interior and exterior girder cross section. As discussed in Chapter 4, the data from many of the concrete gages located at the crowns were unreliable. Therefore, the neutral axis depths for some of the interior girders were calculated using strain readings from one concrete gage and two concrete gages were used for other girders. The difference in neutral axis depth due to the two calculation procedures is shown in Figure 5.9 as a function of the longitudinal truck position. The bumps shown in the figure are due to the tires going over the holes in the slab. Strain readings from reinforcing bar gage RB6 and concrete gages C5 and C6 were used in the plots. No significant difference is observed in neutral axis depth for truck location 3 because the truck was positioned symmetrically with respect to the two concrete gages. But as shown in Figure 5.10, a significant difference is observed in the neutral axis depth for the same gages with the truck positioned at truck location 5. From these two figures, it appears that the neutral axis depth is sensitive to the number of concrete crown gages used in the calculation when the truck is positioned away from the measured girder.

The neutral axis depths shown in the following figures were based on the use of one or two concrete crown gages. Large variations in the neutral axis depth as a function of transverse truck location were

found for all girders. These variations are shown in Figures 5.11 and 5.12 for strains measured by reinforcing bar gages RB1 and RB6 during Test Series 2, respectively. The results from Figure 5.11 were based on the strains from at least three strain gages. Because these large variations were observed in neutral axis depths for exterior and interior girders, the neutral axis depths for each girder and all truck locations were averaged to obtain a depth used for analysis of the experimental results.

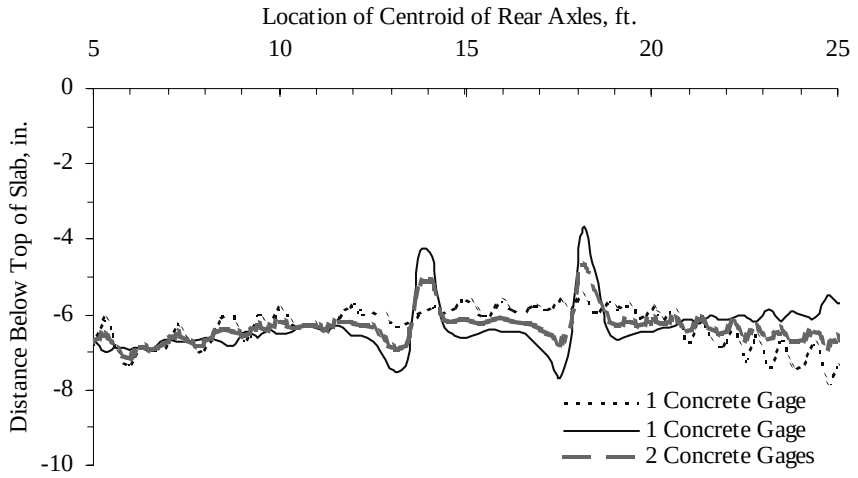

Figure 5.9 Comparison of Neutral Axis Depths in an Interior Girder Calculated Using a Different Number of Concrete Strains, Test Series 2, Truck Location 3, Pass 2

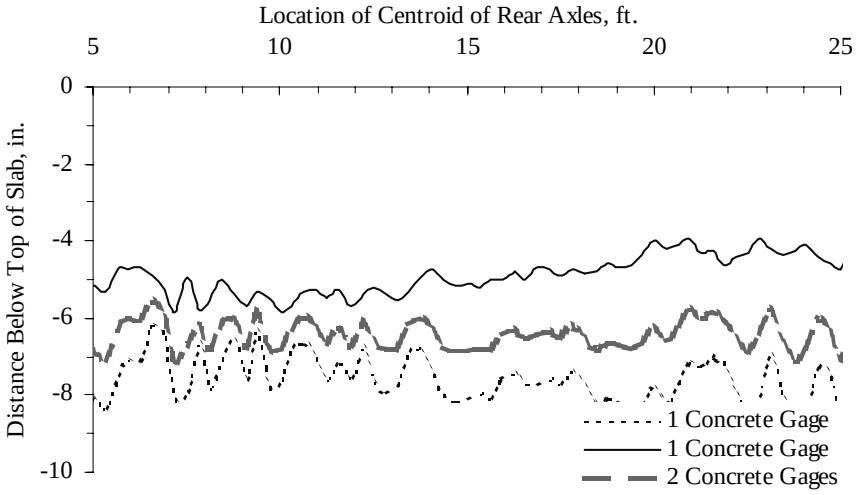

Figure 5.10 Comparison of Neutral Axis Depths in an Interior Girder Calculated Using a Different Number of Concrete Strains, Test Series 2, Truck Location 5, Pass 1

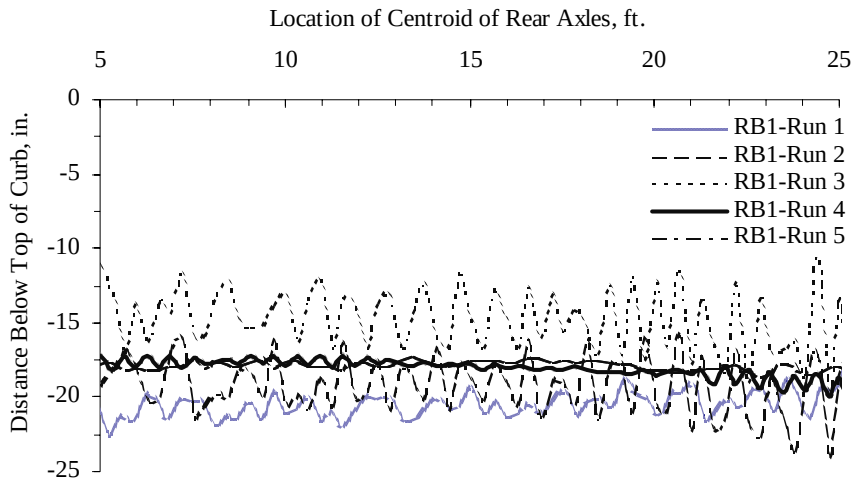

Figure 5.11 Variation in Neutral Axis Depth Calculated from Measured Strains for South Exterior Girder at Midspan

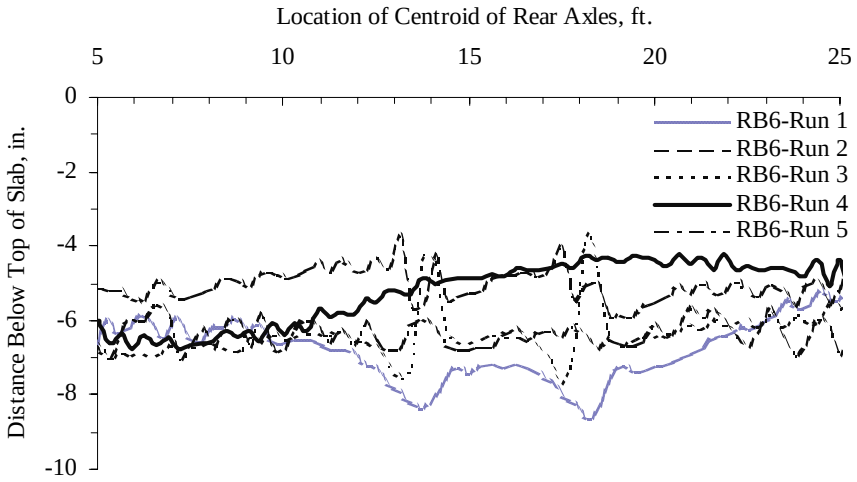

Figure 5.12 Variation in Neutral Axis Depth Calculated from Measured Strains for an Interior Girder at Midspan

Neutral axis depths for a gross and cracked section of the two cross sections were calculated based on their geometric and material properties. The modulus of elasticity used in the calculations for steel was 29,000 ksi, and for concrete it was 4,500 ksi. These values gave a modular ratio of 6.4. Table 5.1 summarizes the location of the neutral axes relative to the top of the curb or slab.

Table 5.1 Summary of Calculated Neutral Axis Depths

	Exterior Girders		Interior Girders	
Cross-Sectional Properties	Gross	Cracked	Gross	Cracked
Neutral Axis Depth*, in.	20.5	14.5	8.4	6.0

* Depth measured from top of curb for exterior girders and from top of slab for interior girders

The neutral axis depths inferred from the experimental data are presented in Figures 5.13 and 5.14. Figure 5.13 represents the average neutral axis depth for the exterior girders, which is denoted by the thick, black line. Additionally, the figure shows the calculated neutral axis depths for gross and cracked cross-sectional properties. The average depth inferred from the measured strains was approximately 18.5 in. below the top of the curb, which is bounded by the values summarized in Table 5.1. This average depth of 18.5 in. was used in all calculations involving the exterior girders.

Figure 5.14 represents the average neutral axis depth for all of the interior girders. The average depth inferred from the measured data was approximately 5.5 in. below the top of the slab, which is slightly higher than the calculated neutral axis depth corresponding to cracked cross-sectional properties. The calculated value of 6.0 in. based on cracked cross-sectional properties was considered to be more appropriate due to the large variability in the concrete strains measured at the crowns and the presence of flexural cracks at both midspan and quarter-span. The calculated neutral axis depth corresponding to cracked sections was used to calculate moments in the interior girders at midspan and the quarter-point.

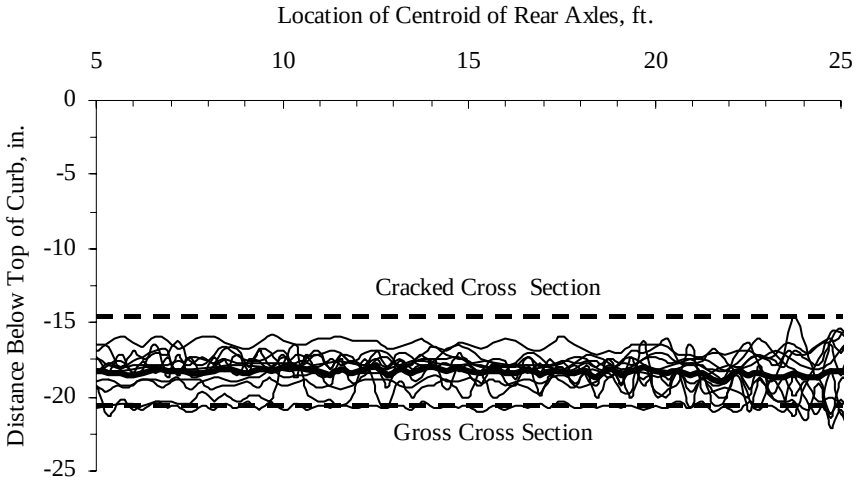

Figure 5.13 Average Neutral Axis Depth for Exterior Girders

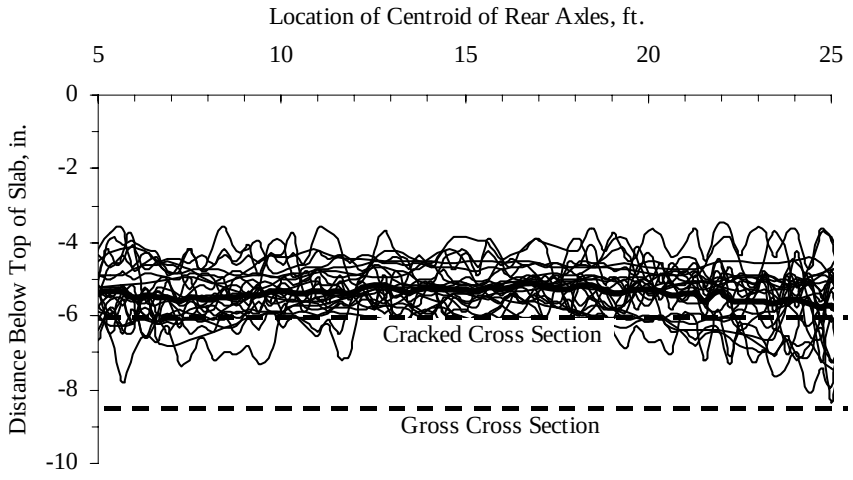

Figure 5.14 Average Neutral Axis Depth for Interior Girders

In summary, the neutral axis depths used for calculating the moments carried by each girder were obtained from analytical and experimental results. The strains from the concrete gages located at the top of the crowns experienced more variability than the strains from the concrete gages located on the curbs. Therefore, the neutral axis depth for the interior girders was based on calculated cracked cross-sectional properties, and the neutral axis depth for the curbs was based on experimental results.

5.2.2 Calculation of Moments in Girders

Determining the distribution of moments among the girders was one of the primary objectives of this investigation. The moments in each girder were calculated using the measured strains from the reinforcing bar gages and the average neutral axis depths discussed in the previous section. Plane sections were assumed to remain plane in all calculations.

Typical exterior and interior girders and the assumed distributions of stress and strain are shown in Figures 5.15 and 5.16. For analysis, each cross section was divided into 0.1-in. increments so that the strains, stresses, and ultimately the forces in each layer of concrete could be calculated. A linear relationship between stress and strain was used for both concrete and steel. This assumption was considered to be valid due to the low measured strain levels.

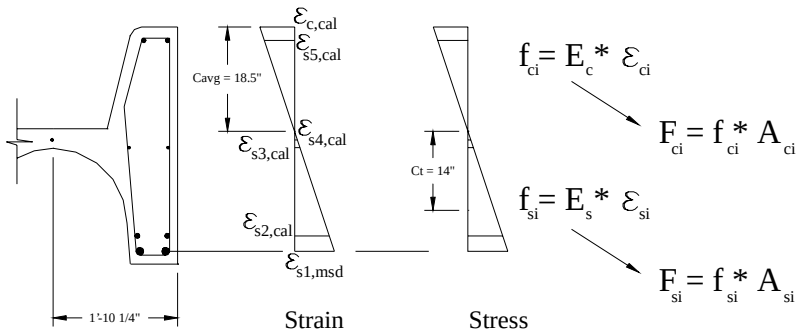

Figure 5.15 Schematic of Strains and Stresses for Calculating Moments in the Exterior Girders

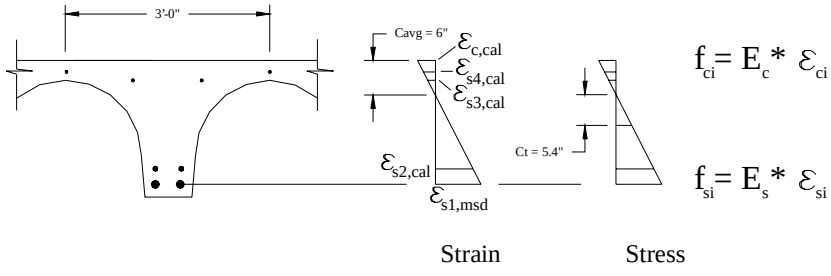

Figure 5.16 Schematic of Strains and Stresses for Calculating Moments in the Interior Girders

The following notation is used in Figures 5.15 and 5.16:

$\varepsilon_{s1,msd}$	=	strain measured in a #11 reinforcing bar
$\varepsilon_{c,cal}$	=	calculated compressive strain at the top of the curb or slab
ε_{ci}	=	calculated strain in layer i of concrete
$\varepsilon_{si,cal}$	=	calculated strains from layers of reinforcing bars
E_s	=	modulus of elasticity for steel, 29,000 ksi
E_c	=	modulus of elasticity for concrete, 4,500 ksi = $57{,}000\sqrt{f_c'}$
f_{si}	=	stress in the reinforcing bars = $E_s*\varepsilon_{si}$
f_{ci}	=	stress in each concrete layer = $E_c*\varepsilon_{ci}$
A_{si}	=	area of the reinforcing bars
A_{ci}	=	area of each concrete layer
F_{si}	=	force in each layer of reinforcing bars = $A_{si}*f_{si}$
F_{ci}	=	force in each layer of concrete = $A_{ci}*f_{ci}$
F_c	=	summation of compressive forces in concrete layers
F_t	=	tensile force in concrete required to satisfy equilibrium
f_c'	=	average compressive strength of concrete using Schmidt hammer and obtained from bottom of girder, 6,500 psi
C_{avg}	=	neutral axis depth
C_t	=	depth of concrete assumed to act in tension

For equilibrium, the summation of internal forces must equal zero. Equations 5.1 and 5.2 show the summation of forces for an exterior girder and an interior girder cross section, respectively, where tensile forces were chosen to be positive.

$$\sum F = F_{s1} + F_{s2} + F_{s3} + F_{s4} - F_{s5} - F_c + F_t = 0 \tag{5.1}$$

$$\sum F = F_{s1} + F_{s2} - F_{s3} - F_{s4} - F_c + F_t = 0 \tag{5.2}$$

In all cases, the compressive forces were larger than the tensile forces in the steel. Therefore, the tensile strength of the concrete was included in the equilibrium calculations, and the required depth of concrete in tension was determined. The same concrete modulus of elasticity was used in tension and compression.

Different values for the depth of the tension zone were calculated for the interior and exterior girders. However, these depths were found to be independent of the longitudinal and transverse position of the truck. The depth of the tensile zone was approximately 14 in. for an exterior girder, and approximately 5.4 in. for an interior girder cross section. Once equilibrium was established, the internal moments were then calculated for each girder using the calculated forces identified in Figures 5.15 and 5.16.

The total moment across the width of the bridge was determined by adding the moments in the longitudinal girders. Moment lines at midspan and quarter-span for each test series are presented in

Figures 5.17 through 5.22. Moment lines from the five transverse truck positions are shown for Test Series 2 and 3. The narrow bandwidth of the total moments indicates repeatability of the results, and that the moment lines at midspan and quarter-span are independent of transverse truck position.

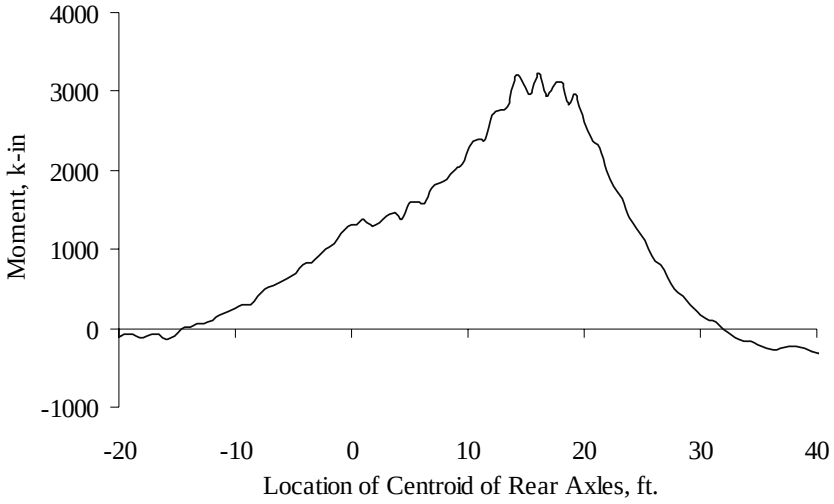

Figure 5.17 Total Moment Line at Midspan for Test Series 1

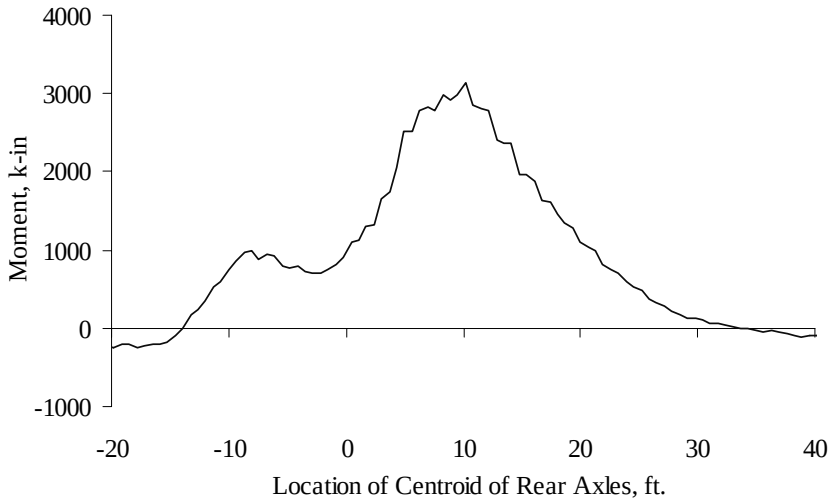

Figure 5.18 Total Moment Line at Quarter-span for Test Series 1

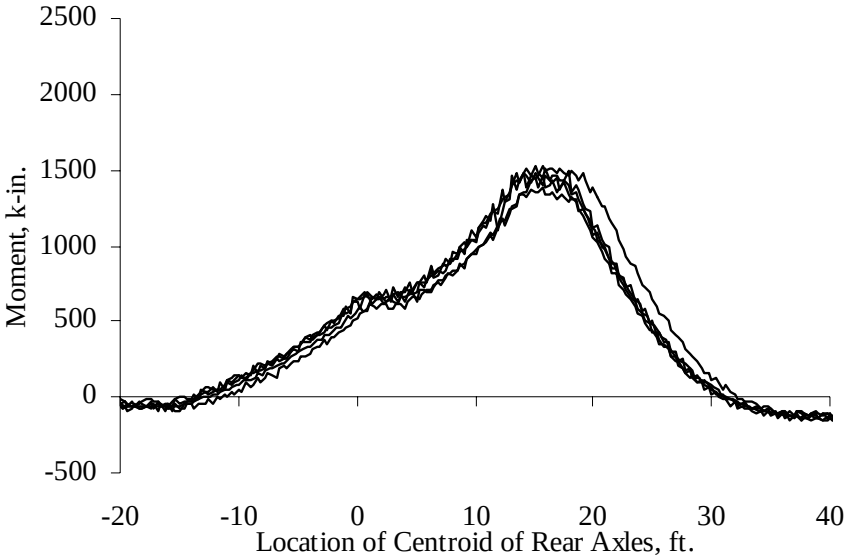

Figure 5.19 Total Moment Lines at Midspan for Test Series 2

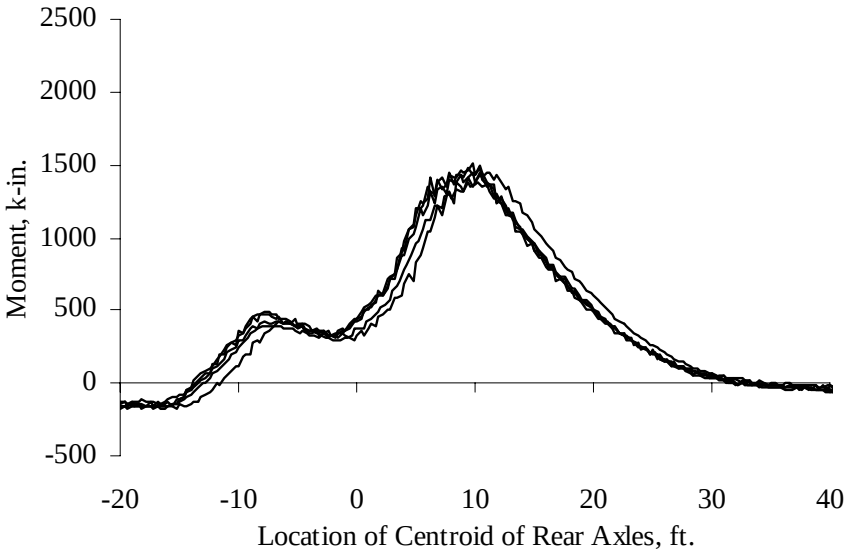

Figure 5.20 Total Moment Lines at Quarter-Span for Test Series 2

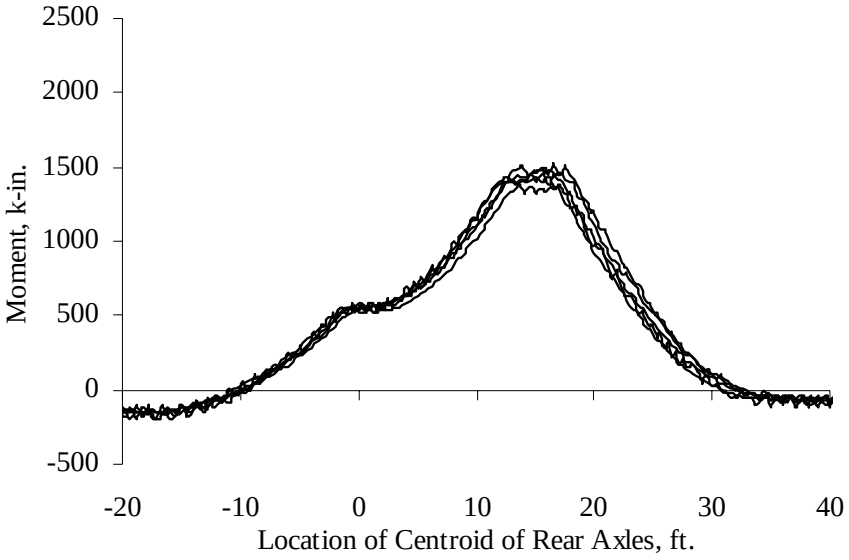

Figure 5.21 Total Moment Lines at Midspan for Test Series 3

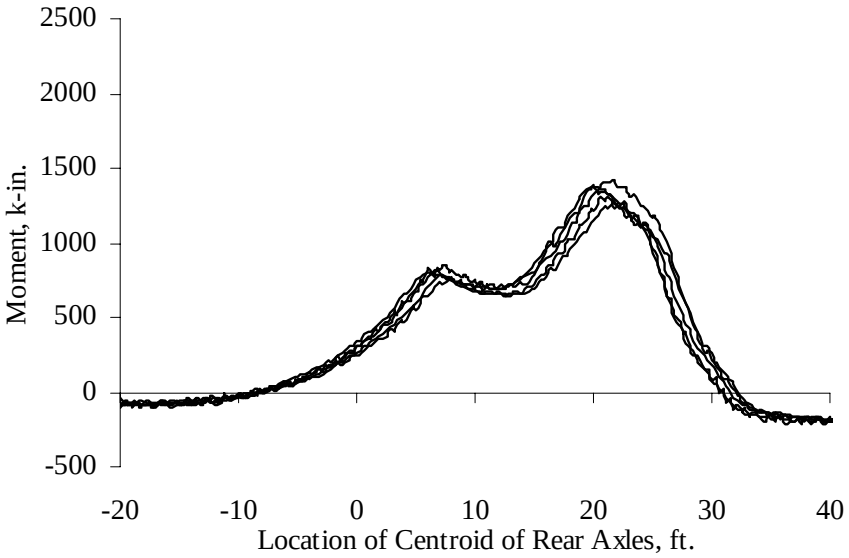

Figure 5.22 Total Moment Lines at Quarter-span for Test Series 3

In Table 4.4 of Chapter 4, reinforcing bar gage RB7Q located at the quarter-span did not produce reliable strain data. To develop the moment lines presented, the bridge was assumed to behave symmetrically. Therefore, the strains from reinforcing bar gage RB3Q were used in place of the strains for gage RB7Q. For example, strains recorded by gage RB3Q during a pass with the truck in location 1 were substituted for strains recorded by gage RB7Q during a pass with the truck in location 5. The validity of this assumption is discussed in the next section.

Summaries of the maximum moments in each girder and the maximum total moment at midspan and quarter-span are presented in Tables 5.2 and 5.3, respectively. The maximum moments at the mid- and

quarter-points were nearly the same, and such a result was unexpected. Girders 1 through 9 correspond to girders instrumented with reinforcing bar gages RB1 through RB9, respectively.

Table 5.2 Maximum Girder Moments and Total Moment at Midspan, k-in.*

Test Series	Truck Location	Girder 1	2	3	4	5	6	7	8	9	Total Moment, k-in.
1	1 & 5	511	243	333	384	406	366	343	286	452	3322
2	1	40	15	21	43	106	201	270	233	475	1404
	2	100	30	42	104	220	248	276	200	281	1500
	3	153	56	87	222	266	241	222	98	179	1524
	4	245	114	191	300	270	191	103	54	121	1588
	5	398	208	238	282	205	79	46	29	66	1550
3	1	61	20	28	65	161	244	267	232	352	1429
	2	120	42	61	170	266	248	256	124	192	1478
	3	187	82	147	285	267	223	135	66	128	1519
	4	296	167	233	278	257	122	65	39	82	1538
	5	553	245	234	281	143	52	33	23	39	1601

* Average of Pass 1 and Pass 2 Data

Table 5.3 Maximum Girder Moments and Total Moment at Quarter-span, k-in.*

Test Series	Truck Location	Girder 1	2	3	4	5	6	7	8	9	Total Moment, k-in.
1	1 & 5	449	231	296	316	384	361	296	338	474	3145
2	1	19	19	37	56	96	222	244	259	464	1416
	2	69	39	68	108	203	250	218	231	314	1500
	3	136	63	114	190	268	251	114	131	215	1482
	4	228	110	218	233	252	203	68	81	141	1534
	5	338	187	244	212	246	94	37	45	80	1483
3	1	39	25	47	68	126	244	207	256	336	1348
	2	94	49	79	141	254	230	240	139	220	1446
	3	157	73	162	218	221	230	162	87	157	1467
	4	234	138	240	196	265	122	79	55	105	1434
	5	373	196	207	204	153	61	47	29	56	1326

* Average of Pass 1 and Pass 2 Data

5.2.3 Sensitivity of Measured Response to Number of Loading Vehicles and Transverse Position of Truck

The testing program used on this bridge was designed to provide information about the linearity and the symmetry of the measured response. This information was considered important for planning instrumentation layouts in future tests. During Test Series 1, two trucks crossed the bridge simultaneously. If the bridge is responding linearly under this load, then superposition of two measured response histories during Test Series 2 and 3 when a single truck was used should equal the response during Test Series 1 (Figure 5.23). Comparison of the maximum total moment at midspan and the quarter-point are summarized in Table 5.4. The differences in the moments ranged between 8 and 16%. In all cases, the maximum moment calculated from strains measured during Test Series 1 exceeded those obtained by superimposing the responses during Test Series 2 and 3.

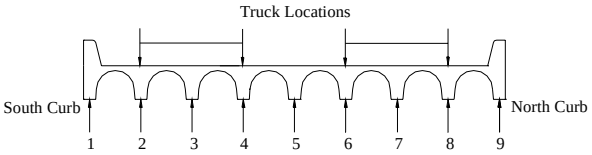

Test Series 1 equal to the sum of truck locations from Test Series 2 and 3

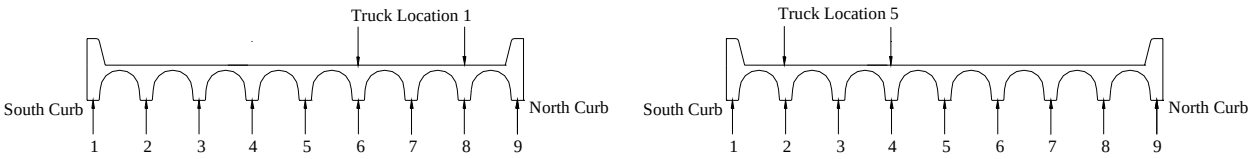

Figure 5.23 Superposition of Loads

Data from Test Series 2 and 3 could also be used to determine if the maximum moment depends on the direction of travel by the truck as it crosses the bridge. In Test Series 2, the truck traveled in the direction of the normal traffic flow in truck locations 1 and 2, while the truck traveled in the direction of normal traffic flow in truck locations 4 and 5 in Test Series 3. As summarized in Table 5.4, the maximum moment at midspan was not sensitive to the direction of the truck. Differences in moments were less that 5% in all cases. The differences were slightly larger at the quarter-point.

Table 5.4 Comparison of Total Moments for Evaluation of Bridge Symmetry

Test Series	Truck Location	Total Moment at Mid-span, k-in.	Percent Difference	Total Moment at Quarter-span, k-in.	Percent Difference
1	1 & 5	3322	11.7	3145	8.1
2	1	2954		2899	
	5				
1	1 & 5	3322	9.2	3145	16.2
3	1	3030		2674	
	5				
2	1	1404	1.8	1416	4.9
3	1	1429		1348	
2	2	1500	1.5	1500	3.7
3	2	1478		1446	
2	3	1524	0.3	1482	1.0
3	3	1519		1467	
2	4	1588	3.2	1534	6.7
3	4	1538		1434	
2	5	1550	3.2	1483	11.2
3	5	1601		1326	
2	1	1404	9.9	1416	4.6
	5	1550		1483	
2	2	1500	5.7	1500	2.2
	4	1588		1534	
3	1	1429	11.4	1348	1.6
	5	1601		1326	
3	2	1478	4.0	1446	0.8
	4	1538		1434	

The response of the bridge under unsymmetrical loading conditions could also be evaluated using the measured data from Test Series 2 and 3. As shown in Figures 5.24 and 5.25, the measured response when the truck is positioned close to the north curb should be the mirror image of the response when the truck is positioned close to the south curb. Differences in the total moment tended to be less than 10% at midspan and less than 5% at the quarter-point for these conditions.

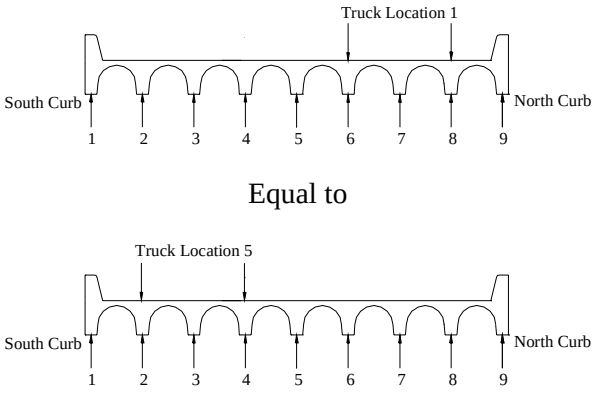

Figure 5.24 Unsymmetrical loading for Truck Locations 1 and 5

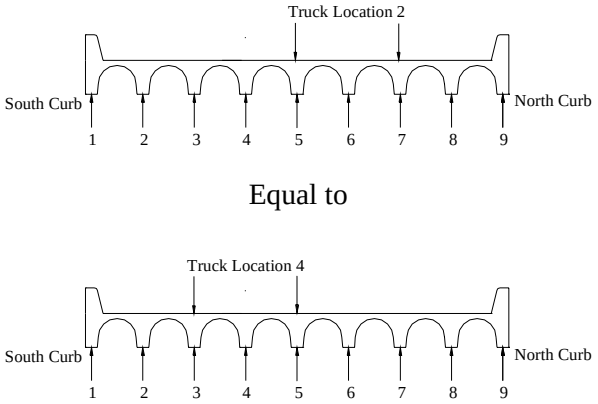

Figure 5.25 Unsymmetrical Loading for Truck Locations 2 and 4

In general, the maximum total moment in the bridge varied by less than 10% from the expected response for the comparisons discussed in this section. These differences are considered reasonable. Slight variations in the position and speed of the loading vehicle provide one possible explanation for these differences.

5.2.4 Comparison of the Moments Inferred from Measured Strains and the Results of Line-Girder Analysis

The moment lines based on line-girder analysis were presented in Section 5.1, and the moment lines based on experimental results were presented in Section 5.2.2. The moment lines are compared in this section. The calculated moment lines at midspan for simply-supported boundary conditions are plotted with the measured data in Figure 5.26, and moment lines for the continuous beam are plotted in Figure 5.27. Figures 5.28 and 5.29 compare similar moment lines at quarter-span.

Figure 5.26 shows that the experimental results do not resemble those obtained from a line-girder analysis with simply-supported ends. The maximum positive moment calculated with simple supports was approximately 60% higher than the maximum positive moments determined from the measured strains. In addition, the moment line for the simply-supported beam varied linearly with truck location whereas the measured response displayed a curved shape.

However, the moment line for moment at midspan closely resembles the results calculated using a continuous beam (Figure 5.27). The magnitudes of the maximum positive moments were within 5% and the overall shape was similar. The only difference between the two results is the amount of negative moment at midspan when the truck is located on an adjacent span. The moments at midspan with the truck on adjacent spans are higher for a continuous system than indicated by the experimental results. This indicates that the adjacent spans are not providing full rotational restraint. The east support shows less transfer of moment between adjacent spans than the west support. This behavior is consistent with expectations because a visual inspection of the two supports showed that the east support had a larger gap between adjacent spans.

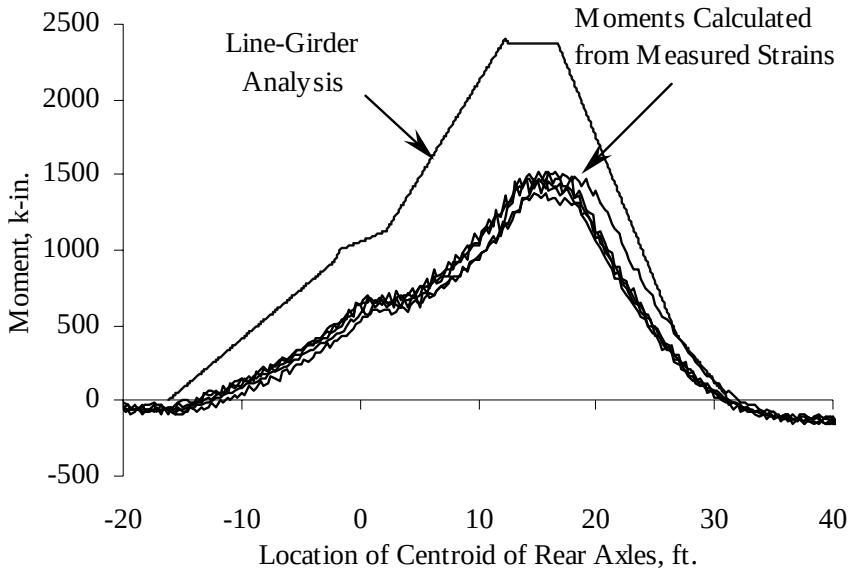

Figure 5.26 Comparison of Measured Moment Lines at Midspan with Line-Girder Analysis of a Simply-supported Beam, Test Series 2

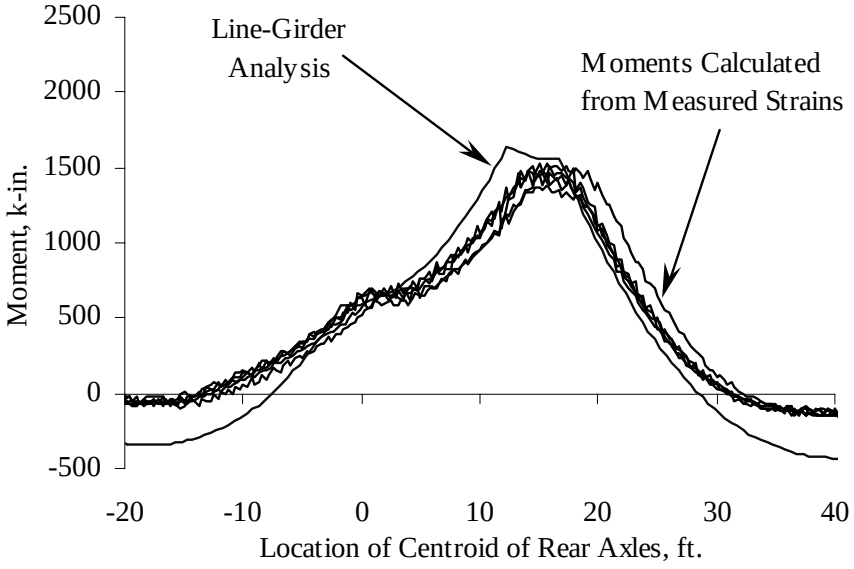

Figure 5.27 Comparison of Measured Moment Lines at Midspan with Line-Girder Analysis of a Continuous Beam, Test Series 2

Figure 5.28 shows that the experimental moment lines at quarter-span follow a similar pattern to the results based on simply-supported boundary conditions. But the maximum positive moments for the simply-supported beam exceeded the experimental moments by 33%. Figure 5.29 shows that the experimental results do not resemble the moment lines calculated for a continous beam. Neither the shape nor the amplitude of the moment lines matched.

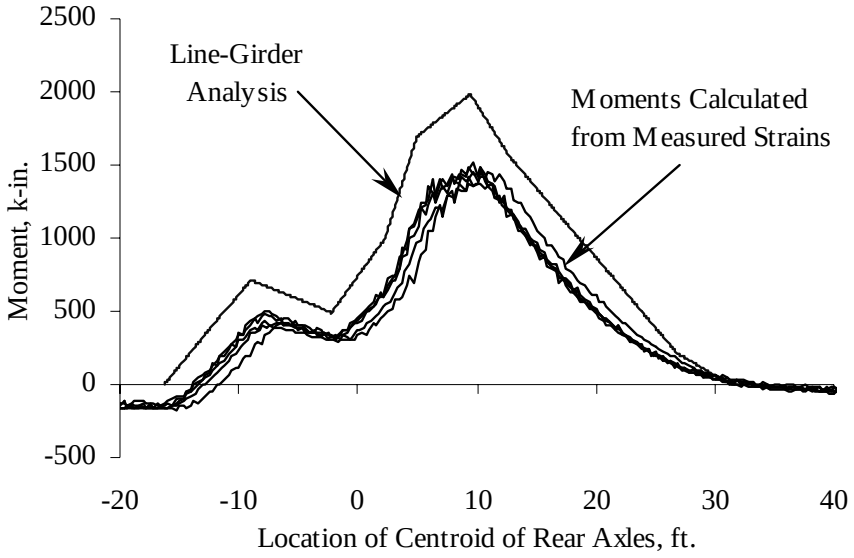

Figure 5.28 Comparison of Measured Moment Lines at Quarter-span with Line-Girder Analysis of a Simply-supported Beam, Test Series 2

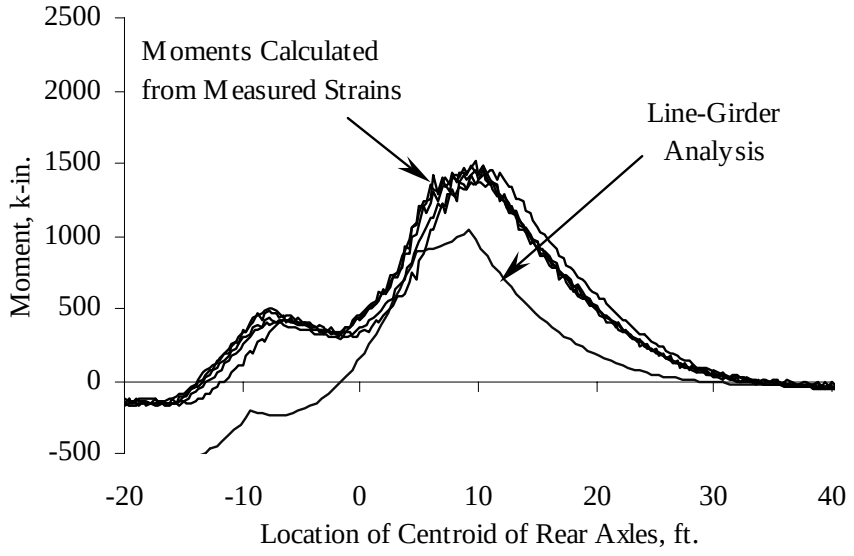

Figure 5.29 Comparison of Measured Moment Lines at Quarter-span with Line-Girder Analysis of a Continuous Beam, Test Series 2

5.2.5 Moment Distribution within Bridge

The percent of moment distributed to each girder as a function of longitudinal truck location was of interest, in addition to the distribution of load as the truck was positioned transversely across the bridge. The distribution factor in each girder was calculated as follows:

$$DF_i = \frac{M_i}{M_{total}} \tag{5.3}$$

where:

DF_i = distribution factor for girder i

M_i = moment calculated from measured strains in girder i

M_{total} = total moment across bridge calculated from measured strains $= \sum_{1}^{9} M_i$

Figures 5.30 through 5.33 present the proportion of moment that was distributed to the midspan of each girder for Test Series 1 and truck locations 1 through 3 of Test Series 2. Figures 5.34 through 5.37 correspond to the moments at quarter-span for the same test series and truck locations. The results for Test Series 3 are similar to those for Test Series 2; therefore, only Test Series 2 results are presented. Additionally, only truck locations 1 through 3 are presented because the bridge responded symmetrically during the tests.

To interpret the figures, the area of the shaded section is proportional to the percent of load carried by a girder. For example, in Figure 5.30 girders 1 and 9 are shown to carry more load than any of the individual girders because the shaded area corresponding to those girders is larger than the interior girders. The range corresponding to the horizontal axis begins when the centroid of the rear axles enters the instrumented span, and the range ends when the centroid exits the instrumented span.

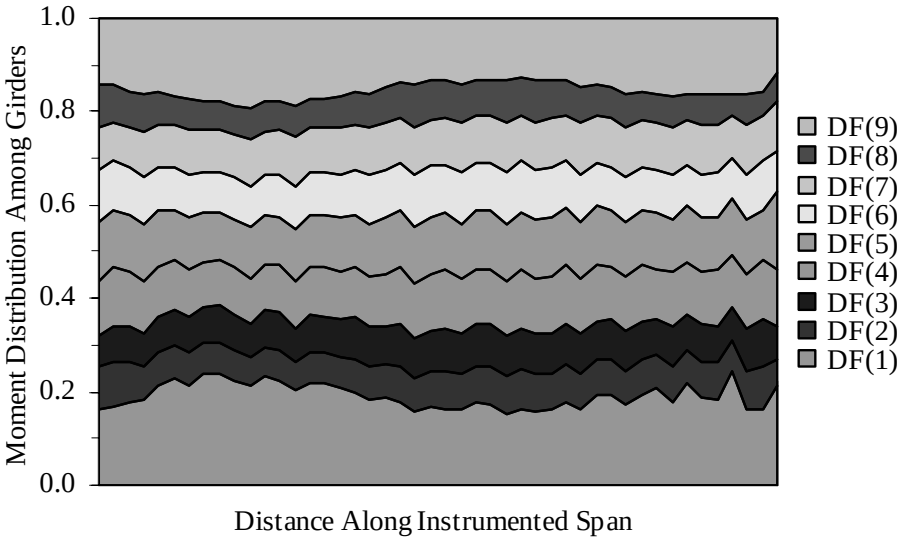

Figure 5.30 Moment Distribution at Midspan, Test Series 1

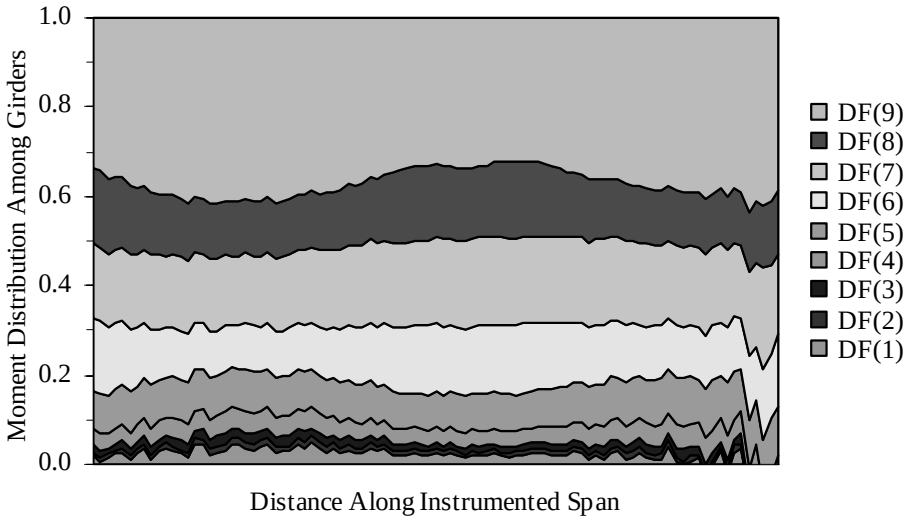

Figure 5.31 Moment Distribution at Midspan, Test Series 2, Truck Location 1

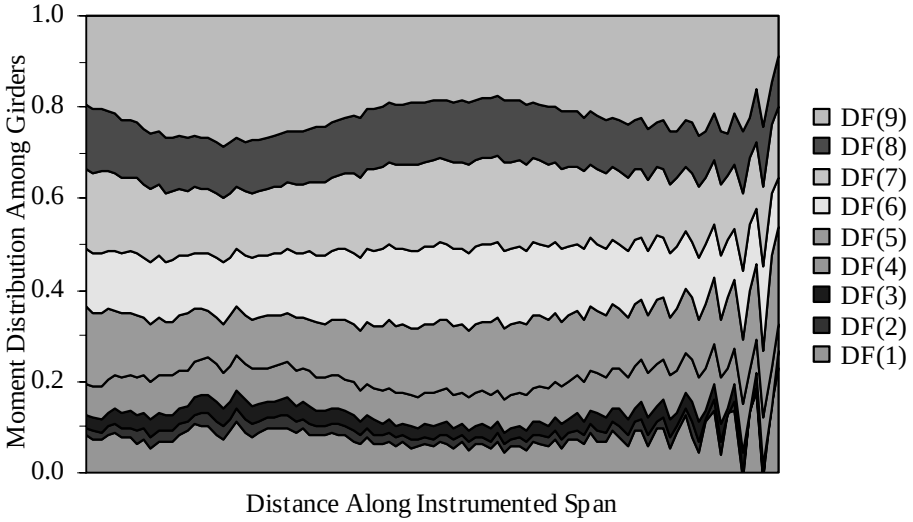

Figure 5.32 Moment Distribution at Midspan, Test Series 2, Truck Location 2

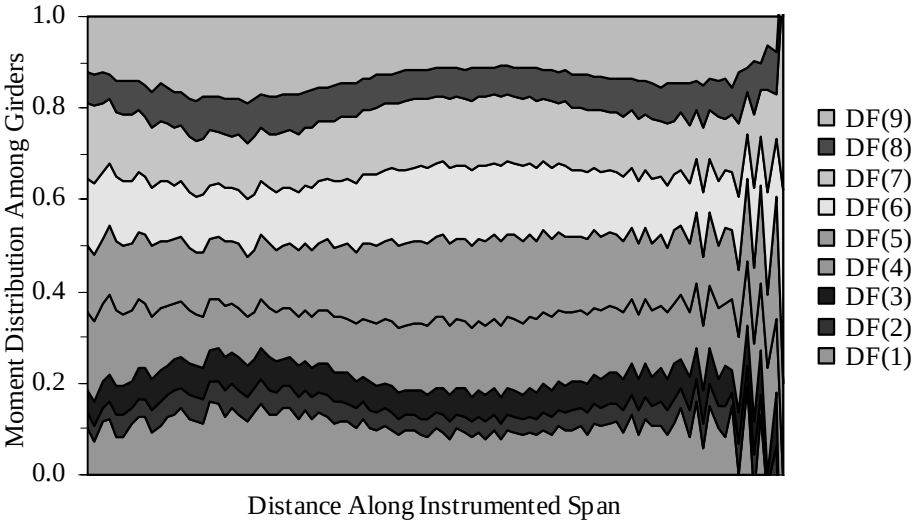

Figure 5.33 Moment Distribution at Midspan, Test Series 2, Truck Location 3

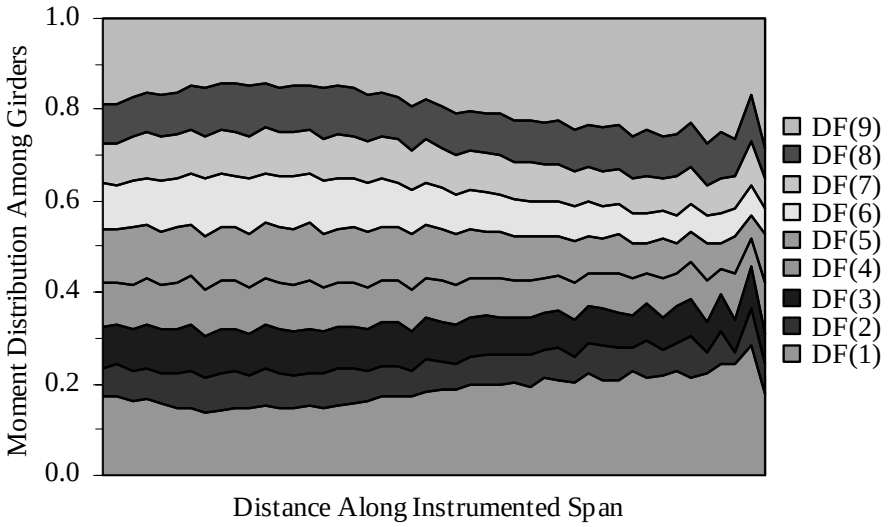

Figure 5.34 Moment Distribution at Quarter-span, Test Series 1

Figure 5.35 Moment Distribution at Quarter-span, Test Series 2, Truck Location 1

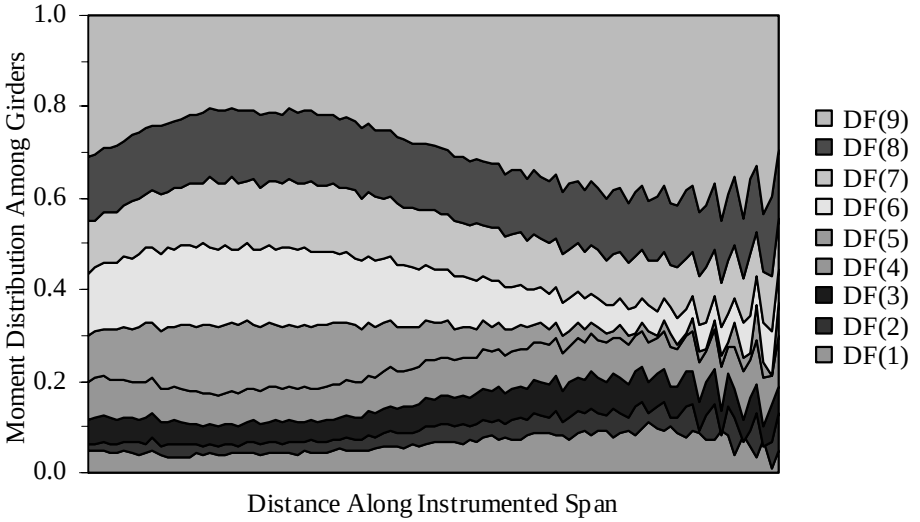

Figure 5.36 Moment Distribution at Quarter-span, Test Series 2, Truck Location 2

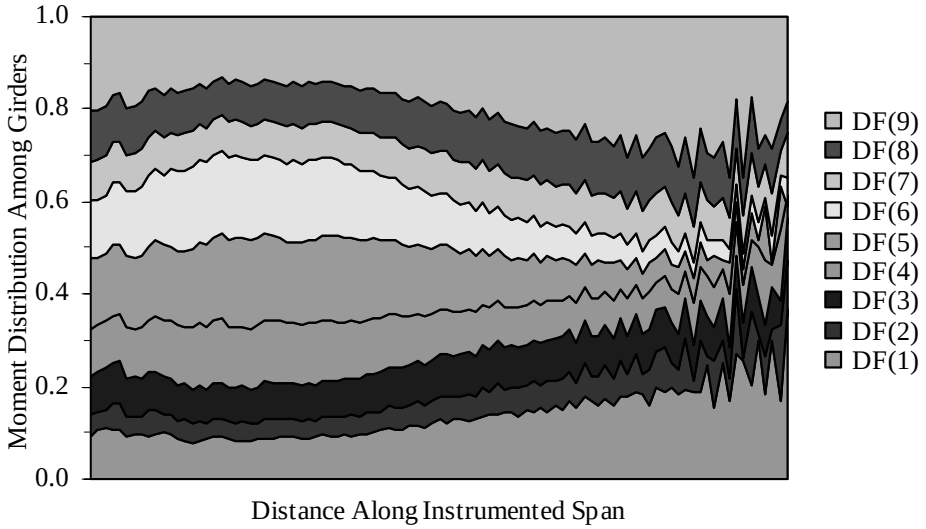

Figure 5.37 Moment Distribution at Quarter-span, Test Series 2, Truck Location 3

The peaks observed at each end of the instrumented span are due to the small amplitude of the strains and noise in the response histories, which represent a large percent of error. Therefore, emphasis should be placed in the central regions of the plots where the boundaries are smoother and the measured strains are larger. The exterior girders are shown to carry a large portion of the total moment for truck locations 1 and 5. But even as the truck moves transversely across the width of the bridge, the exterior girders carry more moment than the interior girders located closer to the truck. The larger distribution of moment to the exterior girders is consistent with the larger stiffness of the girders due to the contribution of the curbs. The maximum and average distribution factors for the above figures are presented in Tables 5.5 and 5.6 for midspan and in Tables 5.7 and 5.8 for quarter-span, respectively. The shaded cells correspond to girders located directly below the truck. Emphasis is placed on the distribution factors that are shaded.

Table 5.5 Maximum Distribution Factors for the Girders at Midspan, Pass 1

Test Series	Truck Location	Girder								
		1	2	3	4	5	6	7	8	9
1	1 & 5	0.24	0.08	0.09	0.13	0.13	0.11	0.11	0.09	0.19
2	1	0.05	0.02	0.03	0.06	0.11	0.16	0.20	0.17	0.42
	2	0.12	0.03	0.04	0.10	0.16	0.17	0.19	0.14	0.28
	3	0.16	0.06	0.08	0.16	0.18	0.17	0.15	0.09	0.19
	4	0.23	0.10	0.12	0.20	0.18	0.14	0.10	0.05	0.12
	5	0.36	0.15	0.16	0.19	0.14	0.07	0.05	0.03	0.07
3	1	0.07	0.03	0.03	0.07	0.12	0.18	0.20	0.17	0.36
	2	0.17	0.05	0.06	0.12	0.19	0.18	0.18	0.10	0.24
	3	0.21	0.08	0.10	0.20	0.18	0.15	0.10	0.07	0.16
	4	0.33	0.12	0.16	0.20	0.18	0.10	0.07	0.04	0.13
	5	0.48	0.16	0.16	0.19	0.11	0.05	0.04	0.03	0.05

Table 5.6 Average Distribution Factors for the Girders at Midspan, Pass 1

Test Series	Truck Location	Girder								
		1	2	3	4	5	6	7	8	9
1	1 & 5	0.19	0.07	0.08	0.11	0.12	0.10	0.10	0.07	0.15
2	1	0.02	0.01	0.02	0.04	0.09	0.13	0.18	0.14	0.37
	2	0.07	0.02	0.03	0.08	0.14	0.15	0.17	0.12	0.22
	3	0.11	0.04	0.06	0.14	0.16	0.14	0.13	0.07	0.14
	4	0.18	0.08	0.11	0.18	0.15	0.11	0.07	0.04	0.09
	5	0.29	0.12	0.14	0.17	0.12	0.06	0.04	0.02	0.05
3	1	0.05	0.02	0.02	0.05	0.11	0.14	0.18	0.13	0.30
	2	0.10	0.03	0.05	0.11	0.15	0.15	0.15	0.09	0.17
	3	0.15	0.06	0.09	0.16	0.16	0.12	0.09	0.05	0.11
	4	0.23	0.10	0.12	0.18	0.14	0.08	0.05	0.03	0.07
	5	0.39	0.13	0.14	0.15	0.09	0.04	0.02	0.01	0.03

Table 5.7 Maximum Distribution Factors for the Girders at Quarter-span, Pass 1

Test Series	Truck Location	Girder								
		1	2	3	4	5	6	7	8	9
1	1 & 5	0.23	0.08	0.10	0.11	0.12	0.12	0.10	0.11	0.26
2	1	0.05	0.04	0.06	0.08	0.08	0.18	0.20	0.21	0.48
	2	0.11	0.07	0.08	0.09	0.15	0.18	0.16	0.16	0.42
	3	0.20	0.11	0.09	0.14	0.19	0.18	0.09	0.12	0.35
	4	0.34	0.11	0.15	0.16	0.17	0.14	0.08	0.11	0.19
	5	0.38	0.13	0.18	0.15	0.17	0.07	0.04	0.07	0.14
3	1	0.05	0.03	0.06	0.07	0.11	0.22	0.17	0.21	0.39
	2	0.11	0.05	0.08	0.11	0.20	0.18	0.21	0.13	0.26
	3	0.18	0.08	0.12	0.17	0.16	0.18	0.12	0.10	0.19
	4	0.27	0.11	0.20	0.16	0.20	0.10	0.08	0.07	0.13
	5	0.38	0.19	0.18	0.18	0.15	0.07	0.06	0.04	0.07

Table 5.8 Average Distribution Factors for the Girders at Quarter-span, Pass 1

Test Series	Truck Location	Girder								
		1	2	3	4	5	6	7	8	9
1	1 & 5	0.18	0.07	0.09	0.09	0.11	0.09	0.09	0.10	0.19
2	1	0.02	0.02	0.04	0.06	0.05	0.12	0.16	0.16	0.39
	2	0.07	0.03	0.06	0.08	0.08	0.12	0.13	0.15	0.30
	3	0.13	0.05	0.08	0.10	0.13	0.11	0.08	0.10	0.20
	4	0.22	0.08	0.12	0.11	0.12	0.09	0.06	0.07	0.13
	5	0.28	0.11	0.13	0.12	0.15	0.07	0.03	0.04	0.07
3	1	0.03	0.02	0.04	0.06	0.08	0.15	0.14	0.17	0.31
	2	0.08	0.04	0.07	0.10	0.14	0.14	0.14	0.11	0.20
	3	0.14	0.06	0.11	0.12	0.13	0.12	0.11	0.08	0.13
	4	0.21	0.09	0.14	0.12	0.16	0.09	0.07	0.05	0.09
	5	0.33	0.13	0.14	0.12	0.12	0.06	0.04	0.03	0.04

As presented in Chapter 1, the load distribution factor, K_A, is related to a constant C for design. This constant may be determined from the measured data. From the above distribution factors summarized in Tables 5.5 through 5.8, the minimum and average C values corresponding to the midspan and the quarter-

span of all nine girders were calculated. The equation used to calculate the C value for each girder is as follows:

$$C_i = \frac{S}{N_w} * \frac{1}{DF_i} \tag{5.4}$$

where:

C_i = constant for girder i

S = average spacing between girders = 3 ft.

N_w = number of wheel lines = 4 for Test Series 1, and
the number of wheel lines = 2 for Test Series 2 and 3

DF_i = maximum or average percent of moment distributed to girder i

The minimum C values were calculated using the maximum percent of moment distributed to each girder when the truck was located at a longitudinal distance between 5 and 25 ft of the instrumented span. This range was selected to avoid the peaks observed at each end of the span. The average C values were calculated to avoid the influence of the peaks in obtaining the maximum moment distribution to a girder. Tables 5.9 and 5.10 summarize the minimum and average C values corresponding to midspan, while Tables 5.11 and 5.12 present the minimum and average C values corresponding to the quarter-span, respectively. The shaded cells correspond to girders located directly below the truck.

Table 5.9 Minimum C Values for the Girders at Midspan, Pass 1

Test Series	Truck Location	Girder								
		1	2	3	4	5	6	7	8	9
1	1 & 5	3.1	9.0	8.1	6.0	6.0	6.6	6.9	8.3	3.9
2	1	31.3	93.8	57.7	27.3	13.9	9.7	7.5	8.6	3.6
	2	12.1	50.0	36.6	15.5	9.3	8.8	7.8	10.9	5.3
	3	9.5	23.8	19.0	9.4	8.2	9.0	9.8	16.7	7.9
	4	6.4	14.6	12.1	7.4	8.2	11.1	15.5	30.0	12.2
	5	4.2	10.3	9.4	7.7	10.7	22.4	31.9	46.9	21.7
3	1	21.4	57.7	45.5	23.1	12.7	8.5	7.6	8.8	4.2
	2	8.9	31.3	24.2	12.4	8.1	8.6	8.3	14.7	6.4
	3	7.0	19.0	14.4	7.5	8.2	9.8	14.4	20.8	9.4
	4	4.6	12.9	9.1	7.6	8.3	15.8	23.1	34.1	11.4
	5	3.1	9.1	9.6	8.1	14.3	28.8	37.5	53.6	31.9

Table 5.10 Average C Values for the Girders at Midspan, Pass 1

Test Series	Truck Location	Girder								
		1	2	3	4	5	6	7	8	9
1	1 & 5	4.0	10.3	9.0	6.6	6.4	7.7	7.4	10.4	4.9
2	1	62.5	136.4	88.2	36.6	17.0	11.6	8.2	10.6	4.1
	2	20.3	71.4	46.9	19.2	11.1	9.9	9.0	12.4	6.8
	3	13.6	34.9	23.8	11.0	9.3	10.5	11.2	20.8	10.9
	4	8.6	18.8	13.9	8.5	9.7	13.6	21.1	39.5	17.4
	5	5.1	12.2	10.9	8.9	12.6	26.3	42.9	75.0	31.3
3	1	31.9	88.2	65.2	28.8	13.9	10.8	8.4	11.3	5.0
	2	15.6	44.1	31.9	14.0	10.2	9.8	9.9	16.5	8.7
	3	10.3	24.2	16.5	9.3	9.3	12.1	16.3	30.0	13.5
	4	6.6	14.6	12.2	8.6	10.9	18.3	30.0	53.6	20.5
	5	3.9	11.3	10.9	9.9	16.9	40.5	65.2	115.4	50.0

Table 5.11 Minimum C Values for the Girders at Quarter-span, Pass 1

Test Series	Truck Location	Girder								
		1	2	3	4	5	6	7	8	9
1	1 & 5	3.3	9.0	7.6	7.1	6.1	6.1	7.6	6.8	2.9
2	1	30.0	37.5	25.0	19.5	20.0	8.2	7.7	7.1	3.1
	2	13.6	22.7	18.5	16.5	9.9	8.4	9.7	9.4	3.6
	3	7.5	13.4	16.1	11.0	7.8	8.3	16.1	12.3	4.3
	4	4.5	13.2	10.2	9.3	8.6	10.4	18.5	13.4	7.9
	5	4.0	11.4	8.5	9.9	8.6	20.3	39.5	22.7	10.6
3	1	33.3	46.9	26.8	20.5	14.0	6.8	9.0	7.1	3.8
	2	13.9	29.4	18.1	14.0	7.6	8.2	7.2	11.6	5.7
	3	8.2	18.8	12.7	9.0	9.2	8.2	12.7	15.5	8.0
	4	5.6	13.5	7.4	9.4	7.5	15.5	17.9	21.4	11.5
	5	4.0	8.1	8.5	8.5	10.3	22.1	26.8	40.5	22.4

Table 5.12 Average C Values for the Girders at Quarter-span, Pass 1

Test Series	Truck Location	Girder								
		1	2	3	4	5	6	7	8	9
1	1 & 5	4.1	10.9	8.6	8.3	7.1	8.1	8.6	7.7	3.9
2	1	75.0	88.2	38.5	27.3	27.8	12.4	9.7	9.7	3.9
	2	22.7	44.1	25.0	19.0	18.5	13.0	12.0	10.3	5.1
	3	11.6	28.8	17.9	14.7	11.6	13.3	17.9	14.6	7.4
	4	7.0	18.8	12.3	13.2	12.7	16.7	25.4	20.3	11.7
	5	5.3	14.2	11.6	12.9	9.9	22.7	48.4	34.9	20.3
3	1	50.0	75.0	35.7	25.9	18.8	10.1	10.6	9.0	4.8
	2	19.5	41.7	23.1	15.8	10.7	10.8	10.7	13.3	7.7
	3	10.8	26.3	13.5	12.4	11.7	12.1	13.5	20.0	11.2
	4	7.3	16.1	10.6	12.7	9.7	17.6	22.7	30.0	17.0
	5	4.6	11.7	10.6	12.5	12.1	26.8	35.7	55.6	41.7

The C values in Tables 5.9 and 5.11 are smaller than those in Tables 5.10 and 5.12. Smaller values indicate that the girder is carrying more moment. Each girder carries its maximum moment when the truck straddles the girder or a wheel line is directly over the girder. The C values corresponding to the

exterior girders are much smaller than the interior girders even when the truck is positioned away from the exterior girder.

Overall, the majority of the load is distributed to the girders immediately adjacent to the truck wheels and the percent carried decreases with distance. But the exterior girders carry a significant portion of the load for all truck positions.

5.2.6 Continuity at Supports

The degree of continuity at the supports was unknown. In order to quantify the rotational restraint at the supports, the bridge was instrumented at two locations: midspan and the quarter-span. The reason for instrumenting the two locations was to use internal moments obtained at those locations to calculate the moment at the east support, and ultimately the moment at the west support, as shown in Figure 5.38. Moments at the midspan and the quarter-span corresponding to tandem axle locations between 18 ft. and 30 ft. were obtained. The reason for this range was because the shears at the section between midspan and the east support would be equal, and thus the end moment could be easily calculated.

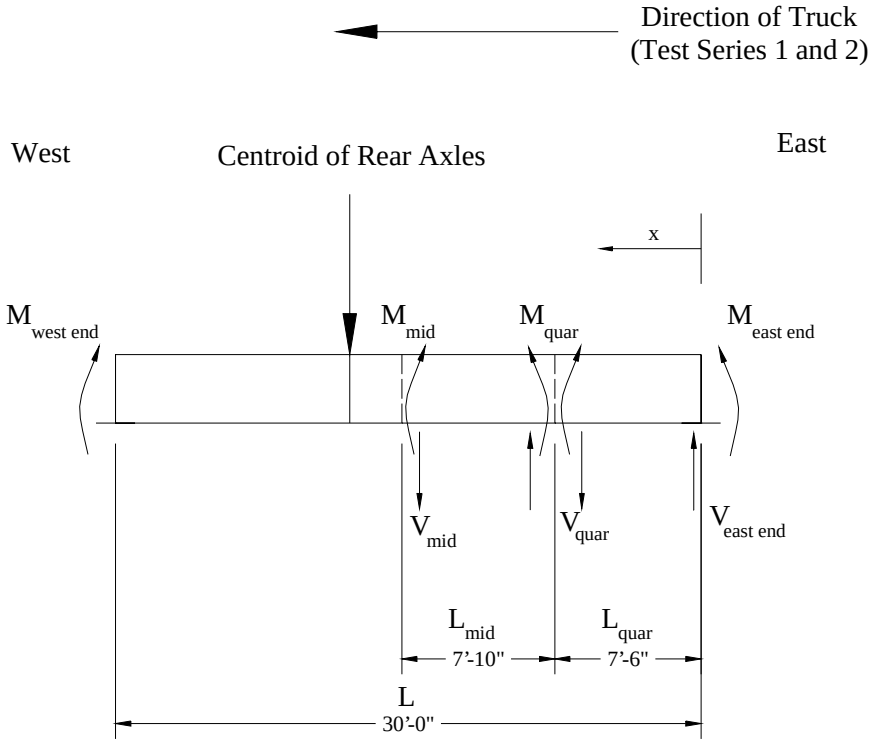

Figure 5.38 Diagram of Calculation for End Moment

To calculate the end moment at the east support due to live loads, Equations 5.6 and 5.7 were used. The end moment at the west support for a longitudinal truck location between 18 ft. and 30 ft. was calculated using Equation 5.8. The shears in the east half of the span were taken to be equal as shown in Equation 5.5:

$$V_{mid} = V_{quar} = V_{east,end} \tag{5.5}$$

$$V_{quar} = \frac{M_{mid} - M_{quar}}{L_{mid}} \tag{5.6}$$

$$\sum M = M_{quar} - V_{quar} * L_{quar} - M_{east,end} = 0 \tag{5.7}$$

$$\sum M = M_{west,end} + P * (L - x) - M_{east,end} - V_{east,end} * L = 0 \tag{5.8}$$

where:

V_{mid}	=	shear at midspan
V_{quar}	=	shear at quarter-span
$V_{east\ end}$	=	shear at east support
M_{mid}	=	moment at midspan
M_{quar}	=	moment at quarter-span
$M_{east\ end}$	=	moment at east support
$M_{west\ end}$	=	moment at west support
L_{mid}	=	length of section between 7.5 ft. and 15.3 ft.
L_{quar}	=	length of section between 0 ft. and 7.5 ft. measured from the end of the span
L	=	length of instrumented span
P	=	combined rear axle weight = 32.2 kips

Figures 5.39 through 5.44 show the end moment at the east support inferred from the measured data as a function of longitudinal truck location. Only end moments based on data from pass 1 of Test Series 1 and 2 were used for the analysis. Equation 5.5 is not valid in Test Series 3 because the direction of travel was reversed. Positive moments are plotted as positive numbers in these figures.

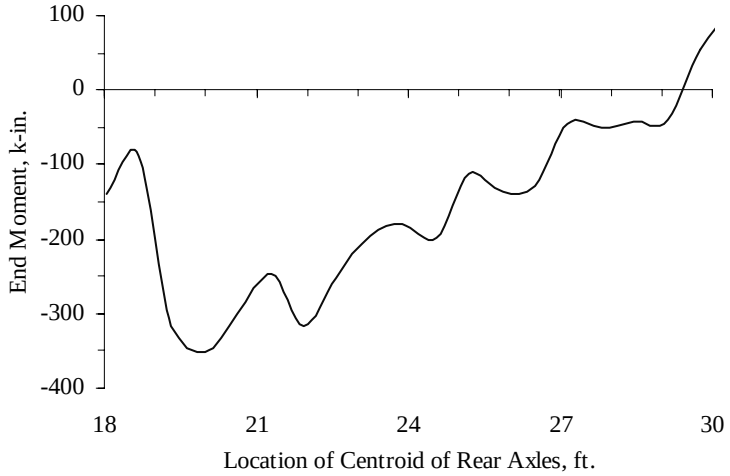

Figure 5.39 End Moment at East Support, Test Series 1

Figure 5.40 End Moment at East Support, Test Series 2, Truck Location 1

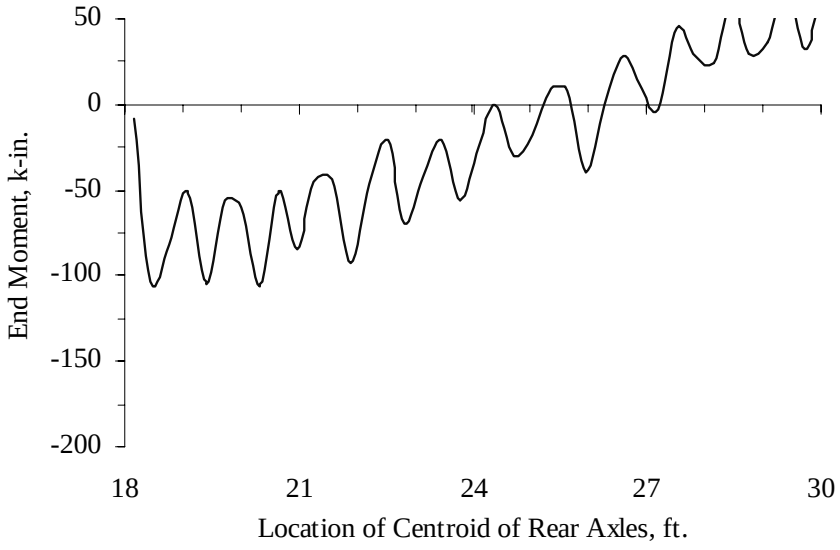

Figure 5.41 End Moment at East Support, Test Series 2, Truck Location 2

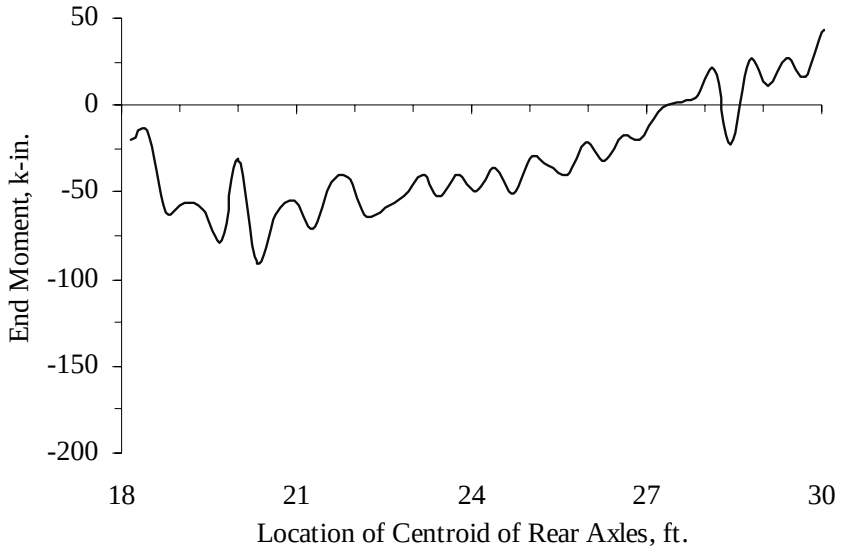

Figure 5.42 End Moment at East Support, Test Series 2, Truck Location 3

Figure 5.43 End Moment at East Support, Test Series 2, Truck Location 4

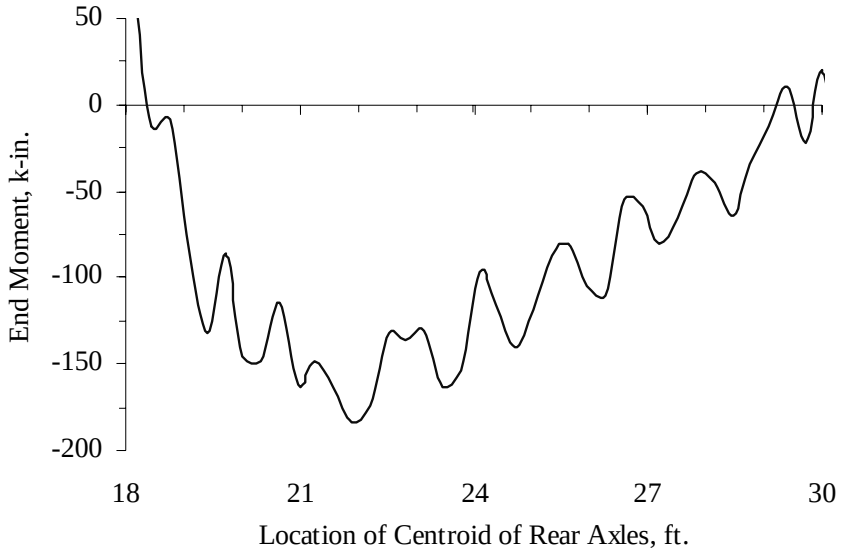

Figure 5.44 End Moment at East Support, Test Series 2, Truck Location 5

As the figures show, rotational restraint was observed at the east support. Figure 5.39 shows the maximum end moment to be approximately 350 kip-in. when the centroid of the rear axles was located at 19 ft. from the east support. For truck locations 1 through 3 for Test Series 2, the maximum end moment was approximately 100 kip-in. Truck locations 4 and 5 had maximum end moments of about 150 kip-in.

Figure 5.45 through 5.50 show the end moments at the west support as a function of longitudinal truck location inferred from the end moments and shears at the east support.

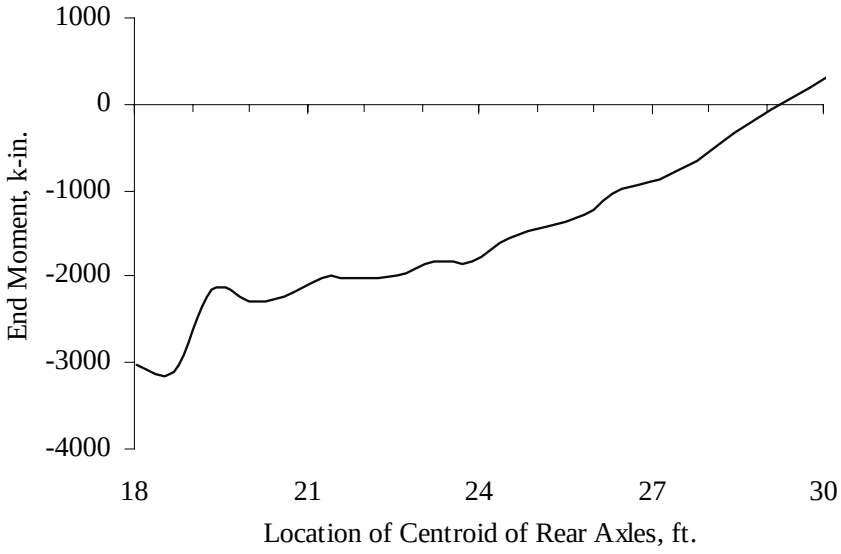

Figure 5.45 End Moment at West Support, Test Series 1

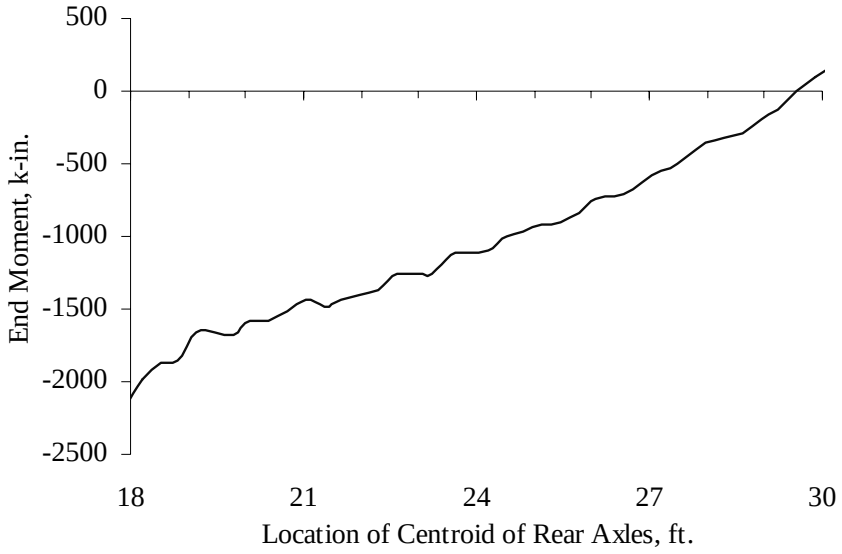

Figure 5.46 End Moment at West Support, Test Series 2, Truck Location 1

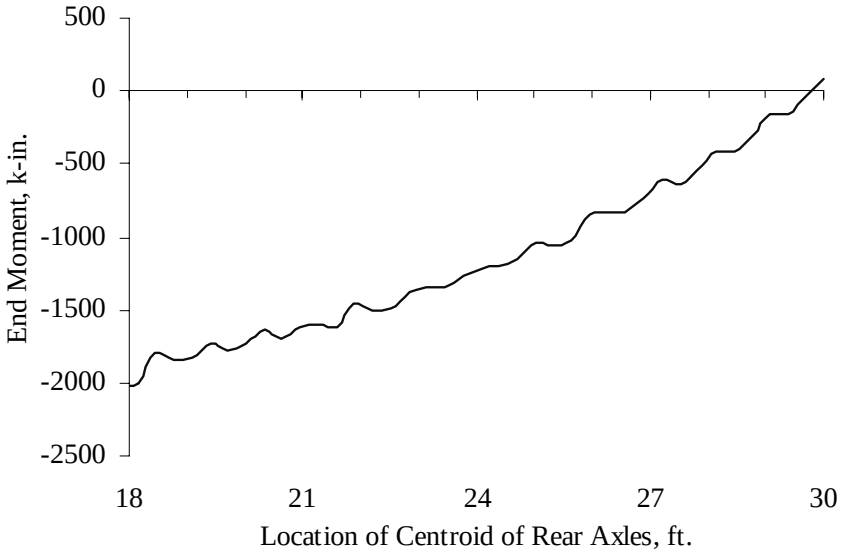

Figure 5.47 End Moment at West Support, Test Series 2, Truck Location 2

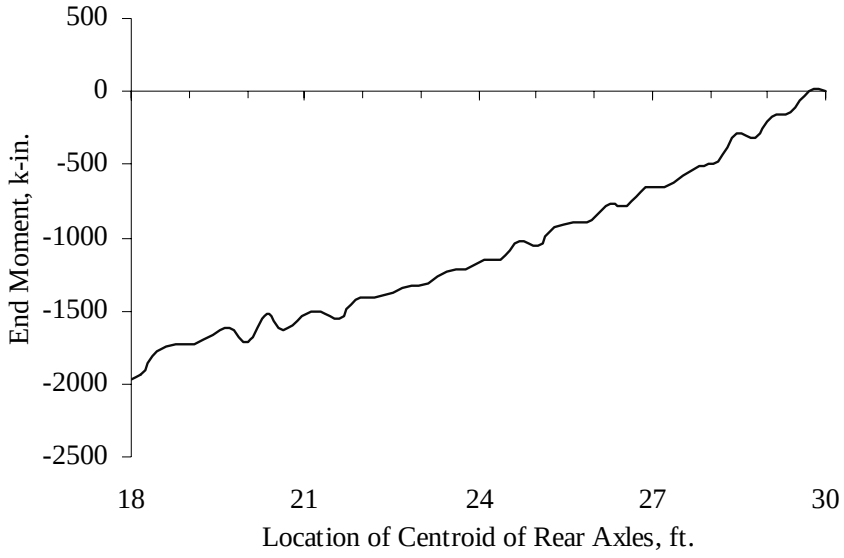

Figure 5.48 End Moment at West Support, Test Series 2, Truck Location 3

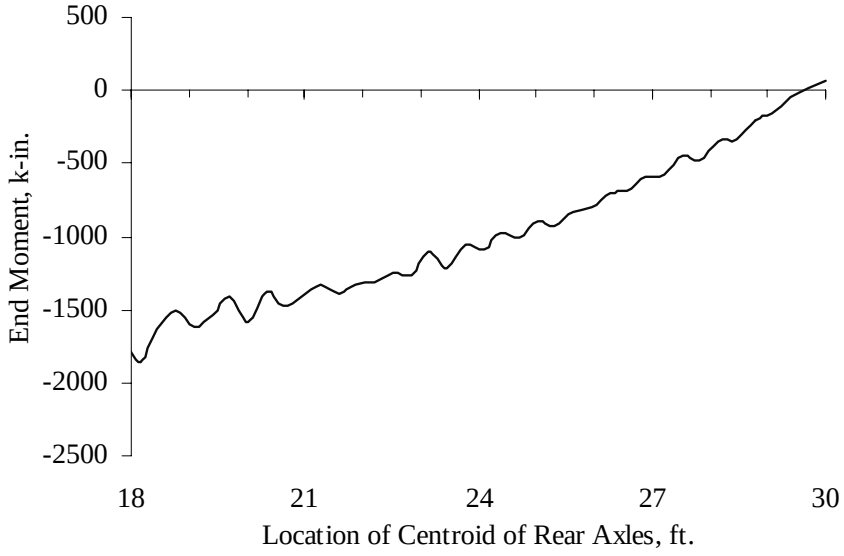

Figure 5.49 End Moment at West Support, Test Series 2, Truck Location 4

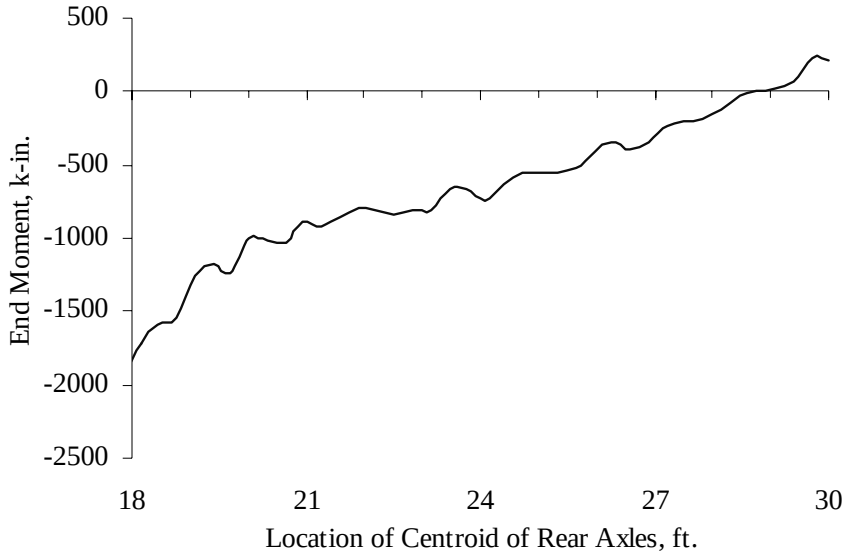

Figure 5.50 End Moment at West Support, Test Series 2, Truck Location 5

As the figures show, some rotational restraint was observed also at the west support. Figure 5.45 shows the maximum end moment to be approximately 3000 kip-in. This value is approximately ten times larger than the rotational restraint at the east support and is observed in all five truck locations of Test Series 2. The west support was found to have more continuity than the east support, but moment lines of the experimental data do not show values indicating such a large increase in restraint. Because the moments at the west support were calculated using the moments and shears at the east support, the margin of error in the results begins to increase because all of the values used in the calculation have been inferred from experimental data. Essentially, the error is compounded, as more variability exists in the results from the calculations.

The end moments at the east and west supports obtained from experimental data were compared with the end moments obtained from a line-girder analysis of a continuous system, as shown in Figures 5.51 and 5.52. The experimental end moments for all five truck positions do not resemble the end moments from the analytical results. Large variations are observed in the experimental data as the truck moves transversely across the bridge. Figure 5.51 further indicates that the support conditions at the east support are not those of a fully continuous system. In regard to the west support, Figure 5.52 indicates that the support conditions at the west support are not similar to the supports for a continuous system. However, Figure 5.53 shows that the support conditions at the west support are nearly fixed, which is possible since a visual inspection of the west support showed that the adjacent supports were pressed against one another, and also a defined joint between the two supports was not seen.

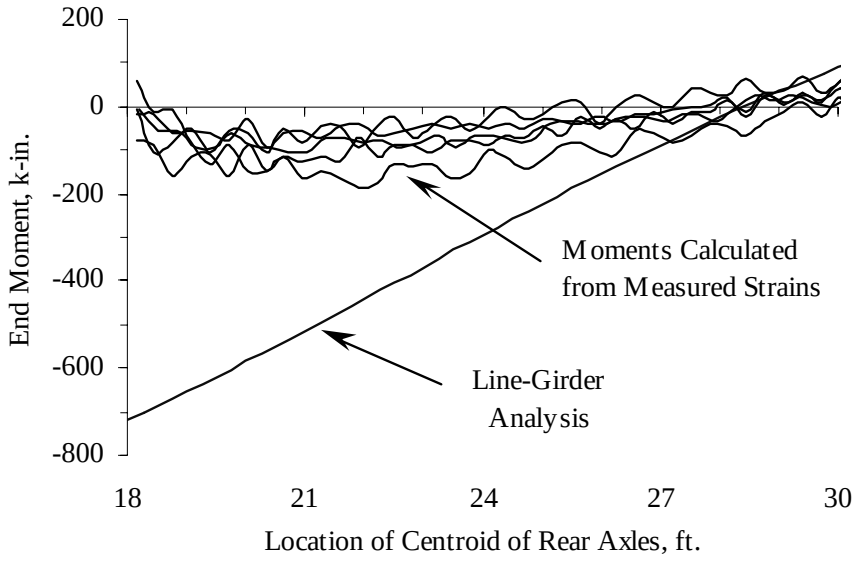

Figure 5.51 Comparison of Measured Moment Lines at East Support with Line-Girder Analysis of a Continuous Beam, Test Series 2

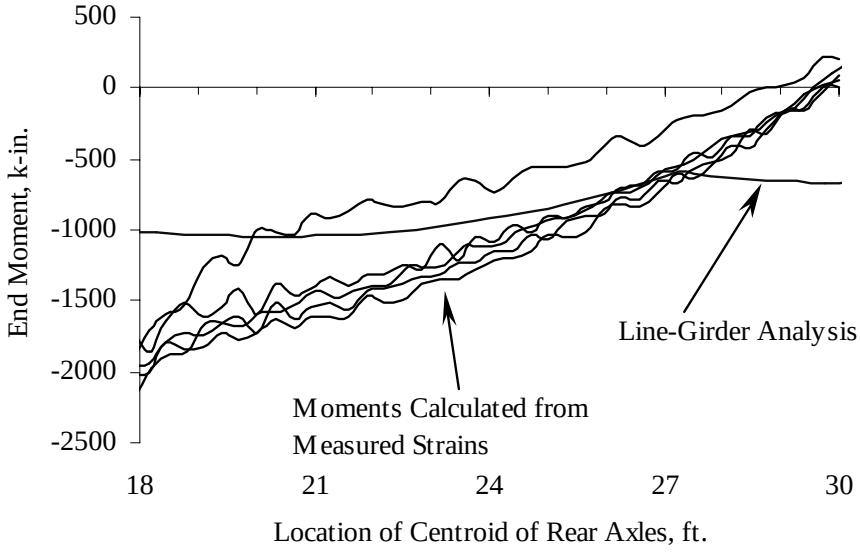

Figure 5.52 Comparison of Measured Moment Lines at West Support with Line-Girder Analysis of a Continuous Beam, Test Series 2

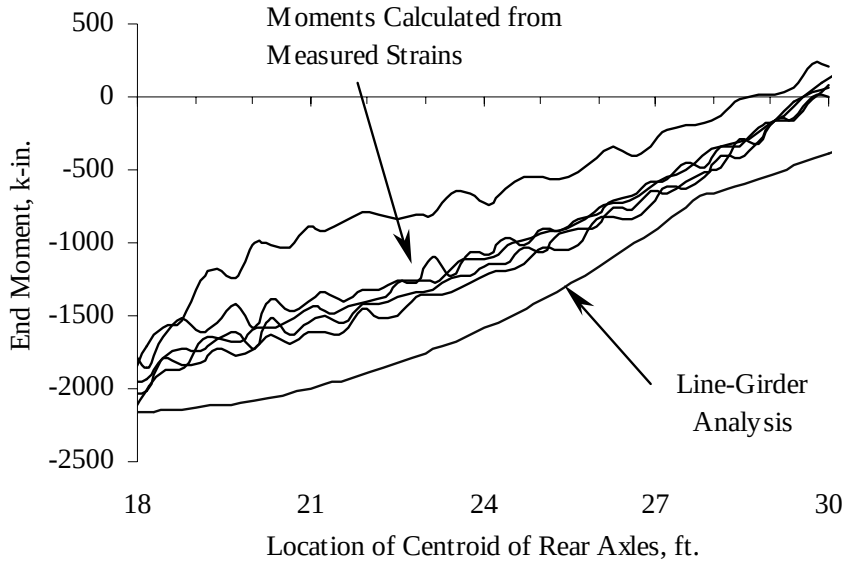

Figure 5.53 Comparison of Measured Moment Lines at West Support with Line-Girder Analysis of a Propped-Fixed End Beam

5.2.7 Summary

The response of the bridge to a diagnostic load test was presented and discussed. The neutral axis depths based on the experimental results were obtained for the two typical cross sections of the bridge. The experimental neutral axis depths for both cross sections were found to vary as the truck moved transversely across the bridge. Therefore, an average depth for each cross section was calculated in order to compare it with the neutral axis depths obtained from analysis. The experimental neutral axis depth for an interior girder was similar to the calculated neutral axis depth assuming cracked cross-sectional properties. A neutral axis depth of 6.0 in. was used for the interior girders in calculating moments. The neutral axis depth of 18.5 in. obtained from the experimental data was used in calculating moments in the exterior girders.

The moments calculated from strains measured on the surface of the reinforcing bars were compared with results from line-girder analyses of simply-supported and continuous beams, to determine the distribution of loading among the girders, and to assess the continuity at the supports. The results indicated that the maximum moments at midspan from the experimental results were within 5% of the maximum moments from a line-girder analysis of a continuous beam. The results also showed that more load was distributed to the exterior girders than to the interior girders because of the larger stiffness of the exterior girders. In reference to the rotational restraint at the supports, continuity at both supports was observed but because of changes in vehicle speed, level of noise in the measured response, and the variability in measured response, the cause and the quantity of the continuity could not be assessed.

CHAPTER 6: COMPARISON OF LOAD DISTRIBUTION WITH A PREVIOUS FIELD TEST AND DESIGN SPECIFICATIONS

This chapter discusses and compares the C values obtained from the measured response of the pan-girder bridge with those values obtained from a previous field test and the 1996 AASHTO Standard Specifications for Highway Bridges [8].

6.1 COMPARISON OF LOAD DISTRIBUTION WITH PREVIOUS FIELD TEST

The load distribution results obtained from the 1998 field test of the pan-girder bridge in Buda, TX were compared with those from the 1968 field test conducted in Belton, TX [4]. The two bridges are different because the Buda bridge has been in service for forty years and the Belton bridge was new at the time of the field test. Emphasis was placed in comparing the experimental C values from the two tests. The experimental C values from the 1968 test were obtained for four load patterns, shown in Fig. 6.1 through 6.4 with the equivalent load pattern for the 1998 test presented to their right. For example, the 1968 loading pattern for truck location 3 has the truck placed near the centerline of the bridge similar to the 1998 loading pattern for Truck Location 3. Therefore, the C values for girders E, F, and G were compared with those for girders 4, 5, and 6. One major difference between the two bridges was that the 1968 bridge did not have any curbs and the 1998 bridge did. The contribution of the curbs to the C values is important and is discussed later in this chapter.

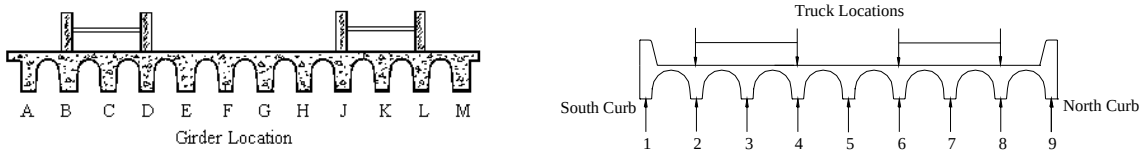

Figure 6.1 1968 Load Pattern Equivalent to Test Series 1 [4]

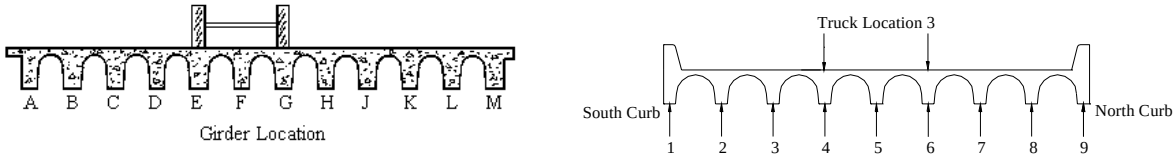

Figure 6.2 1968 Load Pattern Equivalent to Truck Location 3 [4]

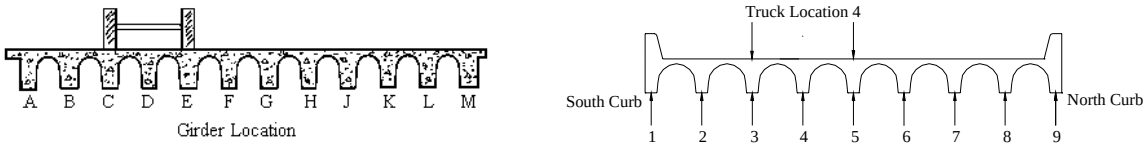

Figure 6.3 1968 Load Pattern Equivalent to Truck Location 4 [4]

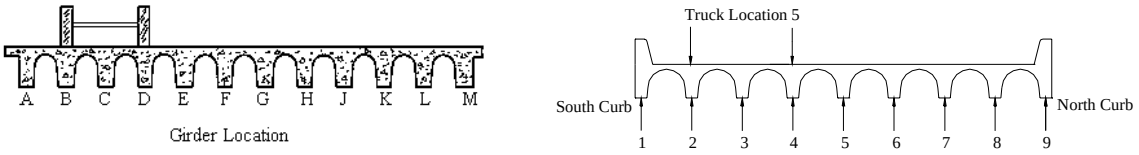

Figure 6.4 1968 Load Pattern Equivalent to Truck Location 5 [4]

Tables 6.1 and 6.2 present a reduced version of the minimum and average C values for the 1998 test, respectively. Table 6.3 presents the C values for the 1968 test. Equations 5.3 and 5.4 in Chapter 5 were used to determine the distribution factors and the experimental C values, respectively.

Table 6.1 Minimum Experimental C values obtained from 1998 Field Test of Bridge in Buda, TX

Test Series	Truck Location	Girder								
		1	2	3	4	5	6	7	8	9
1	1 & 5		9.0	8.1	6.0		6.6	6.9	8.3	
2	3				9.4	8.2	9.0			
	4			12.1	7.4	8.2				
	5		10.3	9.4	7.7					

Table 6.2 Average Experimental C values obtained from 1998 Field Test of Bridge in Buda, TX

Test Series	Truck Location	Girder								
		1	2	3	4	5	6	7	8	9
1	1 & 5		10.3	9.0	6.6		7.7	7.4	10.4	
2	3				11.0	9.3	10.5			
	4			13.9	8.5	9.7				
	5		12.2	10.9	8.9					

Table 6.3 Experimental C obtained from 1968 Field Test of Bridge in Belton, TX [4]

Test Series	Truck Location	Girder											
		A	B	C	D	E	F	G	H	J	K	L	M
1	1 & 5	*	8.2	7.2	9.1	*	*	*	*	7.6	7.6	8.9	*
2	3	*	*	*	*	12.0	11.0	12.0	*	*	*	*	*
	4	*	*	7.1	7.6	10.2	*	*	*	*	*	*	*
	5	*	7.1	6.6	9.3	*	*	*	*	*	*	*	*

* denotes girders where C values were not calculated

The percent difference between the three tables is presented in Tables 6.4 and 6.5 for minimum and average experimental C values, respectively. A negative number in the cells indicates that more load is being distributed to the corresponding girder of the Belton bridge. For example in Table 6.4, girder 2 shows a C value equal to -9.7% for Test Series 1. This value means that approximately 10% more load was carried by girder B of the Belton bridge than by girder 2 of the Buda bridge. Such values are expected because it has been found that the curb carries a large portion of the load when the loading vehicle is placed adjacent to or near the curb.

As shown in the tables, more load is carried by the interior girders of the Belton bridge than the interior girders of the Buda bridge as the truck shifts toward the edge of the bridge, which indicates that the south curb in the Buda bridge is carrying more load. However, as the truck moves away from the curb, the load

is distributed among the interior girders of the Buda bridge, as shown in truck location 3 where the truck is positioned at the center of the bridge. This location shows positive values indicating that less load is being carried by the interior girders of the Belton bridge because the load distributes over a larger area; thereby, more girders are participating in carrying the load. In the loading pattern where two trucks are positioned on the bridge, the table does not show similar trends in the two lanes. Differences such as the exact transverse and longitudinal locations of the two trucks and the number of girders between the two trucks could be the cause for the change.

Table 6.4 Percent Difference between Minimum C Values of 1998 and 1968 Field Tests

Test Series	Truck Location	Girder								
		1	2	3	4	5	6	7	8	9
1	1 & 5		-9.7	-11.3	41.8		13.5	9.9	6.6	
2	3				23.9	29.7	28.2			
	4			-52.1	3.3	21.2				
	5		-36.5	-34.7	18.4					

Table 6.5 Percent Difference between Average C Values of 1998 and 1968 Field Tests

Test Series	Truck Location	Girder								
		1	2	3	4	5	6	7	8	9
1	1 & 5		-20.4	-20.0	37.9		-1.3	2.7	-14.4	
2	3				9.1	18.3	14.3			
	4			-48.9	-10.6	5.2				
	5		-41.8	-39.4	4.5					

In general, the percent difference between the C values from the field test and the 1968 field test ranges from approximately 1% to 52%. The curbs located on the Buda bridge attract load away from the adjacent interior girders, thereby reducing the load carried by the interior girders.

6.2 COMPARISON OF LOAD DISTRIBUTION WITH DESIGN SPECIFICATIONS

According to the 1996 AASHTO Standard Specifications for Highway Bridges [8], the C value for bridges designed for one traffic lane is 6.5 and for two or more traffic lanes, the C value is 6.0. Therefore, C values based on the ratio of experimental girder moment to the moment obtained from a line-girder analysis were compared with the AASHTO design value. The moment influence lines presented in Section 5.1 for a simply-supported beam was used in obtaining the C value used to compare with the AASHTO design value. The results from a line-girder analysis of a simply-supported beam were used because AASHTO uses analysis results from simply-supported beams to design the girders. Only influence lines corresponding to mid-span were used in the analysis because the AASHTO design value was based on maximum moments. The C values were calculated using Eq. 5.3, where the distribution factor in the equation was calculated as follows:

$$DF_i = \frac{M_i}{M_{L.G.}} \tag{6.1}$$

where:

DF_i = distribution factor for girder i

M_i = moment measured from strains in girder i

$M_{L.G.}$ = total moment across bridge from a line-girder analysis of a simply-supported beam

Tables 6.6 summarizes the C values obtained from a line-girder analysis of a simply-supported beam, and Table 6.7 shows the percent difference between the experimental C and the AASHTO design value.

Table 6.6 C Values from Line Girder Analysis of Simple-supported Beam

Test Series	Truck Location	Girder								
		1	2	3	4	5	6	7	8	9
1	1 & 5	3.9	9.7	8.8	6.4	6.4	7.9	7.1	9.6	4.5
2	1						15.0	11.9	13.6	5.8
	2					14.9	13.8	12.3		
	3				14.4	12.3	14.0			
	4			17.4	10.8	12.1				
	5	5.0	13.0	11.7	9.7					
3	1						14.0	13.2	14.9	6.8
	2					13.5	14.3	13.9		
	3				11.9	13.3	14.7			
	4			15.2	12.8	13.6				
	5	4.2	13.8	14.7	12.0					

The negative values in Table 6.7 indicate that the experimental C value was less than the design value. Negative values correspond to correspond to exterior girders, which indicates that the curbs are being distributed more load than what was expected in design. Because of the increase in stiffness due to the integral curb, the exterior girders attract more load. The AASHTO design value does not take into consideration changes in stiffness throughout the bridge cross-section. Therefore, the AASHTO design value of 6.0 is unconservative in quantifying the distribution of load to curbs. But in general, the AASHTO design value is conservative within a range of 7% to 100% for the majority of the interior girders for Test Series 2 and 3.

Table 6.7 Percent Difference between Experimental C from a Line-Girder Analysis of a Simply-Supported Beam and AASHTO Design C

Test Series	Truck Location	Girder								
		1	2	3	4	5	6	7	8	9
1	1 & 5	-43.3	47.5	38.1	6.6	6.6	27.3	17.4	46.3	-29.4
2	1						85.7	66.0	77.8	-3.1
	2					84.9	78.6	68.8		
	3				82.5	68.8	80.1			
	4			97.6	57.1	67.4				
	5	-18.8	74.0	64.6	47.5					
3	1						80.1	74.7	84.9	13.2
	2					77.0	81.7	79.3		
	3				66.0	75.5	84.1			
	4			86.5	72.5	77.8				
	5	-35.0	78.6	84.1	66.7					

In summary, the distribution of load among girders based on the AASHTO design specifications is conservative for interior girders, but unconservative for exterior girders with integral curbs and for loading with two vehicles. Values, which take into account the relative stiffness of curbs to the girders, should be considered in order to assess the appropriate load distribution to the curbs.

CHAPTER 7: CONCLUSIONS AND RECOMMENDATIONS

The objectives of this research were to measure the response of a pan-girder bridge based on a diagnostic load test and to evaluate the response of the bridge. This chapter presents the conclusions and recommendations from the diagnostic load testing of a pan-girder bridge in Buda, TX.

7.1 CONCLUSIONS

The results of this research concluded the following:

1. The mean average compressive strength of the concrete was higher than the compressive strength used in design. Results from Schmidt hammer tests found the average compressive strength to be 8200 psi in comparison with 3000 psi used in design. High variability was observed in concrete compressive strength between the bottom of girders and the top of the curbs. Schmidt hammer results obtained from the top of the curb were higher.
2. Strain gages attached to the surface of reinforcing bars produced more reliable, consistent results than strain gages attached to the surface of the concrete. The repeatability of strains from reinforcing bar gages fell within a ±10% range, whereas the repeatability of strains from concrete gages fell within a ±25% range. The repeatability served as an indicator of the sensitivity of the gages to slight changes in the transverse positioning of the truck.
3. Concrete gages placed at the crown were found to be sensitive to longitudinal cracking, to the impact of truck wheels directly over the gage, and to small changes in transverse position of the truck during passes 1 and 2.
4. The response histories from concrete gages placed on the top of the curbs provided some useable data but were found to drift appreciably during 90-minute tests. Possible reasons were temperature and transverse truck location.
5. Measurements taken by deflection gages resulted in response histories with flattened peaks at locations where maximum displacements were expected.
6. The maximum strains measured under dynamic loading conditions were found to be 10% greater than strains measured from the semi-static loading conditions for the majority of the loading cases.
7. Experimental calculations of neutral axis depths for interior and exterior girder cross sections were very similar to those calculated by analysis. The experimental neutral axis depth for the interior girder cross section was near the neutral axis depth corresponding to cracked cross-sectional properties. For the exterior girder cross section, the experimental neutral axis depth was near the neutral axis depth corresponding to gross cross-sectional properties.
8. The maximum positive moment at the mid-span from experimental results was approximately the same as the maximum positive moment from a line-girder analysis of a continuous beam. However, the maximum calculated negative moments at mid-span due to a truck positioned near the west or east supports exceeded the experimental results. The line-girder analysis of a simply-supported beam resulted in a maximum positive moment approximately 60% greater than the maximum positive moment calculated from the experimental results. Additionally, the maximum positive moments at mid- and quarter-span were almost equal and such results were found to be inconsistent with the line-girder analyses.
9. The bridge responded symmetrically to symmetric loading conditions. For nonsymmetrical loading conditions, the measured response when the truck was positioned near the north curb was a mirror image of the response when the truck was positioned near the south curb. Additionally,

the bridge responds the same to the superposition of loads as it would to loading the bridge with one equivalent load. Therefore, only half of the bridge cross section needs to be instrumented.

10. The curb acts integrally with the superstructure, thereby reducing the load carried by the girders located adjacently to the curb. More load was distributed to the curb when the truck was positioned adjacent to the curb. When the truck was positioned near the centerline of the bridge, the curbs carried approximately the same load as the girders located underneath the truck.
11. Continuity of the west and east supports was observed. Rotational restraint found at the east support was found to be small compared with the results of a line-girder analysis of a continuous beam. Rotational restraint at the west support was found to be approximately the same as the results obtained from a line-girder analysis of a propped-fixed end beam.
12. The experimental C values from this research were larger than the values obtained from a previous test [4] when the truck was positioned near the edge of the bridge. The C values from this research were smaller than the previous test [4] when the truck was located at the centerline of the bridge. These smaller values indicate that the girders located directly below the truck wheel lines were carrying the majority of the load. However, some of the load was transferred to the curbs rather than to other interior girders.
13. The C values for interior girders based on experimental and line-girder results were larger than those obtained from the 1996 AASHTO Specifications, resulting in conservative design specifications. The C values for the curbs, however, were smaller than the 1996 AASHTO Specifications, which results in unconservative design values.

7.2 RECOMMENDATIONS FOR LOAD TESTING

7.2.1 Planning

A thorough investigation of the bridge should be conducted prior to instrumentation. The structural soundness, flow of traffic, and accessibility underneath the spans must be considered in selecting a bridge to load test. The span selected must be accessible to instrument near mid-span by using ladders or preferably scaffolding. The location and width of cracks in the girders and at the crowns should be noted before the load test. In addition, the joints between adjacent supports should be measured and inspected for debris or structural connections between the supports.

7.2.2 Instrumentation

It is recommended that the majority of the strain gages be placed at the mid-span of the primary longitudinal reinforcing bars. Because of the unreliable data obtained from the concrete strain gages located at the crowns, strain gages should be placed on longitudinal reinforcing bars in the slab in an attempt to obtain compressive strain readings. The bottom layer of reinforcing bars of the girders should be instrumented as well to obtain tensile strain readings. Additionally, concrete strain gages should be located at the top of the curbs in order to find the neutral axis depth of the curbs.

Only one half of the mid-span cross-section needs to be instrumented because of the symmetrical nature of the measured bridge response. The quarter-point of the span does not need to be instrumented unless a distinct connection is found between adjacent spans.

7.2.3 Testing

A data-acquisition system with many channels and fast sampling rates is recommended. An increase in channels reduces the slight variations in data due to the repositioning of the truck in an attempt to perform an identical run to obtain data from all the gages.

The loading of the bridge should consist of one truck. Loading the bridge with two trucks is optional to verify the assumption of the bridge responding symmetrically to various loading conditions. The truck

must be positioned transversely across the entire width of the span. Transverse truck locations corresponding to wheel lines directly over the girders are preferred.

7.3 FUTURE RESEARCH

Although the tested bridge was heavily instrumented, many questions remain unanswered. Areas that need further investigation include:

1. Assessing the bi-axial bending of the curb when loads are placed adjacent to the curb. The twisting of the curb in addition to flexure is possible when loads are placed near the curb. The effect of such twisting on the structural behavior of the span should be studied.
2. Quantifying the continuity, if any, that develops where a cold joint is observed, such as the connection between a support and the road abutment.
3. Investigating skewed bridges of this type. Past research [4] indicated that skew angle did not affect the response of a bridge without curbs. However, the curbs in this bridge act integrally with the superstructure, and a skew of the superstructure with respect to the substructure might affect the load distribution patterns.

References

1. American Association of State Highway and Transportation Officials (AASHTO), Manual for Condition Evaluation of Bridges, Washington, D.C., 1994.

2. Lichtenstein, A. G., "Manual for Bridge Rating Through Load Testing," Final Draft, NCHRP 12-28(13) A, June 1993.

3. Leyendecker, E. V., and Breen, J. E., "Structural Modeling Techniques for Concrete Slab and Girder Bridges," Research Report 94-1, Center for Highway Research, The University of Texas at Austin, August 1968.

4. Armstrong, T. A., Leyendecker, E. V., and Breen, J. E., "Field Testing of Concrete Slab and Girder Bridges," Research Report 94-2, Center for Highway Research, The University of Texas at Austin, July 1969.

5. Leyendecker, E. V., and Breen, J. E., "Behavior of Concrete Slab and Girder Bridges," Research Report 94-3F, Center for Highway Research, The University of Texas at Austin, May 1969.

6. Texas Department of Transportation, Bridge Inventory, Inspection, and Appraisal Program (BRINSAP) Database, July 1997.

7. Bussell, L. C., "Diagnostic Testing for Improved Load Rating of Reinforced Concrete Slab Bridges," Master's Thesis, The University of Texas at Austin, May 1997.

8. American Association of State Highway and Transportation Officials (AASHTO), Standard Specifications for Highway Bridges, 16th ed., Washington, D. C., 1996.

9. American Association of State Highway Officials (AASHO), Standard Specifications for Highway Bridges, 8th ed., Washington, D.C., 1957.

10. American Association of State Highway Officials (AASHO), Standard Specifications for Highway Bridges, 9th ed., Washington, D.C., 1965.

11. Velázquez, Blanca M., "Diagnostic Load Tests of a Reinforced Concrete Pan-Girder Bridge," M.S. Thesis, The University of Texas at Austin, 1998.